TESTING CONCRETE FOUNDATION PILES

BY SONIC ECHO

IAN FEGEN

Doctor of Philosophy
University of Edinburgh
1981

Volume 1

ABSTRACT

An acoustic reflection technique for the non-destructive testing of concrete piles has been examined. Currently available non-destructive pile integrity tests have been reviewed with particular attention to systems based on the sonic echo principle.

A practical examination of the method has been conducted on construction sites to identify the inherent problems and to establish areas for research.

Acoustical theory has been studied in relation to the material and the component shape. The relevance of the theory and the problems of practical application of the method have been examined in the laboratory.

The implications for further development of the technique have been considered.

ACKNOWLEDGEMENTS

The author wishes to thank the following for their kind assistance:

Professors A.W. Hendry and J.H. Collins for the provision of facilities within the Departments of Civil and Electrical Engineering.

Dr. M.C. Forde and Dr. H.W. Whittington for their supervision and valuable advice and encouragement.

Dr. D.G. Guild for the translation of Russian papers.

Roberto Morelli for undertaking some of the practical work.

John McCarter for many valuable discussions and assistance with the field work.

His wife, Heather for help with the translation of French and German papers and for her patience and encouragement at all times.

Jan Hollingdale for the proficient typing of this thesis.

C.N.S. Electronics for their cooperation and provision of acoustic transducers.

The financial assistance of the Science Research Council and the sponsorship of Robert Matthew-Johnson Marshall and partners is gratefully acknowledged.

CONTENTS

Page

NOTATION

a	cylinder radius
a_ℓ	angle of incidence and reflection of longitudinal waves
a_t	angle of incidence and reflection of transverse waves
A	cross sectional area
A	constant
A	amplitude
A_0	amplitude at $x = 0$
b	perpendicular distance from bar to transducer
b	length of side of a square cross section
B	constant
c	velocity of wave propagation
c_g	group velocity
c_ℓ	velocity of longitudinal waves
c_0	bar velocity
c_p	phase velocity
c_R	velocity of Rayleigh surface waves
c_t	velocity of transverse waves
C	constant
d	diameter
D	constant
DR	decay rate
E	elastic modulus
E_d	dynamic modulus of elasticity
f	frequency
f_0	resonant frequency
f'	torsional resonant frequency

f''	longitudinal resonant frequency
F	force
F_0	maximum vertical force applied to pile
Fr	frequency
g	gravitational acceleration
G	modulus of rigidity or shear modulus of elasticity
h	height of hammer fall
i	unity for first mode, two for second, etc.
i	$\sqrt{-1}$
I	acoustic intensity
I	moment of inertia
IR	impact/reflection ratio
IRb	impact/rebound ratio
J_0	Bessel function
J_1	Bessel function
k	constant
k_0	propagation constant
k_ℓ	propagation constant
k_t	propagation constant
k_1	constant in Hertz contact theory
k_2	constant in Hertz contact theory
K	bulk modulus
K	radius of gyration
K_1	correction factor
K_2	correction factor
ℓ	length
ℓ	longitudinal wave amplitude

m	mass
m_r	reflection coefficient
m_t	transmission coefficient
M	moment
M	constant
p	acoustic pressure
p	volume ratio of total coarse aggregate to concrete
P	period
P_r	bar stress component
P_z	bar stress component
P_θ	bar stress component
Q	bar stress component
Q	damping constant
r	radial coordinate
r	radius of gyration
r_z	radius of gyration with respect to z-axis
R	characteristic acoustic impedance
R	radius of curvature
R	ratio of polar moment of inertia to the shape factor for torsional rigidity
RP	reflection phase
RtT	return time
RT	toe reflection time
S	constant
SDR	system decay rate
t	time
t	transverse wave amplitude

t_c contact time

T average volume of aggregate particle

T constant

u displacement in the x direction

u_r radial displacement

u_z axial displacement

u_θ angular displacement

U total energy of vibration per unit volume per cycle

ΔU damping capacity

v displacement in y direction

v particle velocity

v_0 hammer impact velocity

V_a pulse velocity in aggregate

V_c pulse velocity in concrete

V_e effective pulse velocity in concrete/steel medium

V_L longitudinal wave velocity

V_m pulse velocity in mortar

V_0 maximum vertical velocity of pile head

V_R surface wave velocity

V_s pulse velocity in steel

w displacement in z direction

W weight of specimen

W_a weight of aggregate

W_m weight of mortar

x coordinate in direction of length

X reactive component

z axial coordinate

Z specific acoustic impedance

α attenuation coefficient

α approach term in Hertz contact theory

α_m maximum approach

γ pulse velocity ratio

Γ gamma function

δ logarithmic decrement

Δ attenuation rate

θ angular coordinate

λ Lamé constant

Λ wavelength

μ Lamé constant

ρ density

ρ_a density of aggregate

ρ_m density of mortar

σ Poisson's ratio

$\mathfrak{T}$ stress

ϕ potential function

ψ single potential function for waves symmetrical about z axis

ω angular frequency

1. INTRODUCTION

Concrete piled foundations are of major importance to many civil engineering works. However due to the nature of sub-surface conditions faults in piles may often pass undetected. Any test which can simply locate defects within a pile would therefore be of value to the industry.

In various forms, load testing is the traditional method of proving the soundness of piled foundations. Preliminary load tests confirm the design bearing capacity and indicate settlement under load. Test loading of constructed working piles confirms preliminary load test results and attempts some quality control of pile construction. These working test piles may be selected purely at random or where the integrity is in doubt because of, for example, difficult ground conditions or suspected poor workmanship. On a large site, test piles may be selected to confirm bearing capacity in several representative areas of sub-surface variation. With the introduction of large diameter bored piles supporting high loads, load testing has become increasingly expensive and less feasible. Additionally, load testing a small number of piles from a large group cannot accurately establish the proportion of defective piles present.

In recent years several non-destructive methods of testing concrete foundation piles have been under development. Their acceptance by the profession has been slow and piecemeal, probably reflecting the level of development

and reliability of the tests. A recent report on problems associated with concrete piles published by CIRIA[7], contained the following recommendation for the pursuance of research:

> "Development of relatively simple, reliable and inexpensive methods of establishing the structural integrity of piles, with particular reference to methods which do not require special means of instrumentation to be incorporated in the piles at the time of construction. Over-sensitivity of equipment should be discouraged, since the existence of minute defects in piled foundations is inevitable."

During the last few years, one such test method has been under development, notably in France. The technique involves the propagation of a sonic impulse down the axis of a pile. The signal is reflected at the pile base, or at a discontinuity if one exists. From the echo time and a knowledge of the velocity of sound in the concrete the length of continuous pile may be estimated. Encouraging results have been obtained but there remains much scope for improvement and development of the method.

In this thesis the present level of development of the sonic echo method is assessed. Theoretical and practical aspects of sound propagation through concrete piles are examined with implications for further development.

2. REVIEW OF PILE INTEGRITY TESTING

2.1 Introduction

Concrete foundation piles are frequently placed under difficult sub-surface conditions and are susceptible to constructional defects. Their inaccessible nature poses special problems in the determination of structural integrity.[1]

Visual inspection of piles is impracticable, therefore more sophisticated means of examination are required. The traditional solution, load testing, has become increasingly expensive and less attractive, especially with the advent of large diameter bored piles now supporting loads in excess of 1000 tonnes.[2] In recent years several non-destructive methods of checking pile soundness have become available.[3,4,5] As yet, no test has been devised which is both reliable and economic.

2.2 Pile Defects

Concrete piles may be broadly divided into two categories; precast and cast in situ. Precast piles are virtually always driven into the ground. Partially preformed piles are sometimes used in which a concrete shell is driven into place and later filled with fresh concrete.[5,6]

Faults which occur in prefabricated piles during manufacture or transport to site may be detected by visual inspection. Any deficiencies which ensue during driving are of more serious import, since they may remain undetected.

Horizontal cracking may often arise but usually this detracts little from the bearing capacity. More serious are longitudinal cracks which can result in shearing failure, especially near the pile head. A driven pile may also break during driving with possibly the lower portion pushed out at an oblique angle.

With cast in situ piles the main problem is to achieve and maintain continuity of the concrete until hardening has taken place. If a shaft lining is used it is advantageous, though more expensive, to leave it in position. Some pile designs specify this practice. When a shaft lining is withdrawn it tends to drag the wet concrete upwards, thus creating voids within the pile body.[7]

Exposure of the pile to the surrounding soil can have several detrimental effects. Pressure on the pile can lead to necking and inclusions of foreign matter. Conversely, the wet concrete may intrude into voids in the soil resulting from overbreak in the shaft bore. Overbreak is often responsible for bulbous projections from the pile body with an associated discontinuity immediately above. Ground water may quickly attack an exposed pile, washing out the fines and leaving a region of weak concrete.[7]

The reinforcing of cast in situ piles can give problems. Close spacing of bars may prevent a stiff mix of concrete from passing through and occupying the complete width of the bore.[7]

2.3 Methods of Pile Testing

The following sections contain a review of pile testing methods including some non destructive techniques which are still under development. Advantages and disadvantages of individual systems are given, with some typical costs.

2.3.1 Load testing[4]

Load testing in various forms is the traditional method of proving the soundness of piled foundations. The test is concerned with two distinct stages in the evaluation of a foundation: design and construction.

As part of the design sequence several test piles are typically constructed on a site. Areas of minimum bearing capacity or difficult ground conditions are usually selected to assess the design fully. These preliminary test piles are then loaded to 1.5-2 times working load to determine suitability of the design. Successful loading confirms bearing capacity and shows settlement under load. If required, the pile design may be modified before construction proceeds.

Test loading of working piles achieves two things:

1: Confirmation of preliminary load tests in proving the design.

2: Quality control of pile construction.

Working piles may be selected for load test at random or where there is some doubt as to integrity because of bad working conditions or poor workmanship.

Load tests are generally performed by simply loading

the pile head (kentledge), or jacking against anchor piles sunk on either side. Cost is high at around £10/tonne of test load. (1980).

Advantages

1: Proves bearing capacity of design and of the tested pile.

Disadvantages

1: Expensive

2: Time and space consuming

3: Cost limits testing to small numbers.

2.3.2 Excavation and inspection [3,4,8]

An expensive though conclusive method of assessing integrity is to pull out or expose the doubtful pile. In the case of large piles a pit or heading may be required. The requirements for heavy plant, labour, the restrictions of safety regulations and problems with ground water may push the cost of investigation beyond that of a load test. Excavation and inspection may be considered in cases of dispute with the piling contractor over responsibility for a failure.

Advantages

1: Positive location of faults.

2: Non-specialist interpretation.

Disadvantages

1: Expensive

2: Time consuming and may interfere with adjacent work.

3: Difficult to apply where piles are close together.

4: Friction piles lose bearing capacity and cannot be used after exposure.

2.3.3 Drilling/coring [2,3,4]

Drilling by percussion equipment permits access of a light and television camera. Breaks in continuity in the path of the drill are easily identified and ingress of water will indicate a break to the exterior of the pile. Inspection is confined to the region of the hole and difficulties may be encountered in maintaining a plumb drilling line. Cost is high at £20-40/m. (1980).

Coring is around twice as expensive but it is easier to locate the cutting path. A core of concrete is recovered for examination and testing and thus regions of weak concrete may be positively identified. T.V. inspection is again possible providing the core diameter is large enough.

Holes produced by coring or drilling may be used for caliper logging. A three armed probe is lowered down the hole giving a surface read-out of the borehole diameter.

Advantages

1: Positive location of faults in the path of the drill.

2: Simple, non-specialist interpretation of information gained.

Disadvantages

1: Expensive

2: Time consuming

3: Fault location confined to immediate vicinity of the hole.

2.3.4 Continuous vibration [2,3,4,9,10-16]

Experience in the development of this dynamic response method has been gained by the organisation Centre Experimental de Recherches et d'Etudes du Batiment et des Travaux Publics (C.E.B.T.P.) in France.[13,14,15] An electrodynamical vibrator placed on the pile head imparts a sinusoidal force of constant amplitude with frequency varying 20 → 1000 Hz. Velocity transducers on the pile head record the steady state response of the pile under the imposed vibrations. (Fig. 2.1)

If V_0 = maximum vertical velocity of the pile head (m/s)

and F_0 = maximum vertical force applied to the pile (N)

then:

$\frac{V_0}{F_0}$ = mechanical admittance of the pile (s/kg)

An automatic plotter records the variation of mechanical admittance with the applied frequency. (Figure 2.2) The resulting curve has a wave-like form with a series of maxima and minima at resonance. At low frequencies, the pile and surrounding soil produce a characteristic lead in slope which indicates pile stiffness. Ideally, maxima

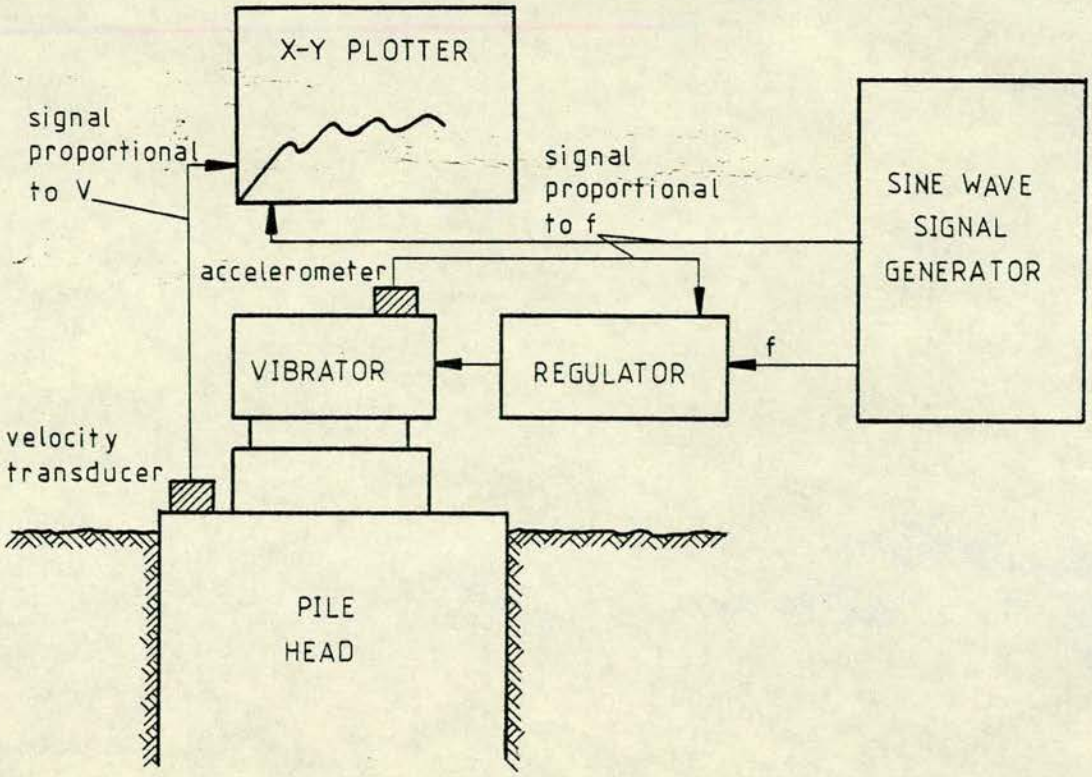

FIGURE 2.1

Diagram of vibration equipment
(After Davis and Dunn [9]).

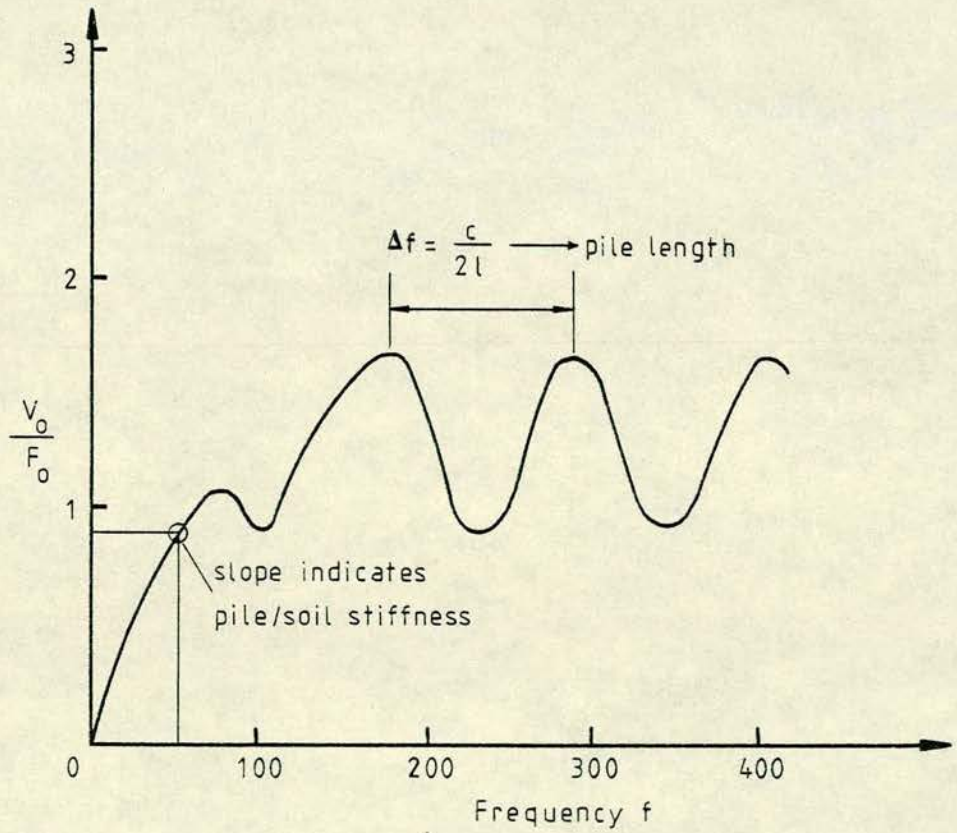

FIGURE 2.2

Ideal response curve
(After Weltman [4]).

will be spaced at intervals of frequency

$$\Delta f = \frac{c}{2\ell} \qquad (2.1)$$

where,

c = velocity of wave propagation

ℓ = length of pile in resonance

Thus, if Δf can be measured, and c determined from tests on samples, the pile length ℓ may be calculated. The test requires some preparation of the pile head to ensure a level base for the vibrator. The equipment requires a skilled operator and resonance curves demand specialist interpretation. Damping of vibrations by the soil limits the length of pile which may be tested. A limiting ratio of pile length to diameter of 30 : 1 is employed in soft alluvium. Under favourable conditions the ratio may be extended to 50 : 1. Gravel layers reduce the ratio or may even rule the method out. Cost is £50-100 per pile tested. (1980).

Advantages

1: Information gained on the stiffness of the pile in the soil as well as structural integrity.

Disadvantages

1: Limitations on length to diameter ratio in some soils.
2: Results weighted to upper part of pile.
3: Skilled operator and specialist interpretation required.

An adaptation of the above method may be used to determine the horizontal stiffness of a pile.[38] The method involves shaking the pile head horizontally and measuring displacement and stiffness at various frequencies. The vibrator consists of two rotating wheels loaded eccentrically. The frequency may be varied through 1 to 14 Hz with an applied horizontal force proportional to the square of the frequency. A horizontal geophone is glued to the pile head. The results are plotted in the form of mechanical admittance against frequency as for the vertical vibration test.

2.3.5 Sonic coring[1-4,11,12,17-23]

Another method developed by C.E.B.T.P. in France.[15] During construction several vertical tubes are cast into the pile. The tubes are of P.V.C. or metal with a diameter of around 40 mm. Transducers are lowered down two of the tubes and a sonic signal is transmitted from one to the other. The tubes are filled with water to ensure sufficient transfer of energy into the concrete. The two probes are raised or lowered together while signals are sent out at regular intervals and the full length of the pile is scanned. (Figure 2.3).

The velocity of sound has the following values: in air (330 m/s), water (1500 m/s), poor concrete (2000-3000 m/s), good concrete (4000+ m/s) and the transmission time therefore gives a good indication of the quality of material intervening between the probes.

The method produces good results and has a high accuracy of fault location.

A single hole technique may be employed using a combined transmitter/receiver unit. A borehole probe approximately 55 mm diameter and 2 m long is lowered down the hole. An ultrasonic transmitter at the top is separated by an acoustic insulator from a receiver at the base. Signals pass through the pile body and continuous monitoring at the surface indicates the quality of concrete adjacent to the probe.

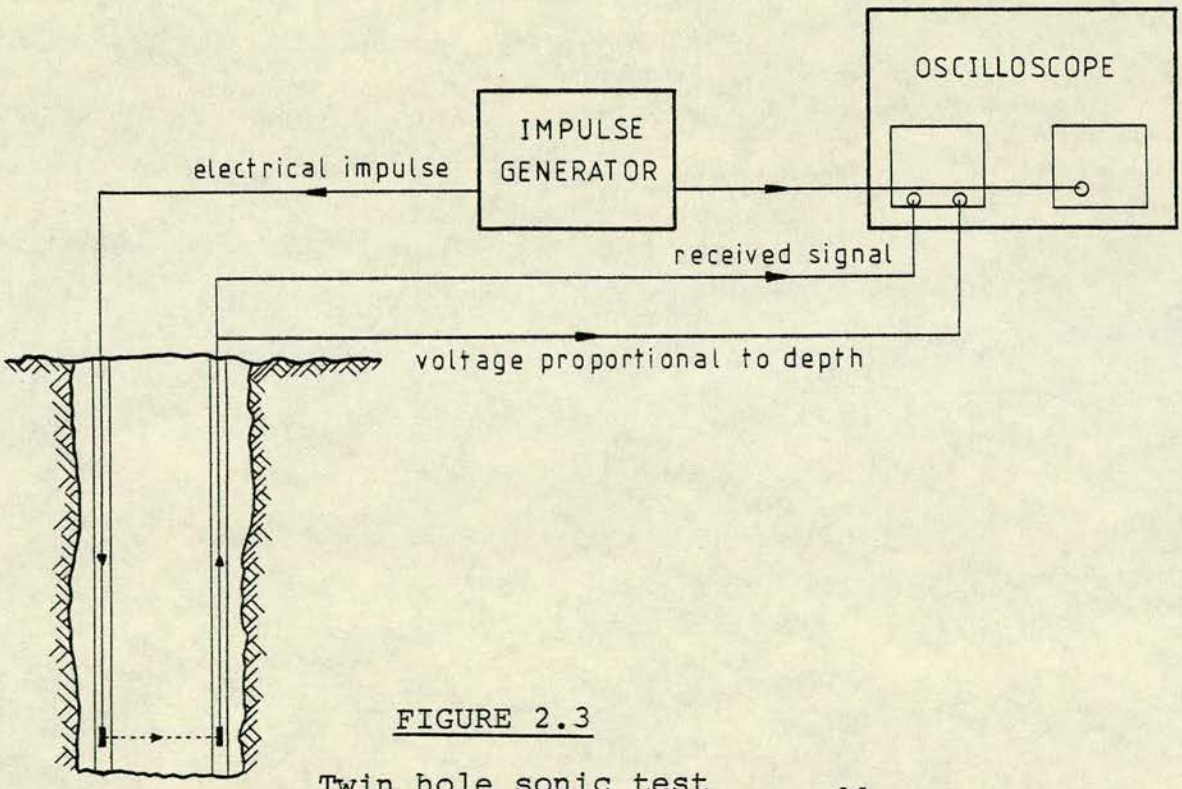

FIGURE 2.3

Twin hole sonic test
(After Davis and Robertson [11])

Contractors often show resistance to use of the technique by quoting high rates for the installation of tubes. Cost is around £50-100 per pile tested.

Advantages

1: High accuracy of fault location.

2: Fairly quick test, (excluding tube placement).

Disadvantages

1: Inspection tubes must be cast into pile during construction.

2: Extent of pile cross-section surveyed depends on the number of tubes employed.

2.3.6 Shaft compression[2-4,24]

In principle this method involves the application of a compressive force over the length of the pile by the stressing of internally cast and recoverable rods or cables. (Figure 2.4). If the pile is significantly weakened by any form of fault this becomes apparent by a downward movement of the top, in the case of a fault near the pile head, or an upward movement of the lower regions in the case of faulting near the base.

Advantages

1: Proves pile bearing capacity.

2: Fault near top of pile may be indicated and remedial action taken.

Disadvantages

1: Expensive.

2: Substantial preliminary work required during casting - contractor resistance.

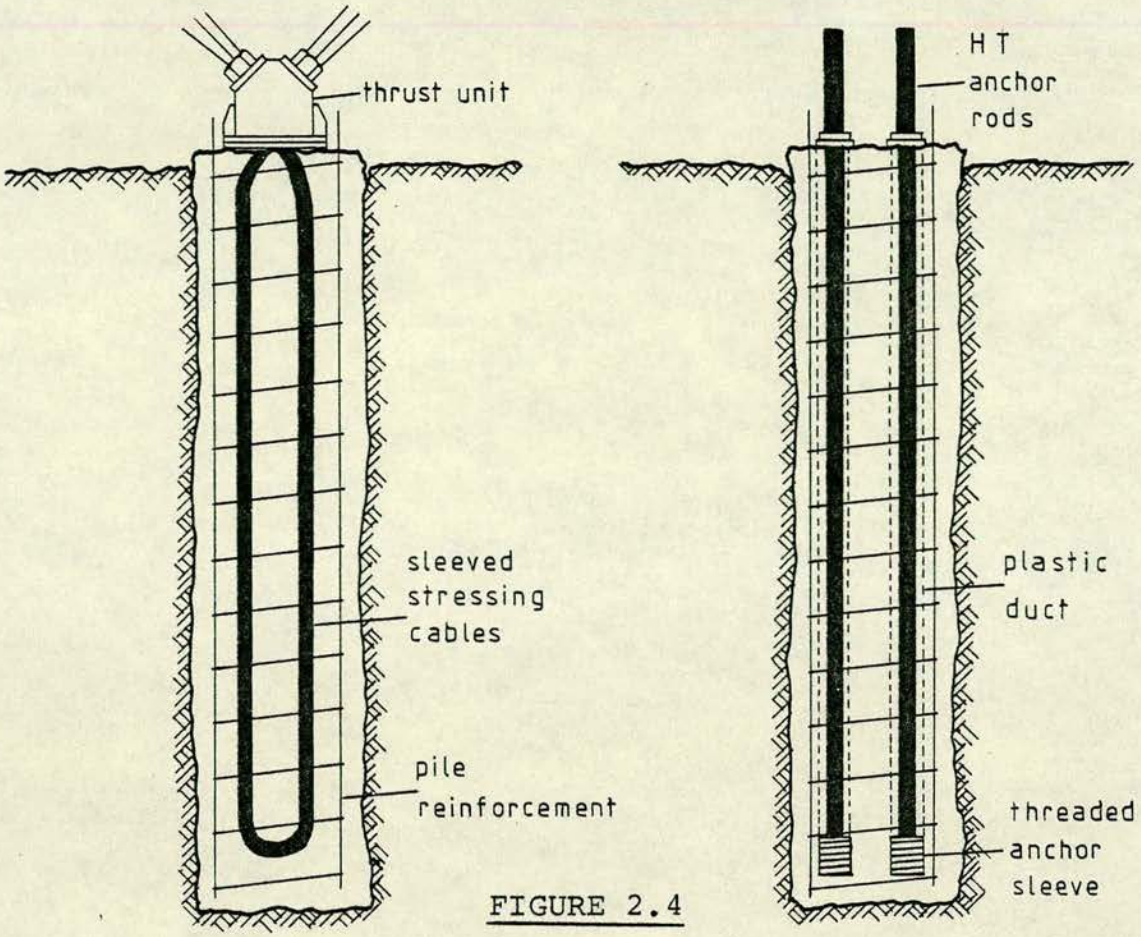

FIGURE 2.4

Shaft compression test
(After Moon[24])

2.3.7 Radiometry[2-4,25]

The method is similar in configuration to that of sonic coring. For single hole inspection a combined radioactive source and detector are employed. The radiation which is deflected after leaving the source by collisions with particles in the pile concrete is picked up by the detector. This is known as the backscatter method. Alternatively a transmission technique may be used across the pile between two tubes. The degrees of absorption or reflection are related to the density of the concrete. Cost is £20-30/m. (1980).

Advantages

1: Can give better penetration from a bore hole scan than caliper logging or T.V. inspection.

Disadvantages:

1: Expensive

2: Preparatory drilling required

3: Safety considerations may restrict use.

2.3.8 Electrical methods [1,2,4,26]

An electrical circuit may be formed between the pile reinforcement and an electrode buried in the soil some distance from the pile. The measurement of various electrical characteristics may then provide some indication of homogenity of the pile body. (Figure 2.5)

The method is currently under study in the Departments of Civil and Electrical Engineering at Edinburgh University.[26]

Advantages

1: Low cost

2: Quick test

3: Light, easily portable equipment carried by one operator.

4: May be used on low cut-off piles.

Disadvantages

1: Anomalous results may arise from variables such as the age or batch of concrete.

2: Experimental method - requires development.

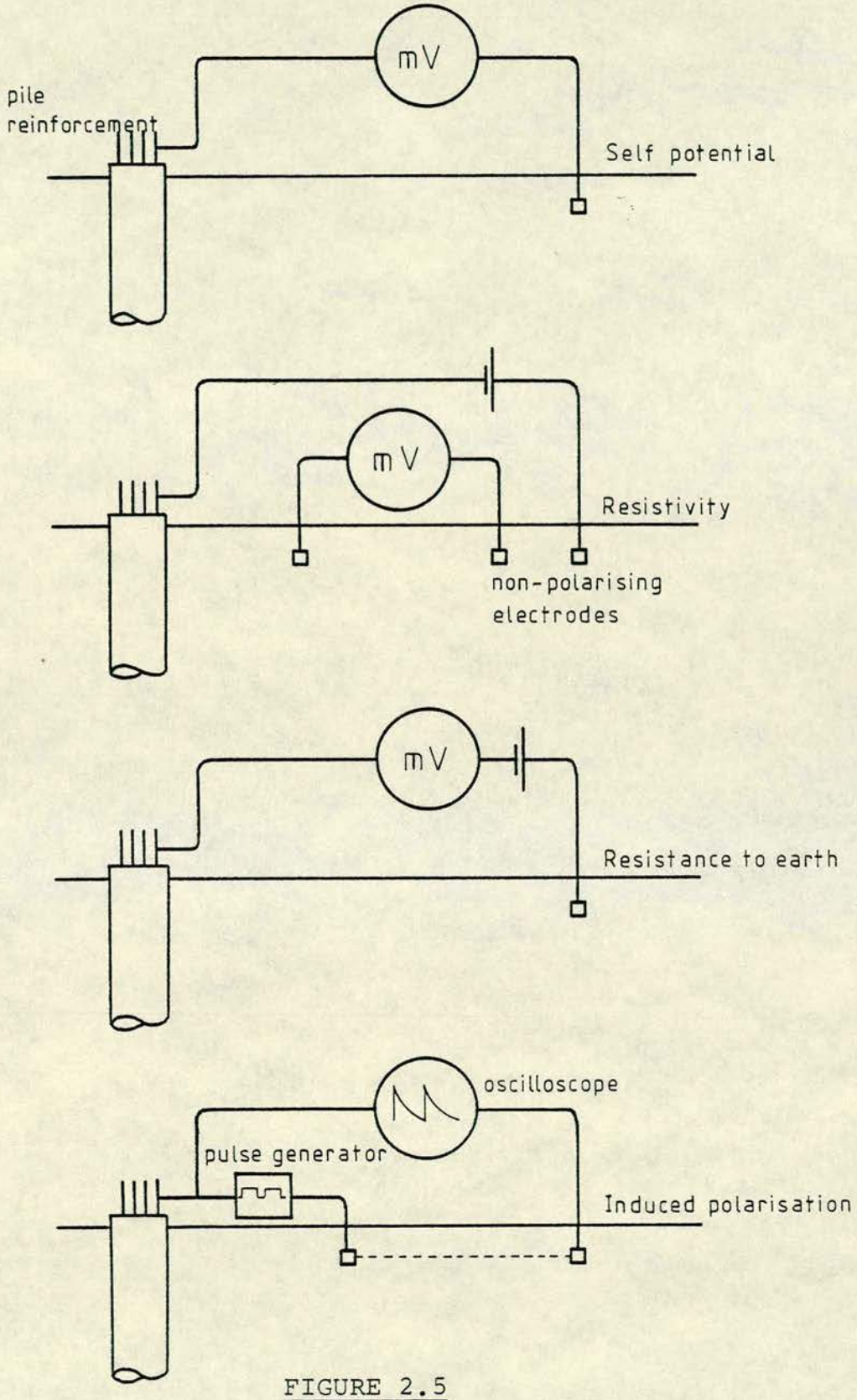

FIGURE 2.5

Electrical methods
(After Weltman [4])

2.3.9 Transient vibration [4,27-30]

The transient response of the pile to a single shock may be monitored through an instrument on the pile head. Dvorak has used a Cambridge vibrograph and has recorded two types of vibration.[27,28] (Figure 2.6). The fundamental mode derives from the vibration of the pile/soil system and is of large amplitude at low frequency. A secondary oscillation at a higher frequency, though not always discernable, is thought to be due to vibration of the pile itself. The fundamental vibration is related to the pile stiffness and the high frequency oscillation depends on the pile length and quality of the concrete.

A recent development of the continuous vibration method (p 8). replaces the mechanical vibrator with a single shock from a hammer.[29] A Hewlett-Packard 2108 computer and x-y plotter are used to analyse the dynamic response as for steady-state vibrations.

In the U.S.A. the Case organisation employs a method which analyses the response to the blow from a pile driving hammer.[30] Records of force and acceleration are recorded in analog form on magnetic tape. Later analysis by computer is then possible on return to the laboratory.

Advantages

1: Low cost

2: No preparation of pile required

3: Quick test.

Disadvantages

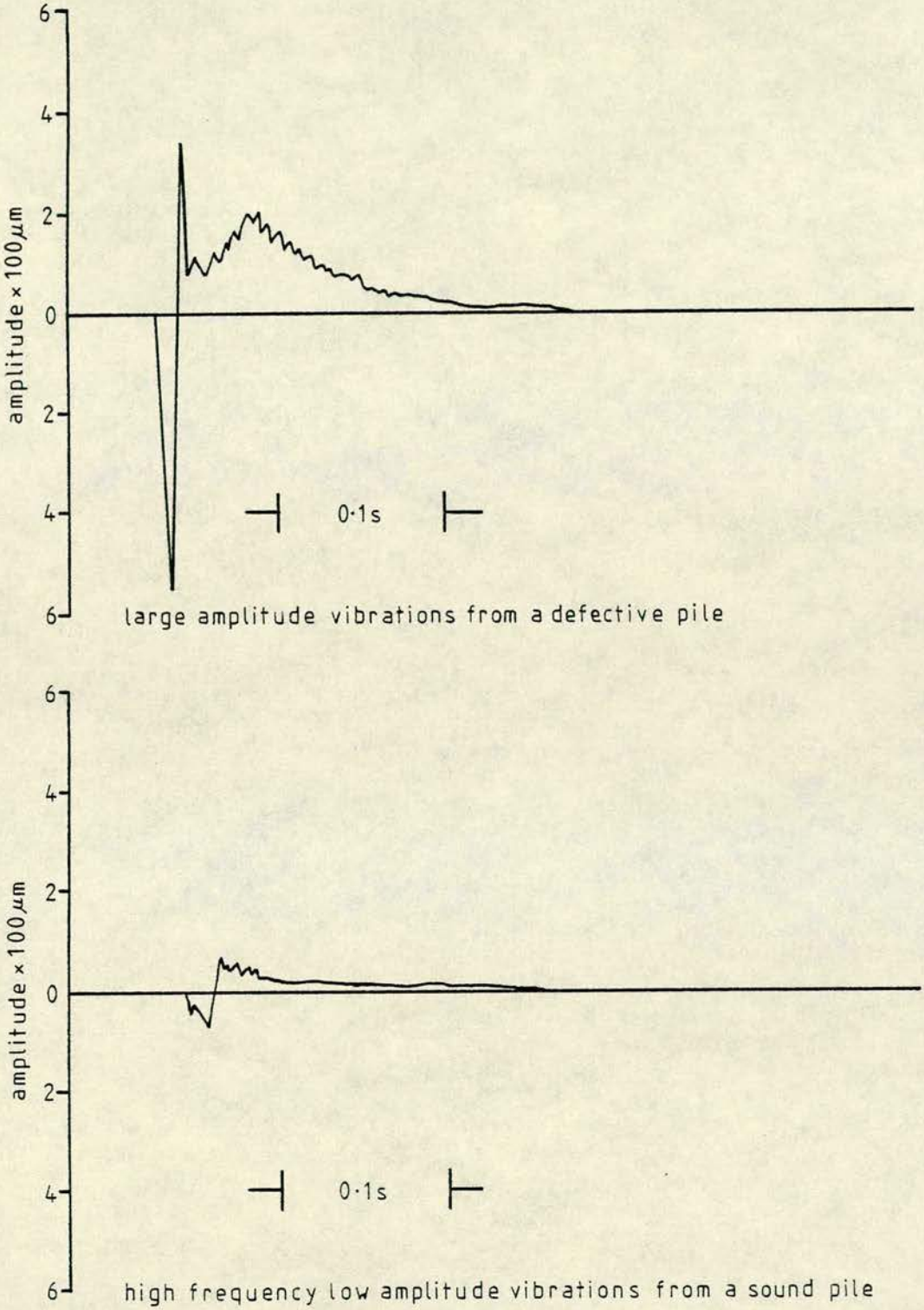

FIGURE 2.6

Vibrograms from a transient vibration test

(After Dvorak [28])

1: Requires experienced operator

2: Specialist interpretation necessary

3: Difficult signal analysis except in ideal conditions, e.g. end bearing precast pile through silt.

4: Case method applicable only to driven piles.

2.3.10 Sonic echo/stress wave[1,2,4,13,15,19,31,37]

This method employs a single hammer blow to the pile head, as in the transient vibration method above. An impulse travels down the pile and is reflected from the base.

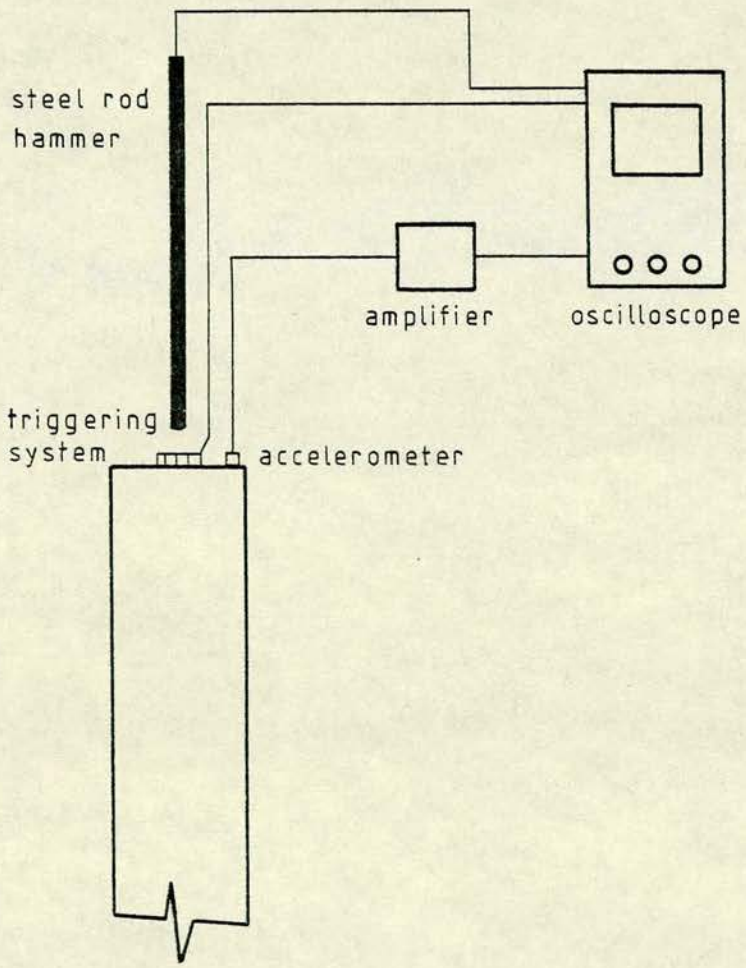

FIGURE 2.7

Diagram of stress wave echo test
(After Steinbach [31])

The velocity of sound in concrete and the echo time may be used to determine the length of the pile to the base or to a discontinuity. The method has been studied in France,[13,15,19,37] the U.S.A.,[31,32] and by the Institute T.N.O. in Holland.[34] Some successful tests have been made in the U.K. by Geophysical Prospection Services of Bristol. (Howell, 1978, private communication).

Advantages

1: Low cost

2: Rapid test, 30-50 piles per day

3: No preparation of pile head required.

Disadvantages

1: Requires experienced operator

2: Specialist interpretation

3: Experimental method - requires development.

Study of the response of concrete piles to a single hammer blow is the work reported in this thesis. A literature review of research and development of this method is given in chapter 3.

2.4 Discussion

Concrete foundation piles are prone to constructional defects which, because of limited access, are difficult to detect. Cast-in-situ piles where the casings are withdrawn are worst in this respect. The civil engineering/ construction industry thus has need of a simple and

inexpensive non-destructive test to assess the integrity of piled foundations. Experience suggests that if at all possible any test method should operate from the pile head with a minimum of prior preparation. At present there is no method which meets all the requirements economically. Correctly executed construction with thorough supervision is therefore a first essential in achieving sound piles. Integrity testing that does not involve loading gives no direct information about the behaviour of a pile under load. However, a low cost rapid test may yield information on a pile population as a whole. Such a test used in conjunction with a limited number of load tests will be statistically of greater significance than random load testing.

2.5 Conclusions

1: Defective piles may be avoided to a large extent by careful design and construction.

2: Defects which do occur are usually difficult to detect.

3: Load testing small numbers of piles, usually at random, is an inefficient way of detecting faulty piles.

4: None of the non-destructive tests presently available has an acceptable combination of accuracy and economy.

5: There has been little attempt at the coordinated use of load testing with non-destructive techniques.

6: Test results are generally viewed in the narrow context of the tested piles with no quantative prediction on the state of the pile group.

7: Electrical methods, transient vibration and stress wave/echo techniques merit further investigation.

3. TESTING BY SONIC ECHO

3.1 Introduction

The principle behind the sonic echo method of assessing pile integrity is straightforward. An acoustic pulse or stress wave is introduced to the pile head, generally by a hammer blow. The signal travels down the body of the pile and is reflected from the pile base or any discontinuity.

From the echo time and a knowledge of the velocity of sound in the concrete the length of continuous pile may be estimated.

The method is similar to that employed in testing engineering materials such as metals. A direct application of conventional materials testing techniques to concrete foundations is not possible, however. In testing metals it is common to use a train of waves containing a large number of sinusoidal periods of well defined frequency. In addition, the lateral dimensions of transmitters are large in relation to the wavelengths used and so a directional effect is obtained.[39] Such frequencies are very quickly attenuated in concrete and so cannot be used to test piles by a lengthwise transmission. This is doubly so in the case of an echo technique. A low frequency stress wave or pulse is therefore more appropriate.

3.2 Current progress in echo testing techniques

Several trials of the sonic echo method have been conducted with some limited commercial application.[13,14,31,32,34,37,40,41]

All observers record some difficulty in obtaining satisfactory echo signals. In some cases additional equipment is used to aid signal interpretation.[13,34] One investigator has suggested the use of several other parameters to augment the information gained from the simple echo time.[40,41]

The general technique appears to be of greater significance when used on a large number of nominally identical piles. A characteristic similarity between piles then becomes apparent and a deviant pile may be detected more easily.

The following sections contain a review of investigations currently being undertaken.

3.2.1 T.N.O.

A basic acoustic echo testing system has been developed and used with some success by the Institute T.N.O. for Building Materials and Building Structures at Delft, Netherlands.[34]

The equipment comprises:

(a) 5 kg hammer with integral trigger transducer.

(b) Acceleration transducer and pre-amplifier.

(c) Signal processor.

(d) Storage oscilloscope.

(e) Polaroid camera.

When the hammer hits the pile head the attached transducer triggers the oscilloscope. The signal from the acceleration transducer on the pile head passes through

the signal processor and is then displayed on the oscilloscope screen. After several recordings to ensure consistency the result is photographed for later interpretation.

The signal processor operates on the modulations from the acceleration transducer in three stages. The signal is integrated twice for the translation of acceleration into displacement. Bandpass filters are then employed to remove some noise frequencies. Finally an exponential gain amplifier is used to compensate for exponential signal attenuation in long piles.

The majority of tests have been conducted on driven piles of regular cross section. A sonic pulse velocity of 4000 m/s is assumed for location of the base echo. Some reflections have been obtained from cracks across a pile cross section. Generally it has been accepted that a pile is reliable provided that a substantial base echo is evident. An ideal signal is shown in fig. 3.1. This was obtained from a 24 m precast pile with no defects.

3.2.2 C.E.B.T.P.

A similar system to the T.N.O. method has been devised at the laboratories of the Centre Expérimental de Recherches et d'Etudes du Bâtiment et des Travaux Publics in France. [13,15,37]

The basic equipment consists of:

(a) Electrically powered hammer.

(b) Piezo-electric quartz transducer.

(c) Storage oscilloscope.

(d) Polaroid camera.

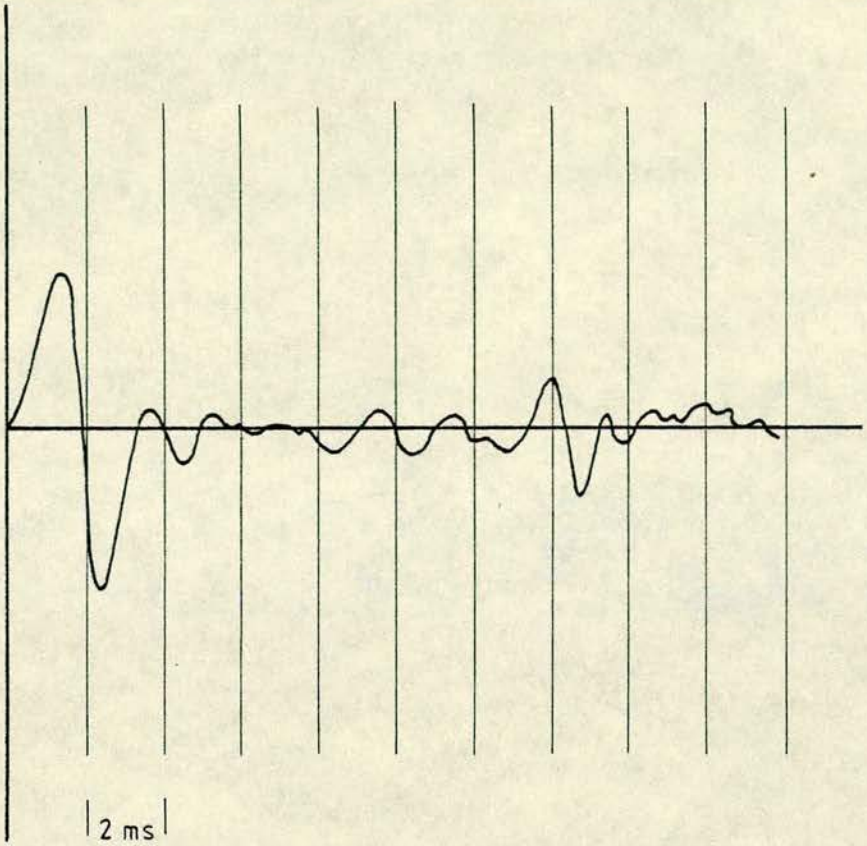

Fig. 3.1 End reflection from a 24 m precast pile (After Institute T.N.O. [34])

The hammer control system incorporates a switch for synchronised triggering of the oscilloscope. A value for the velocity of sound in the pile is obtained from transmission measurements on cubes cast from the pile mix or on core sections cut from the pile at the time of testing.

A typical signal is shown in figure 3.2. In cases of difficult location of the echo point, log amplitudes of the decaying waveform are plotted against time. Since the signal decay is exponential with time, the log plot reduces to a straight line. Any addition of energy from a reflected signal will be indicated by an inflection in

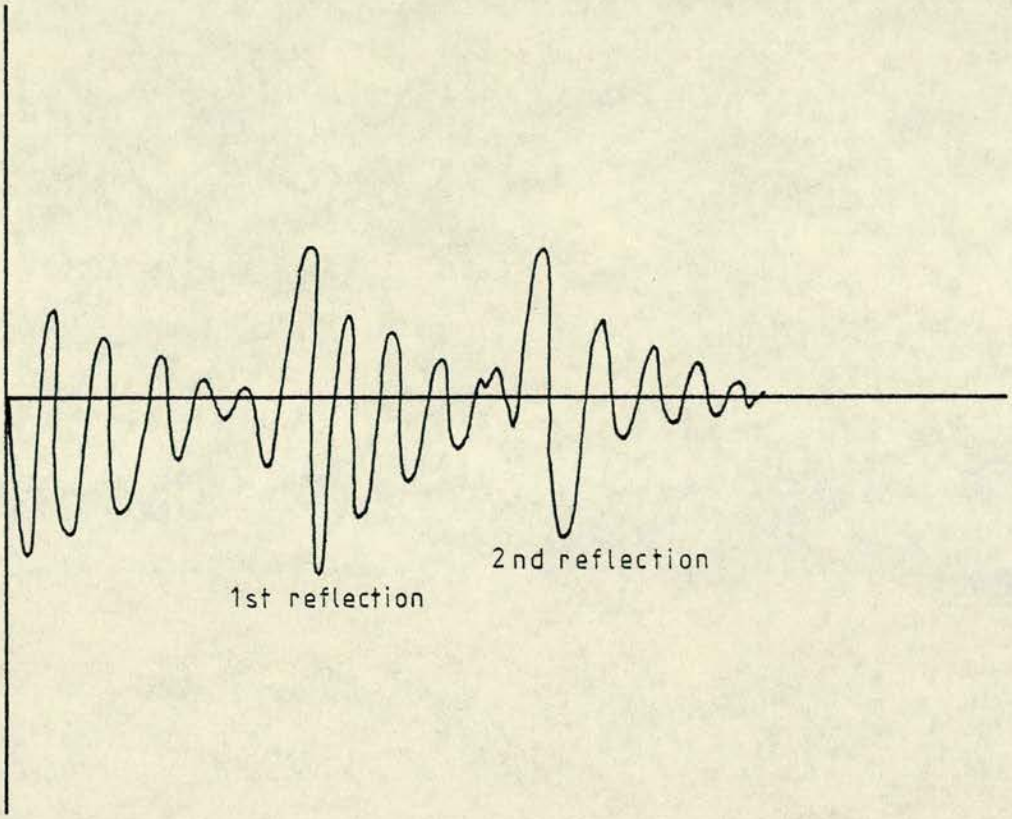

Fig. 3.2 Reflections from the free end of a precast pile (After Menou & Venec[37]).

the linear graph (see fig. 3.3).

Some later additions have been made to the equipment to aid signal interpretation. This takes the form of a signal processor unit containing the following elements:

(a) Mixing circuit to combine the signals from several receivers.

(b) An inverse filter to obtain deconvolution of the end oscillations.

(c) Exponential gain amplifier.

(d) Low pass filter.

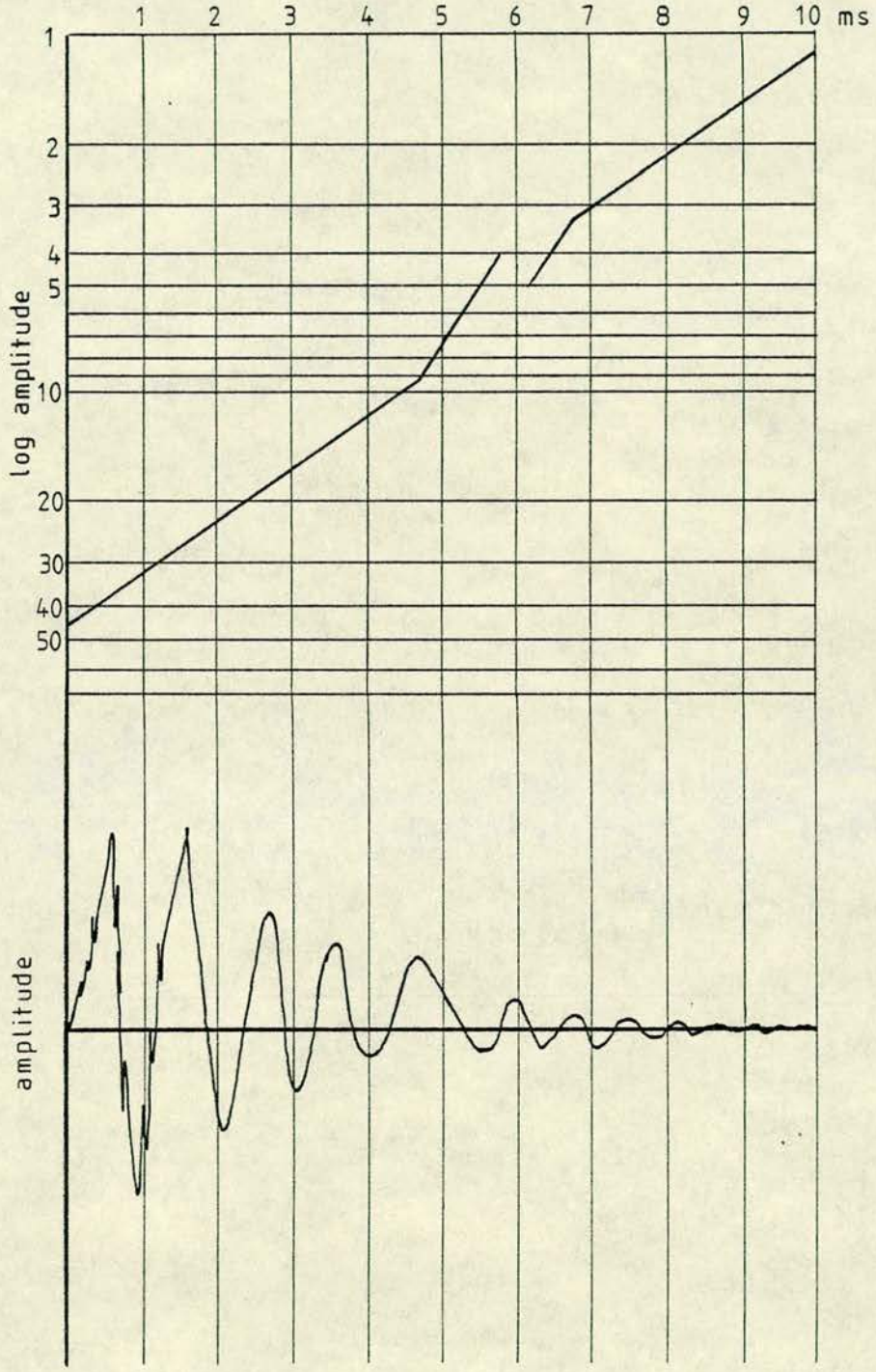

Fig. 3.3 Inflection on log amplitude/time graph caused by the arrival of a reflected signal. (After Menou & Venec[37]).

Several researchers[13,15,37] have evaluated the system and have recommended its use on steel piles and on precast piles up to a length of 15 m. It is generally accepted that beyond this depth the faintness of the echo signal leads to difficulty in its identification. Cast in situ piles have also presented problems because of multiple reflections stemming from the variable cross section.

3.2.3 Steinbach

A useful study of the method was conducted by Steinbach[31,32] at the Illinois Institute of Technology. The apparatus was simple and similar to that employed in the Dutch and French systems. This consisted of:

(a) Steel ball or rod as a hammer.

(b) Metal plate attached to the pile head and forming part of a trigger circuit.

(c) Accelerometer.

(d) Storage oscilloscope.

(e) Polaroid camera.

Laboratory tests were conducted on aluminium and concrete bars. Clear reflections were obtained and multiple reflections in the concrete specimens corresponded to a transmission of 37 m. For this reason the method was considered promising for use on long concrete members in the ground.

Field tests on construction sites showed that attenuation in buried specimens was markedly higher than

in free members. Generally only one reflection could be obtained. Frequently reflections were difficult to locate or did not exist. This was especially true in the case of the longer piles. Wide diameter piles were difficult because of interference due to surface waves of a frequency approaching that of the input pulse.

No signal processing was attempted except for the use of a simple low pass filter to reduce the level of higher frequency components mainly caused by end oscillations.

A typical trace showing multiple reflections is shown in fig. 3.4. This was obtained from a 7 ft. concrete rod buried in the ground.

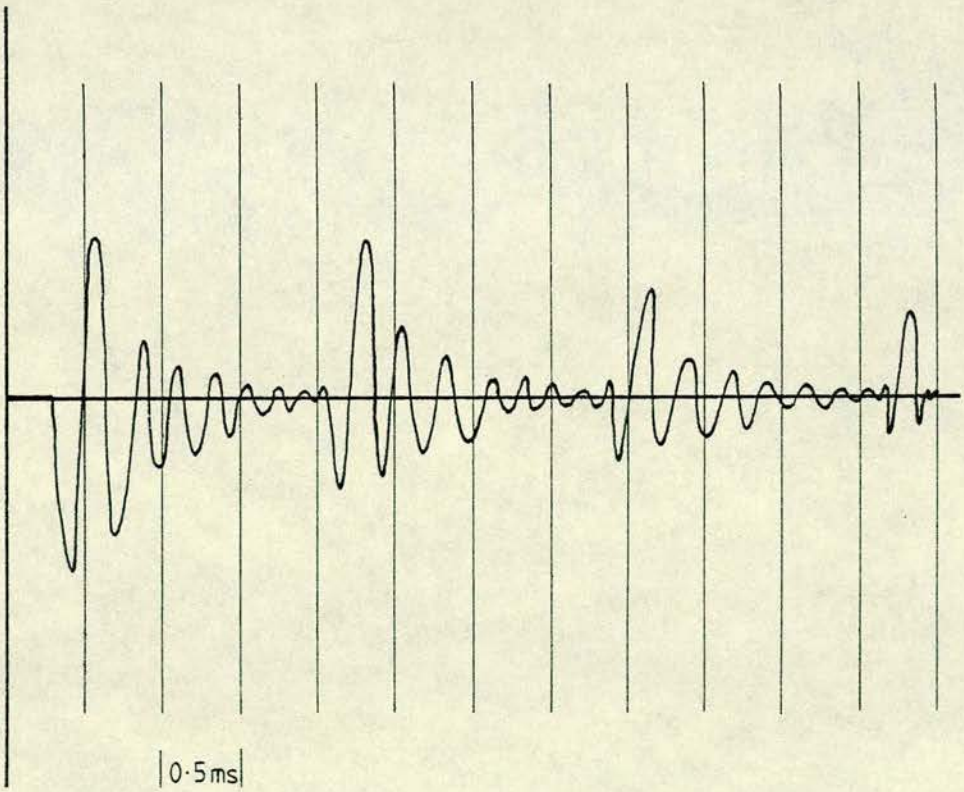

Fig. 3.4 Multiple reflections from a buried 7 ft concrete rod. (After Steinbach and Eben[32]).

The only measurable parameter employed in the testing programme was the echo time. Propagation velocity in the pile was obtained by timing a surface response between the hammer and the pick-up transducer. A conversion was then made to the longitudinal velocity by the equation:

$$V_L = C\ V_R \qquad \ldots\ldots \qquad (3.1)$$

where,

V_L = longitudinal wave velocity

V_R = surface wave velocity

C = constant varying from 1.84 to 1.96.

Clear reflections have been recorded from step tapered piles in excess of 30 m.

3.2.4 C.N.S. Electronics

Echo testing equipment has been developed in Britain by C.N.S. Electronics Ltd.[40] Much of the development work and research was done by Geophysical Prospection Services.[41] The equipment differs from the others slightly in the method of recording the signals. The following units are used:

(a) 6 kg hammer with 1 m guide shaft and conical striking piece.

(b) Transducer of moving coil type.

(c) Chart recorder.

The hammer is a 6 kg steel weight which may be retained at the top of the 1 m long guide shaft by a

spring loaded ratchet. When the weight is released it falls onto a conical nose cone at the base of the shaft. The point of the cone becomes embedded in the concrete after a few blows and then provides a good acoustic contact. The hammer system generally enables production of a consistent and repeatable impact. The cone also permits dry operation when the pile head is submerged in water.

The chart recorder will store a waveform until required for display on the chart. The signals may thus be monitored on an oscilloscope before a print out of the required signal is made. Magnification or reduction of the input may be made up to 256 times. The sweep rate may be set for A3 paper at 2, 4 or 8 ms/inch, or for A4 paper at 1, 2 or 4 ms/cm. The print out from the chart plotter makes measurement easier than from a polaroid photograph. However, the maximum sweep rate of 2 ms/inch (A3) or 1 ms/cm (A4) does not permit an expansion of the input pulse for more exact measurement, and several unwanted reflections may be obtained from short piles.

A propagation velocity of 4000 m/s is assumed for calculation of the reflection time where this cannot be measured directly. Extensive testing has shown the velocity to be generally in the region of 3500 m/s to 4500 m/s. For 28 day old concrete of a typical pile mix the velocity lies between 3800 m/s and 4200 m/s.

In addition to the reflection time several other

parameters have been devised to give a better assessment of pile integrity and the relationship between nominally similar piles on a site.

The complete range of parameters measured is:

(a)	Toe reflection time	RT
(b)	Decay rate	DR
(c)	System decay rate	SDR
(d)	Frequency	Fr
(e)	Impact/rebound ratio	I/Rb
(f)	Impact/reflection ratio	I/R
(g)	Reflection phase	RP
(h)	Return time	RtT

It is stressed in the equipment manual that a comparison of the results from all piles on a site can yield substantially more information than a study of single waveforms in isolation. The characteristic similarity of piles on a site may be readily observed by comparing all the measurable parameters.

The toe reflection time (RT) is the parameter upon which all the echo testing methods are based. A conversion of the reflection time to length using an assumed or measured propagation velocity indicates the intact length of pile to the reflecting surface. A typical signal showing a clear reflection is shown in figure 3.5. This was obtained from a 500 mm diameter bored cast in situ pile 20 m long.

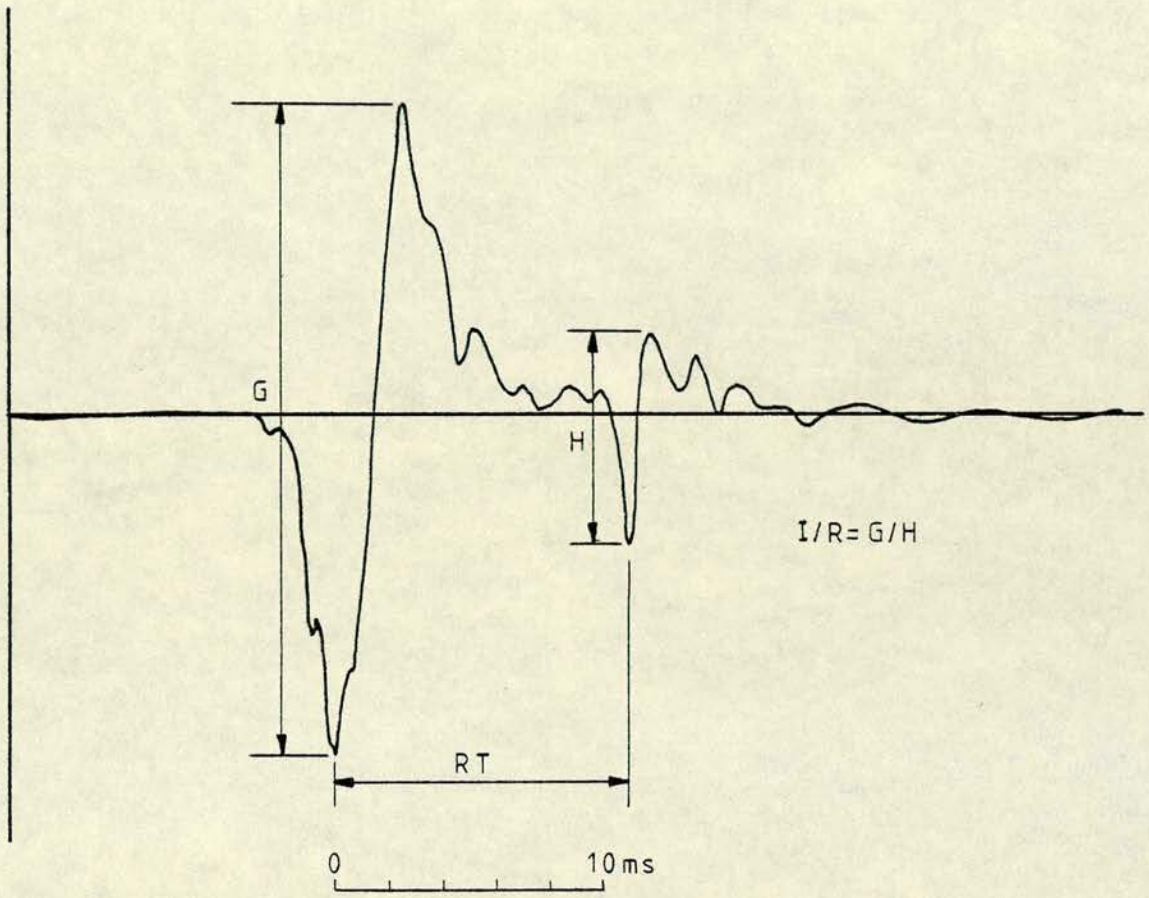

Fig. 3.5 Reflection from the base of a 20 m cast in situ pile. (Courtesy of C.N.S. Electronics Ltd.)[40]

The reflection time may be measured from some convenient point on the input signal to a corresponding point on the reflection.

The decay rate (DR) is a measure of the exponential decay of the impact oscillation. This is obtained as indicated in fig. 3.6.

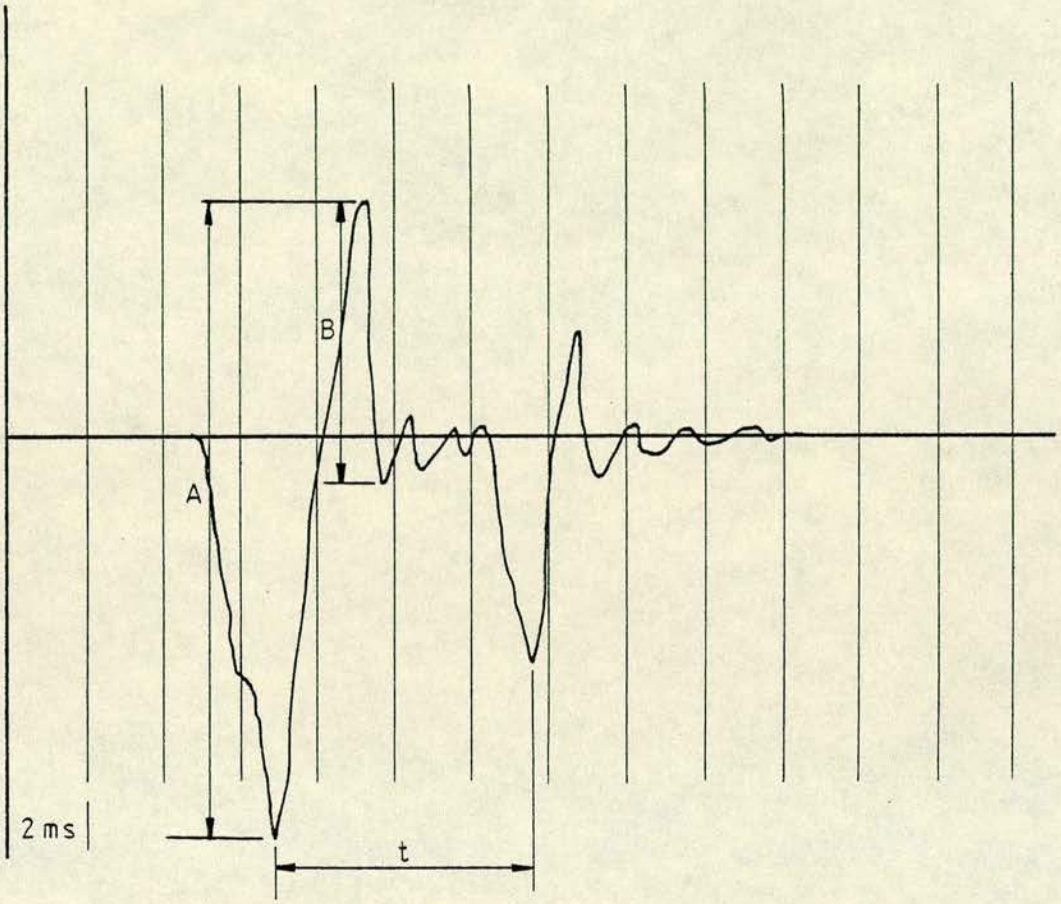

Fig. 3.6 Decay rate of the impact oscillation (Courtesy of C.N.S. Electronics Ltd.)[40]

$$DR = \frac{20 \log\left(\frac{A}{B}\right)}{t} \quad \ldots\ldots \quad (3.2)$$

The units are decibels per second (dB/s).

The system decay rate (SDR) is measured in a similar fashion as shown in fig. 3.7.

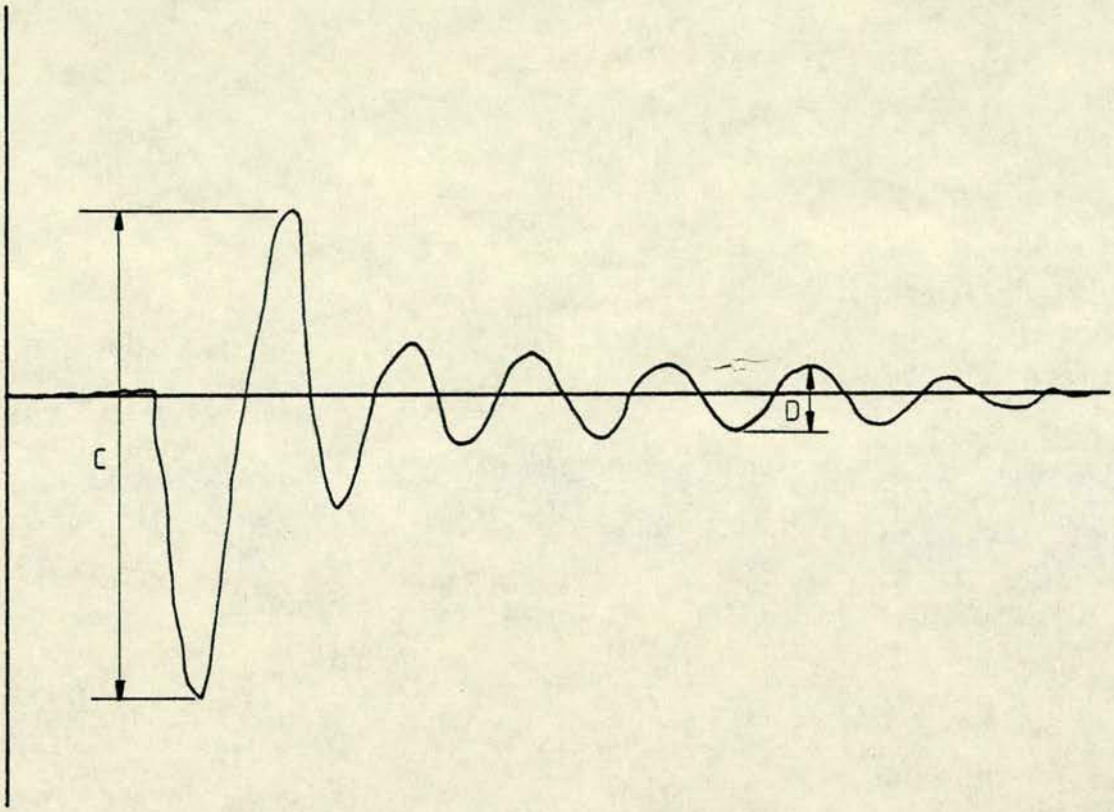

Fig. 3.7 Decay rate of the oscillating pile/soil system (Courtesy C.N.S. Electronics Ltd.)[40]

$$SDR = \frac{20 \log \left[\frac{C}{D}\right]}{t} \quad \ldots\ldots \quad (3.3)$$

The second peak to trough amplitude (D) should be measured at approximately 1.5 times the expected reflection time, so that the reflected signal is well separated from the decay measurement. In the system decay rate (SDR) the reflections within the pile and the effect of the surrounding soil modify the result compared to the decay rate (DR).

The frequency (Fr) in Hz is the total number of profile maxima or minima in the decaying oscillations minus one and divided by the time. The frequency gives an indication of the elasticity and density of the concrete at or near the pile top. The range for normal 28 day concrete is given as between 450 Hz and 780 Hz.

The impact/rebound ratio (I/Rb) is the vertical distance through which the concrete is displaced below its rest position divided by the distance it rises above the rest position on the first rebound. (fig. 3.8)

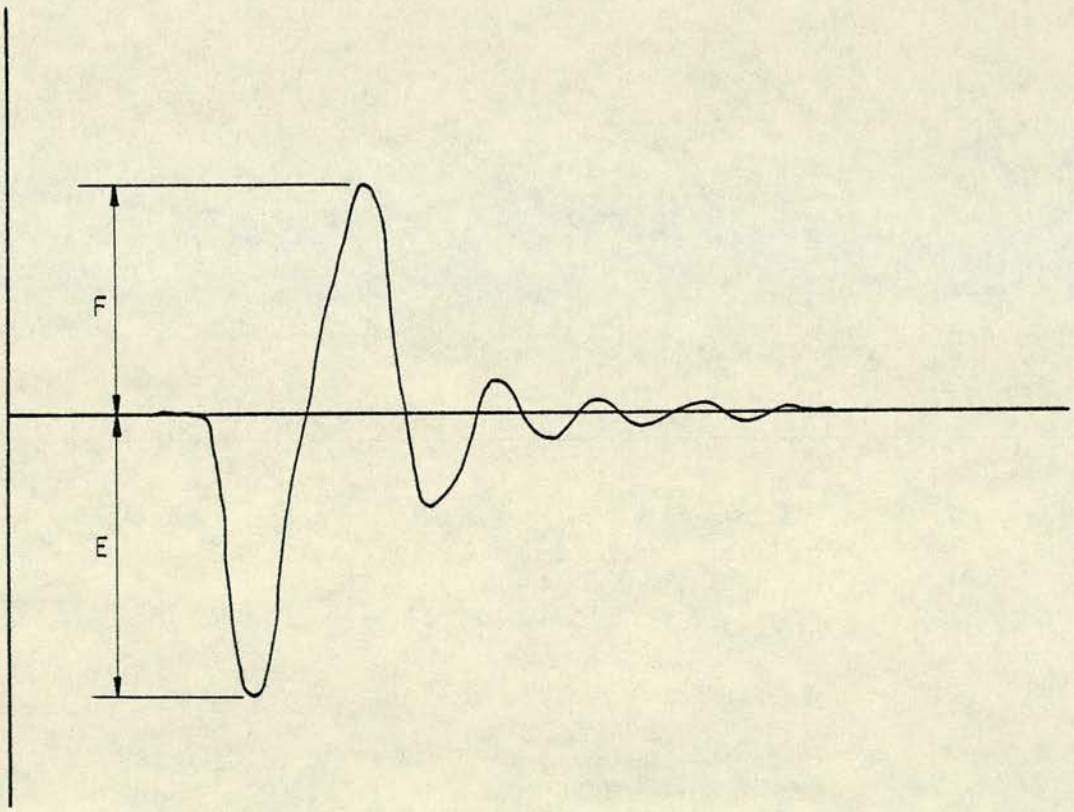

Fig. 3.8 Impact rebound ratio
(Courtesy of C.N.S. Electronics Ltd.)[40]

$$I/Rb = \frac{E}{F} \quad \ldots\ldots \quad (3.4)$$

This ratio is governed by the density and elasticity of the concrete at the pile top.

The impact/reflection ratio (I/R) may be measured on profiles such as fig. 3.5. The first trough to peak amplitude of the impact is divided by the first trough to peak amplitude of the reflection

$$I/R = \frac{G}{H} \quad \ldots\ldots \quad (3.5)$$

The impact/reflection ratio will be affected by the nature of the footing and by the degree of attenuation of the signal in the pile and by the soil.

The reflection phase (RP) will depend on the nature of the pile base. A free end such as on a friction pile founded in an acoustically less dense medium will produce a displayed reflection in phase with the impact waveform. An end bearing pile founded in rock will result in an out of phase reflection. (see chapter 6, p 141).

The return time (RtT) is the bounce interval of the hammer as it rebounds from the nose cone. This parameter is related to the bulk modulus or resistance to deformation of the concrete and should be substantially constant for piles of the same cross section and concrete mix.

3.3 Discussion

The sonic echo test for pile integrity has proved to be a rapid and low cost method within the limitations of present expertise and equipment. Skilled operation of

the testing apparatus is advisable and specialist interpretation of waveforms may often be required.

The several systems described previously are virtually identical in operation and sophistication of signal treatment, the differences being merely in equipment detail. Waveforms containing echo signals are essentially similar in all the methods, even though in some cases a degree of signal processing has been employed. Less clear signals showing ambiguity or lack of an echo also display similarities throughout the four methods. Two common signals which make interpretation difficult or impossible are:

(a) Absence of any echo signal.

(b) Echo signal masked by other oscillations received at the pile top.

Piles of small length to diameter ratio commonly produce the most difficult signals.

The maximum depth to which a successful test has been made is a little over 30m.[31,32] This is somewhat at variance with the claim by French researchers that the maximum depth to which useful testing may be conducted is 15 m. Tests on concrete beams[31,32] indicate that depths well in excess of 30 m should be possible especially in the case of piles of uniform cross section.

Determination of the propagation velocity can never be exact, and therefore only an approximate length may be given to a tested pile, but indirect methods of

measuring the velocity, such as cubes, cores or across the pile head can be sufficiently accurate. In the case of friction piles the length is not of crucial importance. For end bearing piles, a phase change in the reflected signal is excellent evidence that the pile has reached the bearing stratum.

It is generally accepted that the geometry of a pile and the nature of the soil contact will influence the amplitude and form of a reflection. In most cases, however, the reasons for the non appearance of an echo signal are not clear. Testing personnel are frequently unable to explain such waveforms. Some laboratory research has been conducted,[31,32] but this aspect is by no means exhausted. Other researchers have made field tests on piles with known irregularities,[13,15,34,37] and have obtained some limited correlation with the received signals.

The design and selection of equipment must be an important factor in successful testing, particularly in the area of signal processing. In some cases choice appears to have been arbitrary. There are four distinct parts to any echo testing system:

(a) The signal generation device (hammer).

(b) Receiver.

(c) Signal processor (if included).

(d) Display unit.

Some research appears to be required to determine the most suitable impact and how this may best be achieved.

Experience indicates that the most suitable signal may vary with pile geometry. Consistency throughout repeated blows should be attainable.

The type of receiving device does not seem to have a great influence on the waveforms since researchers using different devices have obtained broadly similar results.

The general requirements are:

(a) Sensitivity in the frequency range of received signals.

(b) Absence of natural vibrations at these frequencies.

The extent of signal processing can only be determined accurately through exhaustive research. Several areas in which electronics might be applied are:

(a) Filtering.

(b) Amplification.

(c) Addition of signals.

(d) Correlation between impact and reflected signals.

The method of signal display is a matter of preference. A storage oscilloscope with a polaroid camera is quite convenient. A chart recorder producing a paper print is cheaper in running costs. The operator may still feel the need for an oscilloscope to monitor signals, thus adding an extra item to the system.

In many instances it may prove difficult to interpret the signal from one pile in isolation. When viewed in the context of the overall pattern obtained from a site

the task may become easier. This concept of characteristic similarity between nominally identical piles is important. The comparison of many measured parameters, as suggested by one researcher,[40,41] is therefore a valuable technique.

3.4 Conclusions

1: The four systems examined are very similar in equipment and the form of received signals.

2: The technique in its present state of development is most useful for testing thin piles of regular cross section.

3: It appears feasible that the range may be extended beyond the 30m maximum depth reached so far.

4: Research is required to determine the most suitable form and range of signal generation.

5: A more extensive knowledge of sound transmission in long concrete members is indicated.

6: Additional research is needed before the most suitable form of signal processor may be produced.

7: The concept of characteristic similarity across a wide range of parameters is valuable.

4. PRELIMINARY FIELD TESTS

4.1 Introduction

In order to gain an insight into the sonic echo method of pile testing, a series of field trial tests were conducted on full-scale piles on a number of construction sites.

The philosophy behind the exercise was two-fold. Firstly, to examine the practicalities of site testing and the technique of signal waveform interpretation, and to correlate these with other workers' findings. Secondly, to identify possible problems and limitations of the method and to establish areas for theoretical and practical research.

In addition, a set of records from full-scale piles was obtained for subsequent analysis and comparison in parallel with the other experimental work.

4.2 Equipment

The choice of equipment was based on the four systems reviewed in chapter 3. The main consideration was to keep the items simple and easily portable in a system which could operate without any prior preparation of the piles.

The equipment consisted of:

(a) 4.5 kg rod used as a hammer

(b) 30 mm diameter piezo electric transducer (cased)

(c) 30 mm diameter piezo electric transducer (uncased)

(d) Silicon grease

(e) Tektronix 7632 storage oscilloscope

(f) Polaroid camera

(g) Portable generator.

4.3 Operation

A transducer was attached to the pile head and connected to the oscilloscope by screened cable. A suitable flat area on the pile head could be conveniently obtained by pounding the concrete with the hammer until smooth. Silicon grease was then used to achieve a good acoustical contact. With the oscilloscope sweep made ready the hammer was dropped from a measured height onto the pile head. Triggering of the oscilloscope sweep was from the input signal. In the early field tests the initial part of the trace of the input pulse was lost, due to late triggering of the oscilloscope, but satisfactory measurements could still be obtained. This problem was overcome for the more accurate laboratory work by the use of a separate trigger transducer adjacent to the hammer-pile head contact (section 7.4.2). This system was not adopted for the field work in the interests of simplicity.

After several runs to ensure consistency of the signals, a typical signal trace was photographed for later interpretation. The signal amplitude and sweep rate are printed on the display. On several tests, a second transducer was cast into the base of a pile to monitor the arrival of the hammer pulse. This signal is shown on

the lower trace of the display (fig. 4.1). Each photograph is identified by a number on the lower surround, and the photographic records from the tests are given in appendix 2.

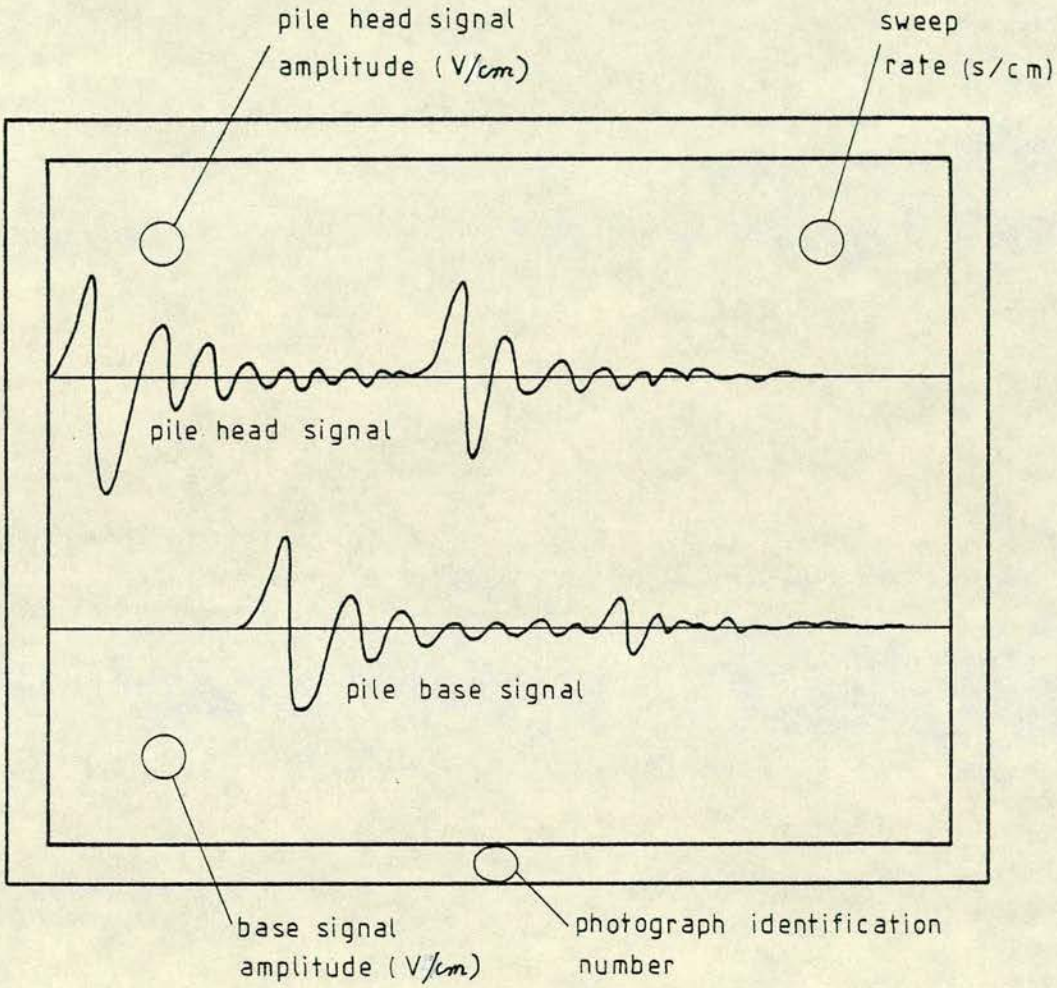

Fig. 4.1 Photograph record of oscilloscope display

4.4 Results and analysis

Testing was conducted on two sites. Two short cast in-situ piles were made available at the underpinning of local authority houses in Kelso. Thirty-five West shell piles and twelve cast in-situ retaining wall piles were

tested at the IBM factory extension in Greenock. Access to the sites was by arrangement with the sponsoring body.

4.4.1 Kelso

Two cast in-situ piles of 200 mm diameter were tested. The 4.5 kg rod was used from a drop height of 500 mm. The signal traces are shown in photographs 1 and 2, and measurements from the photographs in table 1. Pile 1 was tested 24 hours after casting. The concrete had thus only achieved a fraction of its final strength. The signal was weak with a characteristic slow rise to the front of the input signal. Pile 2 was tested 3 days after casting. The input signal was stronger and of shorter period. No echo signal could be detected in either pile with certainty. These piles were short, 2.5 m and 3.0 m, and hence any base reflection would be obscured by the input signal oscillations.

4.4.2 Greenock shell piles

Thirty two shell piles of 406 mm diameter and varying lengths, were tested using the 4.5 kg hammer rod from a height of 500 mm (photographs 3 - 34). Measurements taken from the photographs are given in table 1. In most cases a base reflection is evident. Using the contractor's measured depth of the pile cores, the velocity of propagation was calculated for each pile, giving values of from 3167 m/s to 5272 m/s.

Where possible, additional parameters were measured following the form of analysis due to Geophysical Prospect-

ion Services,[41] as described in section 3.2.4. The measurements where taken show some fluctuation, particularly those based on the input signal.

A further three shell piles of 406 mm dia. and 10 m in length were tested at this site. A transducer was cast into the base of each pile to detect the arrival of the transmitted signal. A drop height of 1 m was employed. Only in one instance was a possible reflected signal evident at a time corresponding to twice the transmission time (photograph 36). Comparing the amplitudes of the base signal and the input signal it may be seen that substantial attenuation occurs after one travel through the pile. If similar attenuation occurs on the return journey, which is reasonable, then the amplitude of the reflected signal would be of the order of 1 mV amplitude and not the 10 mV amplitude of the apparent reflection. The results in photographs 35 and 37 present an even worse case for the amplitude level of a reflected signal. The supposition is either that the base transducer did not register at the sensitivity of the pile head transducer, or that the reflected signal was too weak to detect. If the latter were the case, then signals designated as echos in these and other tests are due to some other cause. It is considered likely, however, that the base transducers had a reduced sensitivity. These transducers were necessarily cased in insulating tape to attach the signal leads, by which means they were also lowered down the pile shaft.

In addition it was difficult to control the attitude of a transducer as the concrete was poured onto it.

4.4.3 Greenock retaining wall piles

A number of 10 m × 1 m diameter piles were contiguously cast to form a retaining wall on the same site. Several of these piles were tested using the 4.5 kg hammer from a drop height of 1 m, (photographs 38 - 73). A base transducer was cast into pile 6 and records were taken with the transducer and impact point in various locations, (photographs 43 - 65). Measurements from the photographs are given in table 2.

A reflected signal was apparent on most of the waveforms. Only in two cases was a possible reflected signal identified at approximately twice the transmission time on pile 6. The base transducer signal was very weak with a probable explanation as discussed above.

The measurements of the transmission times from a variety of transducer/hammer separations show a discrepancy which is due to the time of travel of the initial surface wave from the impact location to the transducer. If the average transmission time with the impact point close to the hammer is taken as a standard time, (photographs 43, 49, 55, 60, 65), then a correction may be made for the input delay by adding the surface wave transit time. The velocity of the surface wave may be obtained by the conversion as used by Steinbach,[31,32] (equation 3.1).

Here, for instance:

$$v_R = \frac{v_L}{1.9}$$

where,

v_R = velocity of the surface wave

v_L = longitudinal velocity along the pile

$$\rightarrow \quad v_R = \frac{3906}{1.9}$$

$$\doteqdot 2000 \text{ m/s} .$$

The corrected transmission times show a closer correspondence, but they should, of course, be equal. The maximum error due to non-allowance for the surface wave delay is approximately 20%.

Change of location of either the hammer or transducer resulted in a different pattern to the signal oscillations. This suggests that the majority of the oscillations succeeding the input pulse are due to pile head motion. Reflections from further down the pile body would arrive in phase and so appear at the same point on the trace.

4.5 Discussion

The signal waveforms recorded during the tests generally were of the form obtained by other workers, [13,14,31,34,37,40] (figs. 3.1 - 3.4). There is rarely a simple trace displaying the input signal followed by a discrete reflection at the appropriate time. Additional signals

from pile head oscillations and multiple reflections from irregularities in the pile cross section tend to obscure the base reflection which is of low amplitude due to attenuation. Reflections from cross section irregularities are of the same wavelength as the base reflection, leading to further difficulties of identification. In the case of very short piles the returning signal becomes involved with the input signal when the time separation is not sufficient.

From the tests with base transducers it is evident that a signal does reach the pile base in a recognisable form, although heavily attenuated according to the length of the pile.

Change in location of the hammer or transducer produced notably different waveforms leading to the conclusion that much of the interfering signals stem from pile head oscillation. If this is the case, then there appears to be scope for a correlation technique based on addition of a series of input pulses with the hammer and/or transducer at varying locations on the pile head. The in phase base reflection would then be reinforced in the presence of the randomly distributed surface effects. Such a technique would not deal with reflections from cross section irregularities since these in phase signals would also be amplified by the correlation addition.

Further substantial research of the method appears warranted as a preliminary to the development of any equipment for signal processing. This would involve a

general review of concrete testing by acoustical methods, the measurable parameters involved, and how these are influenced by variables such as the mix, age, curing conditions and reinforcing steel.

The special case of acoustic propagation in rods is applicable to foundation piles and therefore merits investigation. Several types of wave propagation, with different velocities and propagation characteristics may be generated by the pile head impact. Further study of this aspect is required to clarify the position. In addition, the nature of reflecting surfaces both in the pile body and at the base should be studied to discover their effect on the incident pulse.

An experimental investigation of the method is necessary to determine the relevance of the theory and to establish precepts for equipment design. Such an investigation should be undertaken independently from the additional variables of attenuation due to the soil and from the interfering effects of the irregular cross-section of a cast-in-situ pile.

4.6 Conclusions

1: The field work results have shown a close correspondence with other workers' findings.

2: Signal waveforms are generally complex and rarely display a simple input pulse followed by one base reflection.

3: Reflected signals where present are very weak due to attenuation in the concrete and from the damping effect of the soil.

4: The base reflection is often obscured by pile head oscillations and/or reflections from cross section irregularities.

5: In the case of very short piles (<5m) the reflected signal may be eclipsed by the input signal.

6: An electronic correlation technique based on addition of signals from different hammer and transducer locations could amplify the base reflection in the presence of random interference.

7: Further theoretical research is warranted in the areas of the acoustical behaviour of concrete and the special case of pulse generation and propagation in rods.

8: An experimental investigation is proposed to relate the theoretical treatment to the present experience gained in the application of the method.

5. ACOUSTIC TESTING OF CONCRETE

5.1 Introduction

In common with many construction materials the continuity and consistency of strength of structural concrete cannot be guaranteed. Conventional destructive tests are limited to representative components or test pieces such as cubes. Hence it has been necessary to develop a non-destructive method of in-situ testing to assess the quality and integrity of structural members. In 1938 Powers[42] published the first comprehensive report on the application of sound as a non-destructive test for concrete. Since then the acoustical testing of concrete has proceeded with the study of three important parameters.[43-47]

1: The resonant frequency of vibration of a member.[42,48,49]

2: The velocity of propagation of sound through the material.[50-62,74]

3: The rate of decay of a transmitted signal or vibration.[43,44,52,63,64]

Concrete is a variable combination of several materials formed under a variety of conditions. A knowledge of how these variables affect the behaviour of sound in the material is essential to the application of acoustic testing.

5.2 Measurable Parameters in Acoustic Testing of Concrete

5.2.1 Resonant frequency

The frequency of external impulse applied to a specimen may be adjusted to produce resonant standing waves. Resonance may be transverse, longitudinal or torsional. Generally, a formula relating the dynamic modulus of elasticity to the resonant frequency is employed.

5.2.1(a) Transverse vibrations

The elastic modulus may be obtained from the resonant frequency for transverse vibrations by a formula of the form:[52]

$$E_d = Cwf^2 \quad \ldots\ldots \quad (5.1)$$

where,

E_d = dynamic modulus of elasticity

w = weight of the specimen

f = a resonant frequency

C is a factor which depends on the specimen dimensions, Poisson's ratio and the mode of vibration (fundamental or harmonic).

An appropriate value for C has been the subject of much research and discussion. Pickett[48] has analysed the theoretical basis for the establishment of a value for C. Before C may be evaluated the frequency equation must be known. This equation relates the resonant frequency to the dimensions, density and elastic properties of a specimen. The mathematical derivation of the frequency

equation will depend on the boundary conditions and the form of the differential equation describing the transverse vibration of a prismatic beam. Several differential equations may be considered. The elementary equation is:

$$\frac{E_d r_z^2}{\rho}\frac{\partial^4 v}{\partial x^4} + \frac{\partial^2 v}{\partial t^2} = 0 \quad \ldots\ldots \quad (5.2)$$

where,

ρ = density

r_z = radius of gyration with respect to centroidal z axis.

v = displacement in the y direction

x = coordinate in the direction of length

t = time

Rayleigh[65] has given this equation with a term to correct for rotary inertia, while Love[66] has added a term to correct for lateral inertia. This latter term is never of great importance and is zero for prisms of square cross-section. Another equation has been used by Mason[67] and Thompson[68] including a term to correct for both lateral and rotary inertia. Pickett considers this of doubtful value due to an inadvertent use of a wrong sign. The following equation by Timoshenko[69-71] corrects for the effects of shear and rotary inertia:

$$\frac{E_d r_z^2}{\rho}\frac{\partial^4 v}{\partial x^4} + \frac{\partial^2 v}{\partial t^2} - r_z^2\left(1 + \frac{E_d}{kG}\right)\frac{\partial^4 v}{\partial x^2 \partial t^2} + \frac{r_z^2 \rho}{kG}\frac{\partial^4 v}{\partial t^4} = 0 \quad \ldots\ldots \quad (5.3)$$

where,

G = modulus of rigidity (shear modulus of elasticity).

k = a constant introduced by Timoshenko to account for the effect of shear on the slope of the elastic line.

Pickett suggests a value of $k = 8/9$ for concrete prisms and cylinders.

Goens[72] has given a solution for the frequency equation based on Timoshenko's differential equation. (Equation 5.3). The following relationship may then be deduced:

$$E_d = \frac{4\pi^2 f^2 \rho \ell^4}{r_z^2 k^4} \quad \ldots\ldots \quad (5.4)$$

where,

ℓ = length of the specimen

k = a constant which depends on Poisson's ratio, the relation of dimensions of the specimen in the three axial directions, and the mode of vibration.

From equations (5.1) and (5.4):

$$c = \frac{4\pi^2 \ell^3}{gIk^4} \quad \ldots\ldots \quad (5.5)$$

where,

g = acceleration of gravity

I = moment of inertia of the cross-section.

5.2.1(b) Torsional vibrations

Prisms and cylinders may vibrate in torsion as well as transversly or longitudinally. Torsional vibrations are often confused with transverse vibrations. Pickett[48] gives a general formula for shear modulus, corresponding to equation (5.1) for transverse vibrations, as:

$$G = BW(f')^2 \quad \ldots\ldots \quad (5.6)$$

where,

f' = a torsional resonant frequency

$B = \frac{4\ell R}{gAi^2}$

A = cross-sectional area

i = unity for first mode, two for second mode, etc.

R = ratio of polar moment of inertia to the shape factor for torsional rigidity (1 for a circular cylinder, 1.183 for a prism of square cross-section).

Poisson's ratio for a homogeneous isotropic solid is related to E_d and G by the equation:

$$\sigma = \frac{E_d}{2G} - 1 \qquad \ldots\ldots \qquad (5.7)$$

where,

σ = Poissons ratio

or, from equations (5.1) and (5.6):

$$\sigma = \frac{C}{2B}\left(\frac{f}{f'}\right)^2 - 1 \qquad \ldots\ldots \qquad (5.8)$$

Therefore Poissons ratio may be determined dynamically if the specimen is sufficiently homogeneous and isotropic. A lack of homogenity resulting from differences in the elastic properties of the constituents of concrete does not appear to affect the validity of equations (5.7) and (5.8).[48] Equation (5.8) may have little meaning if the specimen has been weakened by frost action or cracking resulting from excessive shrinkage or thermal action.[49] Equation (5.8) is not applicable to reinforced concrete.[48]

5.2.1(c) Longitudinal vibrations

The modulus of elasticity may also be obtained from longitudinal resonance using the following equation:[65]

$$E_d = \frac{4\ell^2\rho(f'')^2}{i^2} \qquad \ldots\ldots \qquad (5.9)$$

where,

f'' = a longitudinal resonant frequency.

Equation (5.9) is derived from the basic differential equation for the motion of a bar vibrating in the longitudinal mode:[65]

$$\frac{d^2u}{dt^2} = \frac{E_d}{\rho} \frac{d^2u}{dx^2} \qquad \ldots\ldots \qquad (5.10)$$

where,

u = displacement in the x direction.

This equation ignores the effect of lateral inertia. If this effect is accounted for equation (5.9) is modified to:[73]

$$E_d = \frac{4\ell^2\rho(f'')^2}{i^2\left(\ell - \frac{i^2\pi^2\sigma^2r^2}{\ell^2}\right)} \qquad \ldots\ldots \qquad (5.11)$$

For specimens of the size normally used in testing, and vibrating in the fundamental mode the additional term gives a correction of around 1 per cent and can be neglected.[44] For longer members such as piles the term will become more important.

The frequency of longitudinal vibrations will be higher than the frequency of vibrations in the transverse or torsional modes. It is often difficult to produce pure longitudinal vibrations in a member and the fundamental frequency can be confused with higher harmonics of the other forms of vibration.

5.2.2 Velocity of propagation

A second, and more widely used, sonic test of concrete quality makes use of the velocity of propagation of sound through the material. When a solid is exposed to mechanical action elastic waves will propagate through

the material. The velocity of propagation will depend on the properties of the material and on the nature of the source. In an infinite body of homogeneous and isotropic nature two types of wave propagation, longitudinal and transverse, are possible. In finite bodies a third type of wave will develop at the boundaries of the material, and is referred to as a surface or Rayleigh wave.

Longitudinal wave transmission is virtually always used in concrete testing as this wave has the highest velocity and therefore arrives first at a receiving device. The other waveforms can obscure measurements of the longitudinal wave and thus a knowledge of the various velocities is important. Surface waves are sometimes used in particular circumstances where a longitudinal wave is difficult to detect.

5.2.2(a) Longitudinal waves

When longitudinal waves pass through a material in bulk form, the reactions of the non-radiated part of the material on the lateral boundaries of the beam of sound must be considered. These reactions produce shear stresses in addition to the compressive and tensile stresses associated with the waves. The acoustic velocity of plane longitudinal waves will thus be a function of both the bulk modulus and the shear modulus, i.e.:

$$c_\ell = \sqrt{\frac{K + 4/3G}{\rho}} \qquad \ldots\ldots \qquad (5.12)$$

where,

c_ℓ = velocity of longitudinal wave

K = bulk modulus

According to Love[66] the velocity of longitudinal waves in an infinite medium can be found from:

$$c_\ell = \sqrt{\frac{E_d \quad (1-\sigma)}{\rho\,(1+\sigma)\,(1-2\sigma)}} \qquad \ldots\ldots \qquad (5.13)$$

or:

$$c_\ell = \sqrt{\frac{\lambda+2\mu}{\rho}} \qquad \ldots\ldots \qquad (5.14)$$

where,

λ and μ = Lamé's constants.

When the medium is of finite extent in one direction, a plate for example, and the thickness is so small that expansion and contraction at right angles to the surface can take place freely, the velocity of longitudinal waves may be expressed as:[52]

$$c_\ell = \sqrt{\frac{E_d}{\rho(1-\sigma^2)}} \qquad \ldots\ldots \qquad (5.15)$$

In the case of rods where the cross-sectional area is such that transverse deformations do not influence the propagation of the wave, equation (5.15) simplifies to:

$$c_0 = \sqrt{\frac{E_d}{\rho}} \qquad \ldots\ldots \qquad (5.16)$$

This velocity is known as the 'bar velocity' and is approximately 0.9 times the value for propagation in an unbounded medium. This equation derives from an elementary theory of longitudinal wave propagation in a cylinder and is sufficient for general concrete testing. It is assumed that stress at any cross-section is uniform and purely axial, plane cross-sections remaining undistorted by the motion. Wave propagation in cylinders is treated in greater depth in chapter 6 (page 87).

5.2.2(b) Transverse waves

Where a pure shear stress acts on a material only shear strains are involved and the appropriate elastic modulus is the shear modulus or modulus of rigidity.

The velocity of plane transverse waves in a solid are then given by the expression:

$$c_t = \sqrt{\frac{G}{\rho}} = \sqrt{\frac{E_d}{2\rho(1+\sigma)}} \quad \ldots\ldots \quad (5.17)$$

where,

c_t = velocity of transverse waves

or

$$c_t = \sqrt{\frac{\mu}{\rho}} \quad \ldots\ldots \quad (5.18)$$

The characteristic feature of transverse waves is that directions of displacement and propagation are at right angles. The propagation velocity of transverse or

shear waves in an infinite body is about 0.55 times that of longitudinal or compressional waves.

5.2.2(c) Rayleigh waves

A third type of wave is found which affects only particles at or near the surface of a material. Such waves have been treated mathematically by Rayleigh.[65] The velocity of propagation of these waves is about 0.5 times that of longitudinal waves in an unbounded medium, i.e. slightly less than the velocity of transverse waves. This can cause some difficulty in distinguishing between transverse and surface waves.

The particle motion in surface waves is elliptical with amplitude decreasing exponentially with distance from the surface. The horizontal displacement changes sign at a distance from the surface of about 0.19 times the wavelength.

5.2.3 Decay rate

To maintain stationary vibrations in a test specimen energy must be supplied. Part of this energy will be used in overcoming internal resistance and will appear as heat. The rest of the applied energy will be absorbed by the external medium around the specimen.

If the damping capacity, ΔU, is the energy used in overcoming internal losses, the specific damping capacity is $\frac{\Delta U}{U}$, where U is the total energy of vibration per unit volume per cycle.[44]

Analogous to electrical measurements, the damping constant, Q, of a specimen is given as:[67]

$$Q = \frac{2\pi U}{\Delta U} \qquad \ldots\ldots \qquad (5.19)$$

Q may be determined in two ways. Firstly, from the sharpness of the resonance curve, (Fig. 5.1).

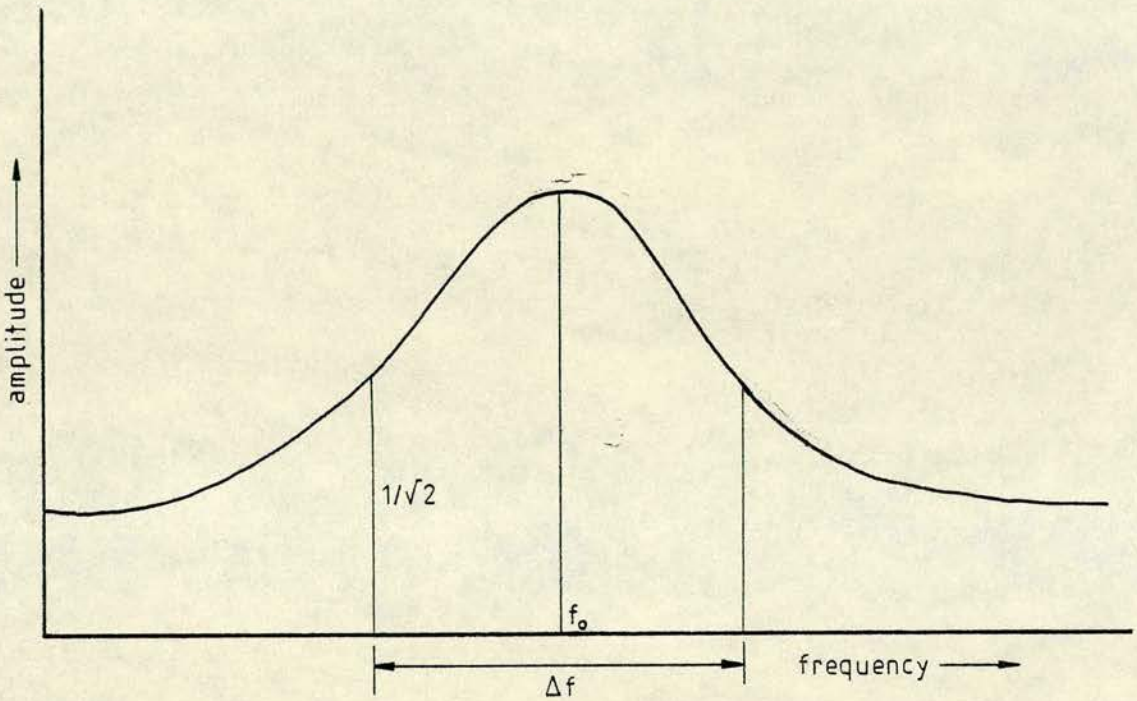

Fig. 5.1 Determination of damping constant Q
(After Obert & Duvall[44])

If f_0 is the resonant frequency and Δf the width of the resonance curve in Hz at $\frac{1}{\sqrt{2}}$ of the maximum amplitude, then:

$$Q = \frac{f_0}{\Delta f} \qquad \ldots\ldots \qquad (5.20)$$

A second method is to obtain the logarithmic decrement (δ) of an exponentially decaying free vibration. Then:

$$\delta = \log_e \frac{A_1}{A_2} \qquad \ldots\ldots \qquad (5.21)$$

where,

A_1 and A_2 are amplitudes of successive vibrations.

Q is then related to δ by:

$$Q = \frac{\pi}{\delta} \qquad \ldots\ldots \qquad (5.22)$$

Additionally, if the amplitudes at the source and some point distance can be measured, then:

$$A = A_0 \, e^{(-\alpha x)} \qquad \ldots\ldots \qquad (5.23)$$

where,

A_0 = amplitude at $x = 0$

A = amplitude at distance x

α = attenuation coefficient.

The following relationship between logarithmic decrement and attenuation coefficient may be deduced:

$$\alpha = \frac{\delta}{\Lambda} = \frac{\delta f}{c} \qquad \ldots\ldots \qquad (5.24)$$

where,

c = velocity of wave propagation

Λ = wavelength.

Assuming that there are no major discontinuities, such as cracks, which will produce large regular reflections and refractions, three main causes of internal

attenuation are apparent; diffraction, scattering, and absorption.

Diffraction and scattering are properties of the shape and macrostructure of the material, while absorption is characteristic of the physical properties and microstructure.

5.2.3(a) Diffraction

A parallel beam of plane waves originating from a vibrating source will diverge after having travelled a specific distance. This distance will depend on the size of the source and the wavelength and is given approximately by:

$$x \simeq \frac{r^2}{\Lambda} \qquad \ldots\ldots \qquad (5.25)$$

where,

x = distance at which divergence occurs

r = radius of source.

The parallel portion of the beam before divergence is called the near field or Fresnel zone. The divergence, which appears to originate from the source centre, is called the far field or Fraunhofer zone.

Equation (5.25) shows that the directivity of the beam increases with the size of the source, but decreases with wavelength, i.e. increases with frequency.

The average intensity over any cross-section in the Fresnel zone remains constant assuming no absorption occurs.

In the Fraunhofer zone, the intensity decreases inversely with the square of the distance from the source, in the same way as spherical waves coming from a point source.

Diffraction is thus not a continuous attenuation. At the frequencies used in concrete testing, the phenomenon of diffraction can present difficulties in measurements of attenuation coefficients. The loss in signal strength may be misinterpreted as attenuation due to other causes.

5.2.3(b) Scattering

It was shown by Lord Rayleigh,[65] that if a large number of small particles of fairly uniform size is distributed homogeneously in a beam of sound, reflection takes place at each of the particles in a random manner. A condition for this Rayleigh type of scattering is that the dimensions of the particles must be small compared to the wavelength, i.e. the particle dimensions must be less than about 0.1 times the wavelength.

The attenuation coefficient is related to the mean particle diameter and the frequency as follows:

$$\alpha = \frac{k f^4 d^3}{c^4} \qquad \ldots\ldots \qquad (5.26)$$

where,

d = mean particle diameter

k = a constant for a particular material.

The constant k depends on the ratio of the characteristic impedances of the suspended particles and

the material through which the sound is propagated.

Akashi[64] gives the following formula for attenuation due to scattering in concrete:

$$= \frac{2\pi^3 pTf^4}{c^4}\left(\frac{\Delta E}{E}\right) \quad \ldots\ldots \quad (5.27)$$

where,

T = average volume of aggregate particle

p = volume ratio of total coarse aggregate in concrete

E = elastic modulus of mortar

$E + \Delta E$ = average elastic modulus of coarse aggregate.

For most polycrystalline metals, the value of the mean grain size is sufficiently low for no appreciable degree of attenuation due to scattering to appear at frequencies much less than 1 MHz. However, the attenuation coefficient then increases very rapidly with frequency, because of the fourth power law, and, except for extremely fine grained materials, it is practically impossible to pass ultrasound through polycrystalline metals at frequencies above 10 MHz. For coarse grained materials, the upper limit may be only 1 MHz or less.

For example, if a beam of ultrasound of frequency 2 MHz is attenuated by 10 dB as a result of Rayleigh scattering, the attenuation is increased to a massive 160 dB when the frequency is doubled to 4 MHz.

In non-homogeneous materials, such as concrete, Rayleigh scattering takes place because of the presence of

the aggregate and air voids. The velocity of sound in concretes is generally much lower than in metals, typically by a factor of a half, and the sizes of aggregates are considerably larger than those of metallic grains. For this reason, measurements on concrete should be made at frequencies of less than 100 kHz.

5.2.3(c) Absorption

Apart from other considerations, energy loss must take place whenever there is relative motion between the various particles comprising a medium. Such losses are due to ordinary frictional forces which will tend to degrade sound energy into heat. In polycrystalline materials friction occurs at the grain boundaries.

In addition to the frictional loss, attenuation may also be caused by thermal conduction effects. Because of the abrupt changes in elastic modulus at the grain boundaries, the strain suffered by each grain is different from that suffered by its neighbour, for a given stress. Consequently, the temperature variations per cycle differ from grain to grain and temperature gradients are set up in addition to those associated with the wave motion. The regular cooling-heating cycles are upset and a general rise in temperature takes place. The energy required to supply this heat is taken from the sound waves, which consequently suffer attenuation.

There are several other minor causes of absorption of sound as it passes through a material. These include

absorption due to imperfections in crystalline lattices and absorption caused by interactions of sound with free electrons.

In general the attenuation due to absorption is proportional to the frequency of the transmitted wave.

5.3 Influence of mix variables on acoustic measurements

Since the measurement of pulse velocity through concrete was first reported by Long and Kurtz[74] in 1943 equipment and techniques for making such measurements have developed rapidly and extensively.

In the early years, as instruments became more generally available and as pulse velocity testing of concrete became more common, there was an increasing tendency for investigators to propose that pulse velocity tests be used for estimating the strength of concrete. Such proposals have great appeal, inasmuch as pulse velocity tests may be conducted quickly and economically, either in the laboratory or in the field, upon concrete of practically any shape and size. For a particular concrete experience has shown that once the strength/velocity relation is established then strength may be predicted, with reasonable accuracy, purely from measurements of the acoustic velocity.

Unfortunately, both strength and acoustic velocity are affected by many variables such as, type of aggregate, mix proportions, water/cement ratio, curing environment and age. Thus two concretes of identical strengths can

display widely differing velocities of sound propagation, and vice versa.

5.3.1 Aggregate type and mix proportions

Elastic theory indicates that if a material is composed of an isotropic medium containing a number of particles of a second phase, then the elastic properties of the material are dependent on the relative proportion and elastic properties of the included phase.

Concrete may be regarded as consisting of mortar and coarse aggregate. Although the distribution of the fine aggregate, cement and water voids will be affected by the coarse aggregate, it is reasonable to assume that the elastic properties of concrete will be a function of the elastic properties of the mortar and coarse aggregate.

Kaplan[75] suggests the following formula to relate pulse velocity and proportions of mortar and coarse aggregate:

$$t = \frac{W_a}{\rho_a V_a A} + \frac{W_m}{\rho_a V_m A} \quad \ldots\ldots \quad (5.28)$$

where,

t = transmission time through a test beam

W_a and W_m = weights of coarse aggregate and mortar

ρ_a and ρ_m = densities of coarse aggregate and mortar

V_a and V_m = pulse velocities in coarse aggregate and mortar

A = area of cross-section of test beam.

The formula is not an exact relationship. An exact formula derived from the theory of elasticity would be very much more complex and would involve Poisson's ratio of the two phases.[75]

The time taken by an acoustic pulse to pass through concrete is thus approximately the sum of the times taken for the pulse to pass through the coarse aggregate and the mortar.

The first term in equation (5.28) suggests that the pulse velocity through concrete will vary with the velocity through the aggregate, i.e. with the type of aggregate used. Similarily, for concrete made with the same type of aggregate, the second term of equation (5.28) indicates that any variation of pulse velocity through concrete will be due to variation in velocity through the mortar. The velocity must also be affected by the percentage of coarse aggregate in the mix, i.e. the mix proportions.

Kaplan has shown this to be true, and has also demonstrated that for any given aggregate and mix proportions there is an approximately linear relation between strength and pulse velocity. The higher the velocity the greater is the strength of the concrete.

Several other investigators have achieved similar results, (Whitehurst[76] and Rajagoplan, et al[54]).

5.3.2 Variation in water/cement ratio

As with variation of aggregate type and proportions, water/cement ratio has a marked effect on the strength/

velocity relationship. Again, velocity varies linearly with strength, but, since strength decreases with increasing water content, the pulse velocity also decreases with a rise in the water/cement ratio. Kaplan[77] has demonstrated an inverse linear relation between pulse velocity and water/cement ratio, the latter varying between 0.4 and 0.9.

Rajagoplan et al[54] show a linear relation between strength and velocity for different water/cement ratios, with lower velocities and strengths corresponding to higher water/cement ratios and vice versa.

The pattern change in compressive strength due to changes in water/cement ratio is not the same as that for pulse velocity. In general, changes in compressive strength at low water/cement ratios are larger than at high water/cement ratios. The opposite is true for pulse velocity; changes in pulse velocity are greater at low strengths than at high strengths. The reasons for this are not clear but it may be that the changes in pulse velocity due to changes in water/cement ratio are more closely related to structural behaviour than to the pattern of changes in compressive strength.

5.3.3 Age

Kaplan[77] has shown that for a given mix and age, the strength/velocity relationship is linear. At early ages the rate of variation of strength with velocity is low, but becomes higher with greater age. Rajagoplan

et al[54] have confirmed these results in later work. They also suggest a relation of the form:

$$T = Mc + S \quad \ldots\ldots \quad (5.29)$$

where,

T = compressive stress

M and S are constants which depend on the mix proportions and age of the concrete.

Provided that the mix proportions are known, it is then possible to estimate the compressive strength of a concrete if the velocity at the required age is determined experimentally.

This estimation of strength of concrete from pulse velocity measurements is more reliable at early ages.

5.3.4 Curing conditions

Effective curing under moist conditions ensures that hydration of the cement particles develops adequately and uniformly, thereby increasing the compressive strength.

Whitehurst[76] has shown that pulse velocity increases with increase in compressive strength through a range of curing conditions.

5.3.5 Reinforcing steel

Pulse velocity measurements on a reinforced concrete member may be affected by the steel bars.[78] The effect of the reinforcement is generally insignificant if the steel bars lie at right angles to the direction of pulse

transmission and the quantity of steel is small in relation to the path length.[79] If the steel bars lie parallel to the pulse path the effect of the reinforcement is more pronounced, since the pulse velocity along a steel bar is much higher than in concrete. Pulse velocity measurements made in the vicinity of a reinforcing bar are thus not representative of the concrete. The apparent increase in pulse velocity will be influenced by the proximity of the measurement to the bar, its diameter and orientation.[78,79]

According to BS 4408 part 5,[78] the pulse velocity in concrete enclosing a steel bar may be obtained from:

$$V_c = \frac{2bV_s}{\sqrt{4b^2+(tV_s-\ell)^2}} \quad \ldots\ldots \quad (5.30)$$

where,

V_c = pulse velocity in concrete

b = perpendicular distance from centre line of bar to nearest edge of transducer

V_s = pulse velocity in steel

t = transit time

ℓ = shortest distance between transducers.

The value of V_s is not constant and is in fact the effective pulse velocity of the steel bar embedded in the concrete.

A measurement of V_s can generally be obtained by propagating a pulse along the axis of an embedded bar, and making due allowance for concrete cover at either end.

Chung[79] has investigated the relationship between the

effective pulse velocity and the diameter of the reinforcing bar. The effect of the steel bar was not detected at diameters less than 10 mm. With a concrete test piece of 750 × 150 × 150 mm and bar diameter of 38 mm the velocity in plain concrete was only 69% of the effective velocity obtained from a reinforced specimen at 7 day strength. At 90 days this had increased to 79%. At 7 days the effective velocity represented 96% of the velocity in a free bar. The measurements were made with a commercially available ultrasonic concrete tester employing pulsed transmission at 50 kHz.

The following empirical formula is suggested by Chung to determine the effective pulse velocity through a steel bar embedded in concrete:

$$V_e = \frac{5.9 - 10.4(5.9 - V_c)}{d} \quad \ldots\ldots \quad (5.31)$$

where,

V_e = effective pulse velocity in the concrete/steel medium (km/s)

d = diameter of bar (mm).

While the zone of steel influence is defined by:

$$\frac{b}{\ell} < \frac{1}{2}\sqrt{\frac{(1-\gamma)}{(1+\gamma)}} \quad \ldots\ldots \quad (5.32)$$

where,

γ = pulse velocity ratio, $\frac{V_c}{V_e}$

5.4 Quality Assessment from Acoustic Measurements

The testing of structural concrete has two objectives. The first is to determine the compressive strength of the mix and this may be determined by cube crushing. The second objective is to ensure that this strength is maintained and that the material is continuous throughout a structure.

Being non-destructive, the acoustical testing of concrete has wide applications in the in-situ determination of structural integrity. However, a direct measure of strength and continuity is not obtainable but must be derived from the three measureable parameters described above.

5.4.1 Resonant frequency

It is common practice to compute the dynamic modulus of elasticity of concrete specimens from their resonant frequencies. The test is inherently limited to use on specimens rather than structures. Although some reports have been made of experiments in which elements which might be called structural have been vibrated[74] it is generally difficult to cause a structure to vibrate at resonance. In some cases it may damage the structure. A second limitation lies in the size of the specimen. As size is increased the power required to vibrate the specimen is increased and the resonant frequency is lowered. The inconvenience associated with providing greater driving power to the vibration is evident.

As frequencies become lower difficulties associated with their generation and measurement are multiplied.

As shown above the equations relating a resonant frequency to the modulus of elasticity invariably include a shape factor for the particular specimen. This factor can be determined to a good approximation for any form of vibration of cylinders and prisms of square or rectangular cross-section. For other shapes the computation of the shape factor becomes extremely difficult.[47]

Although it is generally agreed that some relationship exists between strength of concrete and modulus of elasticity a number of investigators have reported that no reliably useable connection exists.[80-83] In addition, if the modulus of elasticity is determined from a dynamic test method, any uncertainties or errors in computing the modulus from the results of the dynamic test will add to the substantial difficulties in estimating strength from the modulus. This is particularly true in the case of resonant frequency tests where it is necessary that the modulus must first be determined.

5.4.2 Pulse velocity

With pulse velocity tests the errors in estimating the strength from the modulus may be eliminated by directly correlating pulse velocity with strength.

It is known that the velocity of sound in any concrete invariably increases with greater concrete strength. Little evidence exists, however, to show the existence of,

or to define, a general relationship between pulse velocity and either compressive or flexural strength, which would hold for all concretes.

If a sufficiently extensive series of correlation tests are performed on a concrete containing one aggregate system, made from one mix, and cured for the same length of time under similar curing conditions, a relationship can be established between pulse velocity and ultimate strength which will permit reasonably accurate prediction of strength of further concretes made to the same specification. Recent progress in this field has been described by Elvery and Ibrahim.[84]

The basic difficulty is that correlations established for restricted ranges cannot validly be extended outside those ranges.

One way of coping with this difficulty is to include another parameter in the correlation. This approach has been discussed by Facaoaru[85] who employed an impact rebound index as the second variable. More recent work along the same lines has been described by Visvesvaraya et al.[86] Adil[87] has proposed that the product of ultrasonic pulse velocity and density as measured by gamma-ray back-scatter should give a better measure of concrete strength than either measurement alone. Recent work by Reynolds and others [62,88] has shown this to be the case. Their calculations are based on the work of Mashin and Shtriknan,[89] Wolpole[90] and Boucher.[91]

Pulse velocity may be used to investigate the presence and to some degree the extent of cracks and other voids in concrete. If the crack is of appreciable width, not filled with water and is of considerable extent perpendicular to the test path, then no transmitted signal will be detected. If the crack is small or steeply inclined with respect to the test path the impulse will usually travel around the ends of the crack and be detected. In this case, however, the pulse will have taken a longer path and the resulting calculated velocity will be low in comparison with uncracked concrete in the vicinity.

Mitchell[92] has reported tests made on concrete with artificially produced air filled and water filled cracks. He concluded that an impulse could pass through a water filled crack. A 1 mm air crack failed to pass the signal in any detectable form.

Leslie and Cheesman[50] have stated that transmission across an air gap of more than 0.025 mm is negligible and that the amplitude of a signal passing through a water filled crack is only 4 percent of the amplitude through uncracked concrete.

From this it follows that flaw detection should be possible using an echo technique such as that employed in testing materials such as metals. However, in testing metals it is common to use a train of waves of sinusoidal period at a high frequency.

The lateral dimensions of transmitters are large in

relation to the wavelengths used and a directional effect is obtained. Application of an analogous technique to concrete would appear to be limited by the rapidly increasing attenuation with rise in frequency. Akroyd and Jones[51] state: "The reflection of a pulse at an air crack in a material has formed the basis of crack detection studies which have been made on concrete. However, it is rarely possible to use the reflected echo, as in conventional flaw detection, and the presence of cracks is usually inferred from the apparently highly attenuated signal and delayed pulse arrival, or even by complete absence of the transmitted signal".

5.4.3 Decay rate

Part of the energy of vibration of a specimen will be absorbed by the external surroundings, while the rest will be used to overcome internal friction in the specimen. Internal friction in a specimen could be reduced by continued curing or increased due to drying or to internal defects produced by freezing and thawing.[52]

Obert and Duvall[44] have shown that damping varies markedly with water content, indicating that internal friction is increased as water content is reduced. Thomson[43] suggests that the deterioration of a material such as concrete will be accompanied by an increase in internal friction. It seems logical therefore to expect an increase in damping capacity with deterioration. There has been little attempt, however, to make any quantitative connection

between damping capacity and the strength of concrete specimens.

5.5 Discussion

Any system for the acoustic testing of concrete foundation piles must be based on one of the measurable parameters described above. At first inspection a resonant frequency technique does not appear suitable.

Specimen dimensions are required to compute the elastic constants, but pile dimensions are known only nominally, particularly in the case of cast in place piles. The actual length of a pile is essentially an unknown and must therefore be determined by the integrity test. Thus it would be necessary to apply the resonant frequency equations in reverse, employing values for the elastic constants determined by some other means. The elastic constants, the dynamic modulus of elasticity (E_d) and Poisson's Ratio (σ), could be obtained from measurements on test pieces. However, apart from the problems involved in achieving sufficient accuracy in these measurements, there would be a large and inestimable error in applying the measured constants to the piles. Although test pieces may be cast from the same mix, compaction and curing conditions could not be duplicated.

Because of the casting difficulties described in section 2.2, cast in place piles are likely to have a variable cross-section though still maintaining a satisfactory bearing capacity. This variable cross-section

must introduce another unquantifiable variable to the equations. Likewise the degree of contact with the surrounding soil will be unknown and therefore the way in which this alters the resonant behaviour of the pile cannot be assessed. In addition, vibrations would be heavily damped by the soil and so powerful vibrating equipment would be necessary.

Despite the apparent difficulties inherent in a resonant test some research has been undertaken, as described in section 2.3.4. The important feature of this vibration method is the use of the directly measurable parameters of force and velocity rather than the elastic constants. The method still suffers from the general problems inherent to any vibration technique. Davis and Dunn[9] have reported difficulty in interpretation of the information gained from such tests for the following reasons:

"(a) variation in the diameter of the pile,

(b) variation in the quality of concrete within the pile,

(c) variation in stiffness of the soil through which the pile passes,

(d) the top part of the pile being exposed above the ground."

Additionally, interpretable results appear to be weighted towards the top end of the pile where a defect may be more easily detected than one near the pile base.

In contrast, the application of a pulse velocity

technique to the testing of piles has apparent advantages. Since the base of a pile is inaccessible an echo technique must be employed. If an impulse is introduced to the head of the pile by some means (e.g. by a hammer blow) stress waves will develop and propagate down the length of the pile. A reflection from the base or some discontinuity may be received at the surface. A computation of time and velocity will yield the length of pile through which the sound has travelled. The distinct advantage of the method lies in the stress wave velocity. A plane fronted longitudinal wave will travel with the highest velocity and should always return to the surface first. The velocity of this wave, and therefore its time of travel, will be influenced little by variation in the pile cross-section or degree of contact with the soil. In this respect a velocity method appears superior to a resonant technique.

With any echo technique the reflection characteristics of the remote surface will determine the nature of the reflected signal. If the pile base or a discontinuity presents an irregular or angled surface, the assumption of a plane fronted longitudinal wave may be incorrect. In addition, multiple defects along the pile length may produce a confused echo signal. Echo techniques for the acoustic testing of concrete have received little attention. This aspect is examined theoretically in chapter 6 and forms part of the experimental work undertaken by the author.

To obtain an accurate measure of length, the velocity

of sound through the pile must be known. Although a direct measurement cannot be made, test pieces cast from the same mix at the time of casting may be used. Alternatively, the speed of transmission across the pile head should be more representative of that within the pile body. Steinbach [31 and 32] has proposed the use of the surface wave velocity to compute the longitudinal velocity, as described in chapter 3 (page 31). This method should give similar results to a direct measure across the pile head providing that the surface wave arrival can be correctly identified.

The presence of reinforcing steel is unlikely to affect velocity measurements unless the receiver is mounted directly over a reinforcing bar which extends to the surface. This might easily be avoided by mounting the receiver towards the centre of the pile.

Loss of signal within the pile and damping due to the surrounding soil must limit the range of the method but it may be possible to overcome this with electronic signal processing.

The rate of decay of an impulse or vibration must be greatly influenced by the consistency and degree of contact of the surrounding soil. These factors are unknown and therefore it does not seem possible to use a decay rate measurement to assess pile quality.

5.6 Conclusions

1: Pulse velocity appears to be the most useful measurable parameter for the testing of concrete piles.

2: An echo technique must be employed unless a receiver is cast into the pile base.

3: The reflection characteristics of the pile base or discontinuities may determine the nature of the reflected signal.

4: A measure of the pulse velocity and therefore the pile length can be obtained.

5: Pulse velocity is unlikely to be influenced by reinforcing steel, variation in cross-section or the consistency or degree of contact of the surrounding soil.

6: Attenuation within the pile and from the soil will be large and signal enhancement may be necessary for long piles.

6. PROPAGATION OF SOUND THROUGH RODS

6.1 Introduction

Due to the long thin shape of a pile the study of acoustic propagation through a material in rod or beam form is appropriate. Although a long solid cylinder is a simple structure the propagation of stress waves is complicated by the presence of the free boundaries. Reflections from these boundaries modify the propagation characteristics and waves display phenomena which are not present in unbounded media.

The complexity of the problem calls for simplified solutions in most cases and several approximate theories exist. In some cases exact solutions exist but only for infinite trains of sinusoidal waves. Simplified equations usually show a close correspondence with the exact theory only over a limited frequency range. In the case of pulsed propagation, when a wide band of frequencies is present, simple approximate theories frequently give misleading results.

The base of a foundation pile is generally inaccessible once in position. Thus any test method based on the lengthwise transmission of sound must involve an echo technique. Reflection and transmission characteristics of the pile base will then be important. In addition, observations of the echo signal may be complicated by the intervening behaviour of the pile top.

6.2 Continuous Wave Propagation in Cylinders

In the general solution of the wave equations for a solid cylinder, particle displacements will be functions of the co-ordinates r, θ and z,[93]

where,

r = radial co-ordinate

θ = angular co-ordinate

z = axial co-ordinate.

Flexural or transverse waves will involve displacements in all three co-ordinates. Longitudinal displacements will be independent of θ, while torsional waves will be independent of both r and z.[93]

6.2.1 Longitudinal waves

Longitudinal waves are characterised by particle motion which is parallel to the axis of propagation of the wave. The axially symmetrical component of any disturbing force applied to a rod or beam will produce a longitudinal waveform. Other terminology includes compression waves, pressure waves, or dilatational waves where propagation is in an unbounded medium.

Of the types of wave transmission possible in rods the longitudinal is the simplest to analyse mathematically and to measure experimentally. More work has thus been undertaken in this field.

Longitudinal waves generally travel at the highest velocity and are therefore the first to arrive by direct transmission or after reflection. This is of particular

significance in the application of acoustics to the testing of piles.

6.2.1 (a) Elementary theory

In the simplest theory it is assumed that stress over any cross section of the rod is uniform and purely axial, and that plane cross sections remain undistorted by the motion. (Fig. 6.1)

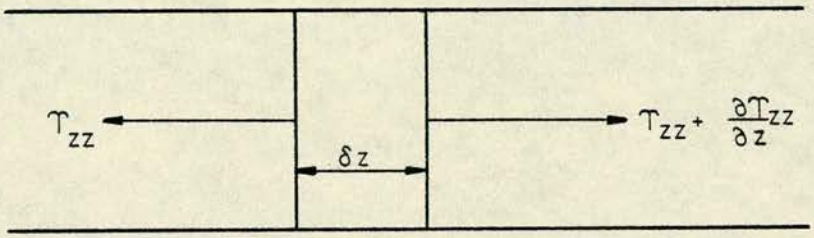

Fig. 6.1 Longitudinal stresses in a cylinder

Under the assumed conditions the following two equations may be written:[94]

$$\rho A \delta z \frac{\partial^2 u_z}{\partial t^2} = A \frac{\partial T_{zz}}{\partial z} \delta z \quad \ldots\ldots \quad (6.1)$$

$$T_{zz} = E \frac{\partial u_z}{\partial z} \quad \ldots\ldots \quad (6.2)$$

where,

u_z = axial displacement.

Combining these equations gives the second order partial differential equation:

$$\rho \frac{\partial^2 u_z}{\partial t^2} = E \frac{\partial^2 u_z}{\partial z^2} \quad \ldots\ldots \quad (6.3)$$

This is the well known wave equation in which the propagation

velocity, known as the bar velocity, is:

$$c_0 = \sqrt{\frac{E}{\rho}} \qquad \ldots\ldots \qquad (6.4)$$

The above equations predict that waves of all frequencies travel with the velocity c_0 (fig. 6.2), curve 1.

Any waveform can be described by means of a Fourier analysis in terms of its sinusoidal components. Since each component sinusoidal part is propagated at the same velocity c_0, no phase differences develop at remote stations along the bar and hence no distortion results.

This is not an exact description of propagation in a cylinder since it does not include the radial motion which must occur at the same time as the longitudinal motion due to the Poisson's ratio coupling.

The theory is useful in the analysis of reflections at the end of a finite specimen such as the base of a pile since it predicts plane fronted waves which are relatively simple to deal with.

6.2.1 (b) Exact theory

In principle it is possible to describe any problem concerned with the vibrations of an elastic solid by use of exact equations of motion governing the medium. The complexity of such an analysis generally precludes the use of the theory in engineering practice but it may serve a useful purpose in demonstrating the adequacy of an approximate theory.

The classical solutions of the exact wave equations

are due to Pochhammer[95] and Chree.[96] The cylinder is assumed to be of circular cross-section, infinite in length, composed of homogeneous linearly elastic material and free of tractions on the lateral surface. The following version of the solutions is as given by Redwood[93] in terms of potential functions. All functions are assumed independent of θ.

In cylindrical co-ordinates the wave equations are:

$$\frac{\partial^2\phi}{\partial r^2} + \frac{1}{r}\frac{\partial\phi}{\partial r} + \frac{\partial^2\phi}{\partial z^2} = \frac{1}{c_\ell{}^2}\frac{\partial^2\phi}{\partial t^2} \quad \ldots\ldots \quad (6.5)$$

$$\frac{\partial^2\psi}{\partial r^2} + \frac{1}{r}\frac{\partial\psi}{\partial r} + \frac{\partial^2\psi}{\partial z^2} = \frac{1}{c_t{}^2}\frac{\partial^2\psi}{\partial t^2} \quad \ldots\ldots\ldots \quad (6.6)$$

where,

ϕ = potential function

ψ = single potential function for waves symmetrical above the z-axis.

Putting:

$$\phi = \phi_0(r)e^{-ik_0 z}e^{i\omega t} \quad \ldots\ldots \quad (6.7)$$

$$\psi = \psi_0(r)e^{-ik_0 z}e^{i\omega t} \quad \ldots\ldots \quad (6.8)$$

gives the two differential equations:

$$\frac{\partial^2\phi_0}{\partial r^2} + \frac{1}{r}\frac{\partial\phi_0}{\partial r} + \left[\left(\frac{\omega}{c_\ell}\right)^2 - k_0{}^2\right]\phi_0 = 0 \quad \ldots \quad (6.9)$$

$$\frac{\partial^2\psi_0}{\partial r^2} + \frac{1}{r}\frac{\partial\psi_0}{\partial r} + \left[\left(\frac{\omega}{c_t}\right)^2 - k_0{}^2\right]\psi_0 = 0 \quad \ldots \quad (6.10)$$

where,

k_o = propagation constant

ω = angular frequency.

Each of these equations may be solved by separation of variables. The most general solutions include both Bessel and Neumann functions. Only the Bessel function solution is not infinite at $r = 0$ and is the one used here. The solutions may be written:

$$\phi = A\, J_0(k_\ell r) e^{-ik_0 z} e^{i\omega t} \quad \ldots\ldots \quad (6.11)$$

$$\psi = C\, J_0(k_t r) e^{-ik_0 z} e^{i\omega t} \quad \ldots\ldots \quad (6.12)$$

where,

$$k_\ell = \sqrt{\left(\frac{\omega}{c_\ell}\right)^2 - k_0^2} \quad \ldots\ldots \quad (6.13)$$

$$k_t = \sqrt{\left(\frac{\omega}{c_t}\right)^2 - k_0^2} \quad \ldots\ldots \quad (6.14)$$

J_0 = Bessel function

A and C are constants.

To find k_ℓ and k_t in terms of ω the boundary conditions are used. The radial and axial displacements are:

$$u_r = \frac{\partial \phi}{\partial r} + \frac{\partial^2 \psi}{\partial r \partial z} \quad \ldots\ldots \quad (6.15)$$

$$u_z = \frac{\partial \phi}{\partial z} - \frac{\partial^2 \psi}{\partial r^2} - \frac{1}{r}\frac{\partial \psi}{\partial r} \quad \ldots\ldots \quad (6.16)$$

$$u_r = \left[-k_\ell A\, J_1(k_\ell r) + ik_0 k_t C J_1(k_t r)\right] \times e^{-ik_0 z} e^{i\omega t} \quad (6.17)$$

$$u_z = \left[-ik_0 A\, J_0(k_\ell r) + k_t^2 C J_0(k_t r)\right] \times e^{-ik_0 z} e^{i\omega t} \qquad (6.18)$$

where,

J_1 = Bessel function.

The stresses are related to the displacements by:

$$T_{rr} = \lambda\left[\frac{u_r}{r} + \frac{\partial u_r}{\partial r} + \frac{\partial u_z}{\partial z}\right] + 2\mu \frac{\partial u_r}{\partial r} \quad \ldots\ldots \qquad (6.19)$$

$$T_{zr} = \mu\left[\frac{\partial u_r}{\partial z} + \frac{\partial u_z}{\partial r}\right] \quad \ldots\ldots \qquad (6.20)$$

At the radial boundary ($r = a$) these stresses must be zero. Substituting from equations (6.17) and (6.18) into equation (6.19) and putting this equal to zero at $r = a$ gives the equation:

$$A\left[-\tfrac{1}{2}(k_t^2 - k_0^2) J_0(k_\ell a) + \frac{k_\ell}{a} J_1(k_\ell a)\right]$$

$$+ C\left[ik_0 k_t^2 J_0(k_t a) - \frac{ik_0 k_t}{a} J_1(k_t a)\right] = 0 \qquad (6.21)$$

Putting equation (6.20) equal to zero at $r = a$ and using equations (6.17) and (6.18) gives the equation:

$$A\left[2ik_0 k_\ell J_1(k_\ell a)\right] - C\left[k_t^3 - k_0^2 k_t\right] J_1(k_t a) = 0 \qquad (6.22)$$

If A and C are eliminated from equations (6.21) and (6.22) the characteristic frequency equation is obtained:

$$k_0^2 kt \frac{J_0(k_t a)}{J_1(k_t a)} - \frac{1}{2a}\left(\frac{\omega}{c_t}\right)^2 + \left[\frac{1}{2}\left(\frac{\omega}{c_t}\right)^2 - k_0^2\right] \frac{J_0(k_\ell a)}{k_\ell J_1(k_\ell a)} = 0 \qquad (6.23)$$

Substituting for A/C from equation (6.22) the

expressions for the displacements u_r and u_z become:

$$u_r = i\,C\left[k_0 k_t J_1(k_t r) - \frac{(k_0^2 - k_t^2)}{2k_0} k_t \frac{J_1(k_t a)}{J_1(k_\ell a)} J_1(k_\ell r)\right] \times e^{-ik_0 z}\, e^{i\omega t} \quad \ldots\ldots \quad (6.24)$$

$$u_z = C\left[k_t^2 J_0(k_t r) + \frac{(k_0^2 - k_t^2)}{2k_0} k_t\, J_0(k_t r)\right] \times e^{-ik_0 z}\, e^{i\omega t} \quad \ldots\ldots \quad (6.25)$$

The frequency equation (6.23) may be solved at any frequency. It expresses the relation between the phase velocity and the wavelength. The phase velocity (c_p) is the rate of travel of a point of constant phase and is obtained from the term $e^{-ik_0 z}$.

The solution of equation (6.23) is laborious. At high frequencies ($> 10^7$ Hz) an approximate solution may be used to find some of the roots, but for low frequencies numerical solution is best. The problem has been studied by Bancroft,[97] Flinn[98] and Davies.[99] The curve of the phase velocity to wavelength relation is shown in figure 6.2, curve 2. In this figure only one of the infinite number of branches of the Pochhammer-Chree theory is shown, corresponding to the fundamental mode. The fundamental is the lowest frequency symmetrical longitudinal mode, known also as the Young's Modulus mode.

At low frequencies it is this mode which is of most

interest since even when the frequency is such that the higher modes are not evanescent, they appear to be excited only to a limited extent. In a highly attenuating medium such as concrete only the fundamental mode is likely to be sustained.

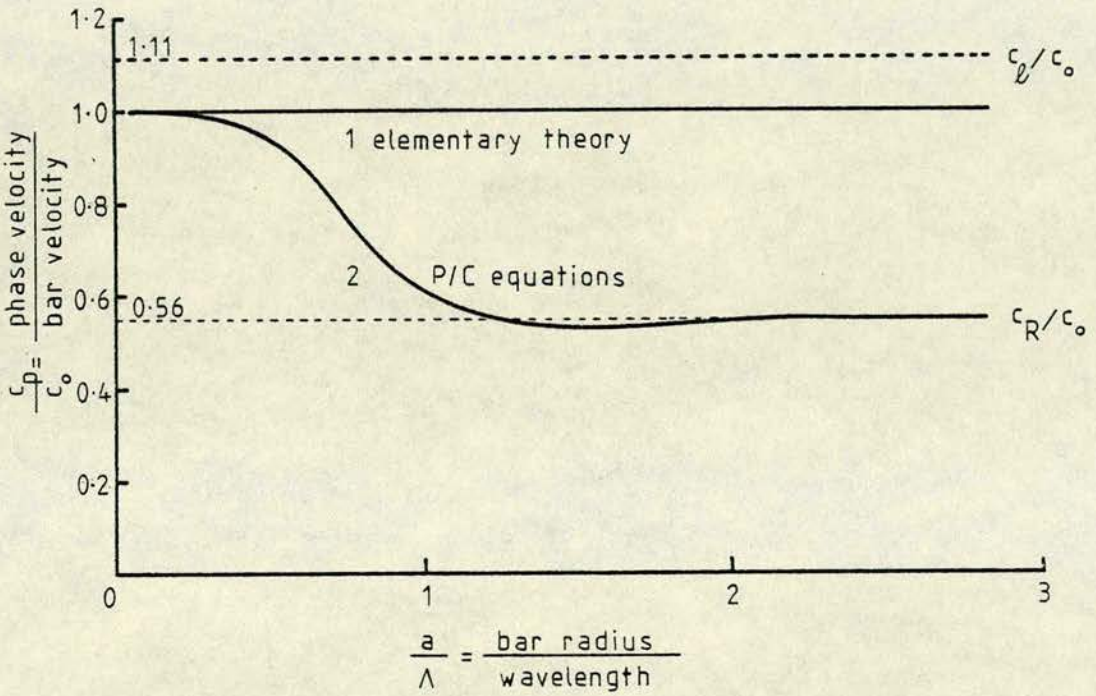

Fig. 6.2 Phase velocity curves for longitudinal waves in a cylinder. (After Bancroft[97]).

From the above figure it may be seen that a wave which has a wide band of frequencies will undergo a change in shape as it propagates along the rod. The previous conclusion from the elementary theory, that the form of the wave is preserved, is therefore incorrect. It is approximately correct for wavelengths which are long in relation to the bar diameter.

Under certain conditions there may be a grouping of a number of waves of nearly the same wavelength which reinforce one another, and produce a local disturbance which is large in comparison with the nearly completely cancelled components surrounding it. This larger disturbance will travel at the group velocity:

$$c_g = c_p - \Lambda \frac{dc_p}{d\Lambda} \qquad \ldots\ldots \qquad (6.26)$$

where,

c_g = group velocity.

The group velocity may be considered as the velocity of a wave packet whose wavelengths do not differ greatly from that of the dominant wave of the group. This velocity is important in the consideration of pulsed propagation. The dispersion curve for group velocity is shown in fig. 6.3.

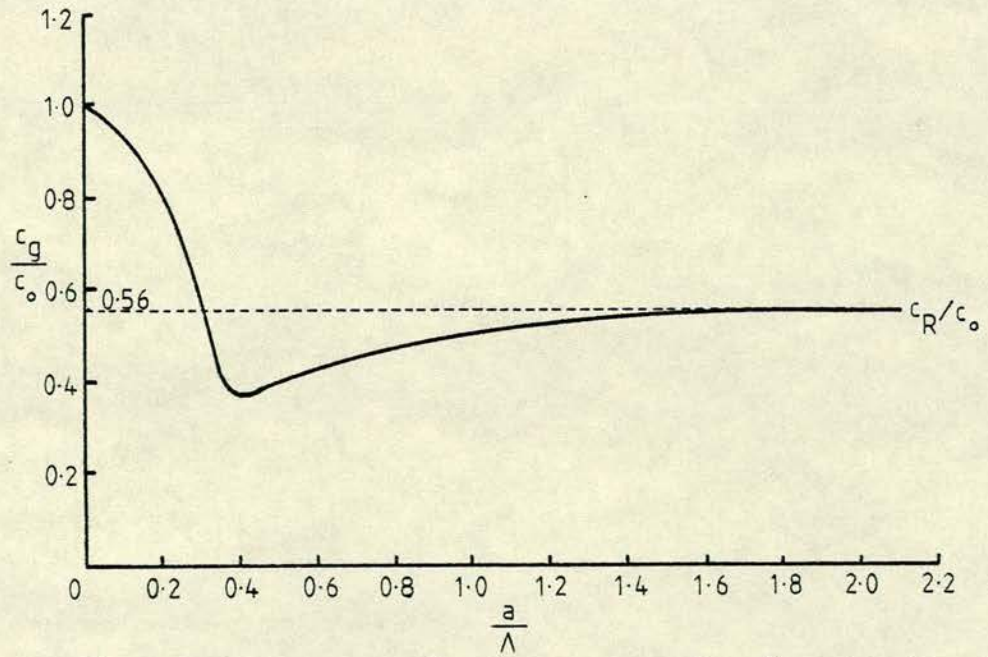

Fig. 6.3 Group velocity curve for longitudinal wave motion in a cylinder. (After Davies [99]).

As $f \to 0$, c_p and $c_g \to \sqrt{\frac{E}{\rho}}$, the bar velocity. As $f \to \infty$, c_p and $c_g \to c_R$, the velocity of Rayleigh surface waves. At some intermediate frequency, c_p has a minimum value slightly less than c_R.[97,100] The group velocity shows a pronounced minimum and there are often two values of frequency corresponding to each value of c_g.[93] The phase velocity of the fundamental mode has been verified by several experiments using both continuous wave and pulse techniques.[101-106] The results of some of these experiments have also been used to check the variation of group velocity with frequency. The problem has been the subject of several theoretical papers.[107-110]

It should be noted that the Pochhammer-Chree theory is applicable only to an infinitely long bar in which sinusoidal wave trains of infinite length are propagated in either direction. It is not directly applicable to a solution for a finite bar since the boundary conditions make solution of the wave equations (6.5, 6.6) impossible, but the approximation at low frequencies is close.

The complexity of the frequency equation (6.23) introduces great difficulties in the analysis of pulsed propagation.

6.2.1 (c) Approximate theories

Several approximate theories have been constructed to contain the essential features of the exact solution but in a simplified form. Love[66] developed an approximate theory to describe the vibrational behaviour of an elastic

bar. This was similar to the correction for the frequency of steady state vibration given by Rayleigh[65] and is sometimes known as the Rayleigh approximation. As in the elementary theory it is assumed that plane cross sections remain plane and that axial stresses are uniformly distributed over the cross section. Terms are included to take account of the inertia associated with the lateral motion resulting from the axial compression or extension.

Love developed his equations by applying Hamilton's principle to an energy expression containing a transverse inertia term.

It is assumed that displacement in the radial direction is proportional to the radial coordinate r, and to the axial strain $\frac{\partial u_z}{\partial z}$, giving the equation:

$$u_r = - \sigma r \frac{\partial u_z}{\partial z} \qquad \ldots\ldots \qquad (6.27)$$

The kinetic energy per unit axial length of the vibrating rod is:

$$\frac{\rho A}{2}\left[\left(\frac{\partial u_z}{\partial t}\right)^2 + (\sigma r_z)^2 \left(\frac{\partial^2 u_z}{\partial z\, \partial t}\right)^2\right] \qquad \ldots\ldots \qquad (6.28)$$

The strain energy per unit length of the bar is:

$$\frac{EA}{2}\left(\frac{\partial u_z}{\partial z}\right)^2 \qquad \ldots\ldots \qquad (6.29)$$

From Hamilton's principle, the first vibration of the total energy integrated between fixed times is zero.

Hence:

$$\delta \int_{t_1}^{t_2} dt \int_0^{\ell} \left\{ \frac{\rho A}{2} \left[\left(\frac{\partial u_z}{\partial t} \right)^2 + (\sigma r_z)^2 \left(\frac{\partial^2 u_z}{\partial z \partial t} \right)^2 \right] + \frac{EA}{2} \left(\frac{\partial u_z}{\partial z} \right)^2 \right\} dz = 0 \qquad (6.30)$$

Integration by parts gives the differential equation for the interior of the bar:

$$\rho \left[\frac{\partial^2 u_z}{\partial t^2} - (\sigma r_z)^2 \frac{\partial^4 u_z}{\partial z^2 \partial t^2} \right] - E \frac{\partial^2 u_z}{\partial z^2} = 0 \qquad (6.31)$$

When used to find the phase velocity as a function of frequency, curve 3 in fig. 6.4 is obtained.

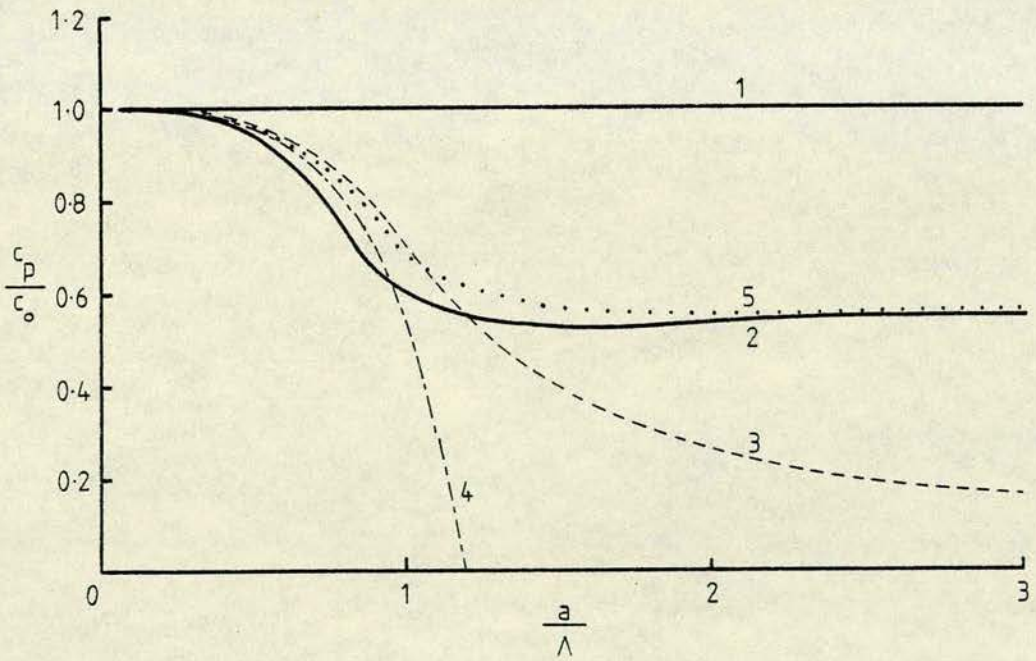

Fig. 6.4 Approximate theories of longitudinal elastic waves in a cylinder. (After Abramson et al.[94])

At low frequencies this curve gives a better approximation to the exact theory than does the elementary theory. Where the wavelength is less than about ten times the cylinder radius the discrepancy becomes considerable. The theory predicts only one branch of the dispersion diagram corresponding to the fundamental mode. Although the theory has a limited region of application it does suggest that the inclusion of terms describing the lateral inertia are necessary.

A slightly different approximation also due to Love[66] is based on the exact characteristic equation (6.23). He expanded the Bessel functions:

$$J_0(ka) = 1 - \frac{1}{4}(ka)^2 + \frac{1}{64}(ka)^4 - \ldots \qquad (6.32)$$

$$J_1(ka) = \frac{1}{2}(ka) - \frac{1}{16}(ka)^3 + \ldots \qquad (6.33)$$

If the first two terms only of the series are employed a constant velocity of $\sqrt{\left(\frac{E}{\rho}\right)}$ is obtained. If the terms (ka) and $(ka)^2$ are included then:

$$c_p = \sqrt{\left(\frac{E}{\rho}\right)}\left(1 - \frac{\sigma^2 k_0{}^2 a^2}{4}\right) \qquad \ldots\ldots \qquad (6.34)$$

and

$$\frac{c_p}{c_0} = 1 - \sigma^2\pi^2\left(\frac{a}{\Lambda}\right)^2 \qquad \ldots\ldots \qquad (6.35)$$

This approximation is shown in fig. 6.4, curve 4 .

A frequently used approximation for longitudinal waves in a cylinder has been given by Mindlin and Herrmann.[111,112] As in Love's theory, it is assumed that

radial displacements are proportional to the radial coordinate and that initially plane sections remain plane. It is further assumed that:

$$u_r = \frac{r}{a} u(z,t) \quad \ldots\ldots \quad (6.36)$$

$$u_\theta = 0 \quad \ldots\ldots \quad (6.37)$$

$$u_z = w(z,t) \quad \ldots\ldots \quad (6.38)$$

Four bar stress components are defined as:

$$P_r = \int_0^a T_{rr}\, r\, dr \quad \ldots\ldots \quad (6.39)$$

$$P_\theta = \int_0^a T_{\theta\theta}\, r\, dr \quad \ldots\ldots \quad (6.40)$$

$$P_z = \int_0^a T_{zz}\, r\, dr \quad \ldots\ldots \quad (6.41)$$

$$Q = \int_0^a \frac{T_{rz}}{a}\, r^2\, dr \quad \ldots\ldots \quad (6.42)$$

Under conditions of zero lateral surface stress the equations of motion in terms of P and Q are:

$$\frac{\partial Q}{\partial z} + \frac{P_r + P_\theta}{a} = \frac{\rho a^2}{4} \frac{\partial^2 u}{\partial t^2} \quad \ldots\ldots \quad (6.43)$$

$$\frac{\partial P_z}{\partial z} = \frac{\rho a^2}{2} \frac{\partial^2 w}{\partial t^2} \quad \ldots\ldots \quad (6.44)$$

The relations between P, Q, u and w are:

$$2P_r = 2P_\theta = 2a(\lambda+\mu)u + a^2\lambda\frac{\partial w}{\partial z} \quad \ldots\ldots \quad (6.45)$$

$$2P_z = 2a\lambda u + a^2(\lambda+2\mu)\frac{\partial w}{\partial z} \quad \ldots\ldots \quad (6.46)$$

$$4Q = a^2\mu\frac{\partial u}{\partial z} \quad \ldots\ldots \quad (6.47)$$

where,

λ and μ = Lamé constants

Corrections for shear and inertia are made by introducing two factors K_1 and K_2 to equations (6.45), (6.46) and (6.47) such that:

$$2P_r = 2P_\theta = K_2^2\left[2a(\lambda+\mu)u + a^2\lambda\frac{\partial w}{\partial z}\right] \quad \ldots \quad (6.48)$$

$$2P_z = 2a\lambda u + a^2(\lambda+2\mu)\frac{\partial w}{\partial z} \quad \ldots\ldots \quad (6.49)$$

$$4Q = K_1^2 a^2\mu\frac{\partial u}{\partial z} \quad \ldots\ldots \quad (6.50)$$

Substitution of these equations into equations (6.43) and (6.44) yields the following two equations of motion in terms of displacements:

$$a^2K_1^2\mu\frac{\partial^2 u}{\partial z^2} - 8K_2^2(\lambda+\mu)u - 4aK_2^2\lambda\frac{\partial w}{\partial z} = \rho a^2\frac{\partial^2 u}{\partial t^2} \quad (6.51)$$

$$2a\lambda\frac{\partial u}{\partial z} + a^2(\lambda+2\mu)\frac{\partial^2 w}{\partial z^2} = \rho a^2\frac{\partial^2 w}{\partial t^2} \quad \ldots\ldots \quad (6.52)$$

Mindlin and Herrmann obtained sinusoidal solutions of these equations of the form:

$$u = A\, e^{-ik_0 z}\, e^{i\omega t} \qquad \ldots\ldots \qquad (6.53)$$

$$w = B\, e^{-ik_0 z}\, e^{i\omega t} \qquad \ldots\ldots \qquad (6.54)$$

where,

A and B are constants.

Substituting for u and w in equations (6.51) and (6.52) and eliminating A and B gives a relation between phase velocity and frequency. Curve 5 in fig. 6.4 is a plot of this equation. In obtaining this curve the constant K_2 was set equal to unity and K_1 was adjusted to make the curve agree with the exact theory at short wave lengths.

Solutions of the Mindlin-Herrmann equations have been given by others. Herrmann[112] has solved equations (6.51) and (6.52) under conditions of free and forced vibration. Miklowitz[113,114] obtained a solution by means of Laplace transforms for a semi-infinite rod subject to an axial force in the form of a step function. Plass and Steyer[115] have rewritten the equations of the Mindlin-Herrmann theory as five first order partial differential equations with respect to time. Families of characteristics are found, together with the differential equations corresponding to each characteristic in a manner similar to that used by Malvern.[116] The characteristics and the associated differential equations are useful for computational purposes and also for

understanding the manner in which wavefronts are propagated.[94]

Bishop[117,118] has given another approximate theory in which Love's[66] assumption of the relation between lateral displacement and axial strain is used. An additional term is included to take account of the shear stresses that result from the rather abrupt changes in diameter as the wave passes. Bishop's theory does not allow a sudden change in radial shear without the accompanying sudden change in axial strain. The Mindlin-Herrmann equations do have this freedom. These equations have been derived directly from the Pochhammer-Chree exact equations by Volterra[108,119] using a method known as internal constraints. It is assumed that displacements in the interior of the bar are restricted in certain prescribed ways. Strains are then computed and substituted into the strain energy integral. Using Hamilton's Principal the partial differential equations of the exact theory are reduced to ordinary differential equations in terms of the variables which represent the variation of displacements with the coordinates of the cross section. The Mindlin-Herrmann equations result when the displacement in the axial direction is assumed to be constant over the cross section, and when the radial displacement is assumed to be proportional to the radial coordinate. Then the parameters are the axial displacement and the

rate of change of radial displacement with radial distance. In this case the values of K_1 and K_2 are not arbitrary.

A similar treatment to that of Volterra has been used by Plass[120] to obtain the same results. Hamilton's Principle was not used but average stresses and strains were assumed from the variation of displacements with the radial distance. The equations of motion were modified in terms of these averages and the wave equation deduced.

Only the Mindlin-Herrmann and the Love theories have been used to analyse the transient behaviour of a rod due to the propagation of a pulse. Pulsed stress wave propagation produced from a hammer blow forms the basis of the echo testing technique for foundation piles. The transient behaviour of pulses is examined at greater length in section 6.4, (p. 124).

6.2.2 Transverse waves

In transverse waves particle motion is at right angles to the direction of propagation of the wave. These waves are only possible in a medium which is capable of transmitting shear forces. The term shear waves is frequently used in seismology. Other terms include distortional waves or flexural waves where the disturbance is travelling in a beam or rod. A transverse or off centre longitudinal impact on a beam

or rod will produce both symmetrical and anti-symmetrical components about the neutral axis. These components will result in longitudinal and transverse waves respectively.

The problem of transverse motions of rods is more difficult than that of the longitudinal motions discussed earlier. Transverse deformations depend on fourth order rather than second order differential equations. Also it is found that even the elementary theory predicts dispersion.

6.2.2 (a) Elementary theory[121]

Transverse waves propagate a bending effect along the length of a beam and so a simple wave theory may be derived from the elementary theory of beam bending. In this analysis it is assumed that cross sectional dimensions are small compared to the length of the beam, and that transverse sections of the beam, originally plane, remain plane and normal to the longitudinal axis after bending, i.e. the only motion of any element is perpendicular to the axis.

In fig. 6.5 the bending moment is:

$$M + \frac{\partial M}{\partial z}\,\delta z \qquad \ldots\ldots \qquad (6.55)$$

This moment is balanced by the shear forces:

$$F \quad \text{and} \quad F + \frac{\partial F}{\partial z}\,\delta z \qquad \ldots\ldots \qquad (6.56)$$

From the laws of motion:

$$\rho A \frac{\partial^2 u_z}{\partial t^2} = \frac{\partial F}{\partial z} \quad \ldots\ldots \quad (6.57)$$

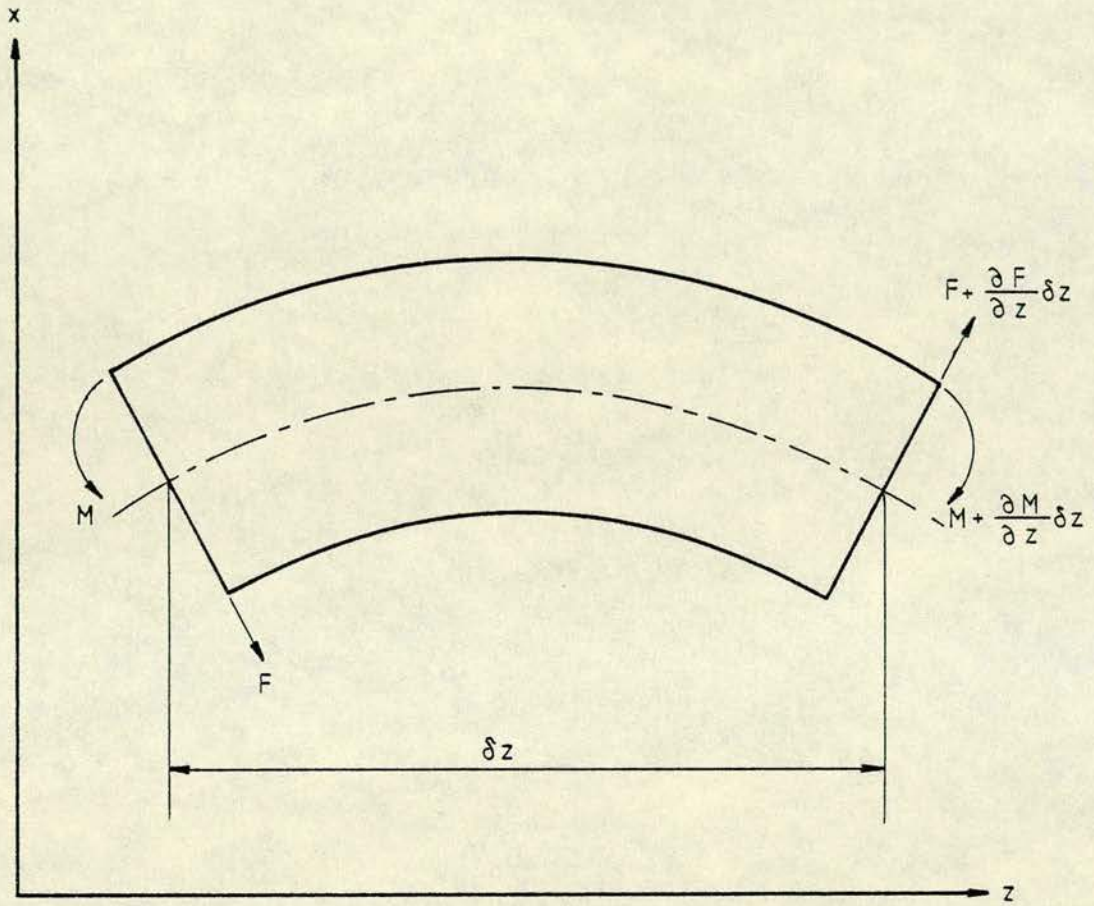

Fig. 6.5 Elementary theory of transverse wave motion in a cylinder.

Taking moments about the y-axis:

$$\frac{\partial M}{\partial z}\,\delta z + \left(2F + \frac{\partial F}{\partial z}\,\delta z\right)\frac{\delta z}{2} = 0 \quad \ldots\ldots \quad (6.58)$$

i.e.:

$$F = -\frac{\partial M}{\partial z} \quad \ldots\ldots \quad (6.59)$$

To find the relation between the axial displacement, u_z and the moment, M, the element is considered as a set of parallel components.

Then:

$$M = \frac{EI}{R} \qquad \ldots\ldots \qquad (6.60)$$

where,

R = radius of curvature

I = second moment of area of the cross section

$$\frac{1}{R} \simeq \frac{\partial^2 u_z}{\partial z^2} \qquad \ldots\ldots \qquad (6.61)$$

$$\therefore \quad F = - EI \frac{\partial^3 u_z}{\partial z^3} \qquad \ldots\ldots \qquad (6.62)$$

and by substituting into equation (6.57):

$$\rho A \frac{\partial^2 u_z}{\partial t^2} = - EI \frac{\partial^4 u_z}{\partial z^4} \qquad \ldots\ldots \qquad (6.63)$$

or:

$$\frac{\partial^2 u_z}{\partial t^2} = - c_0^2 K^2 \frac{\partial^4 u_z}{\partial z^4} \qquad \ldots\ldots \qquad (6.64)$$

where,

$K = \sqrt{\frac{I}{A}}$ = radius of gyration of the cross section about an axis in the neutral surface perpendicular to the axis of the bar. For a cylinder $K = \frac{a}{2}$.

If sinusoidal waves are assumed with propagation constant k_0 then:[93]

$$\omega^2 u_z = c_0^2 K^2 k_0^2 \qquad \ldots\ldots \qquad (6.65)$$

$$c_p = c_0 K k_0 = \frac{2\pi c_0 K}{\Lambda} \qquad \ldots\ldots \qquad (6.66)$$

At low frequencies this equation gives results which are approximately correct.[93] The **phase** velocity, c_p, is inversely proportional to the wavelength and so for infinitely short wavelengths the velocity would be infinite (fig. 6.6 curve 1). Therefore a disturbance containing extremely short wavelengths would be propagated throughout the beam instantaneously. Clearly the theory is incorrect beyond some particular wavelength.

6.2.2 (b) Exact theory

Another set of solutions to the Pochhammer-Chree equations (6.5) and (6.6) may be obtained by choosing some special functions which show a variation with θ as well as with r and z.[66,122] The basic equations only are reproduced here.

It may be shown that the following displacement functions are solutions of the wave equations (6.5) and (6.6):[95,96]

$$u_r = U(r) \cos n\theta \; e^{-ik_0 z} \; e^{i\omega t} \qquad (6.67)$$

$$u_\theta = V(r) \sin n\theta \; e^{-ik_0 z} \; e^{i\omega t} \qquad (6.68)$$

$$u_z = W(r) \cos n\theta \; e^{-ik_0 z} \; e^{i\omega t} \qquad (6.69)$$

where,

$$U = C\left\{- A\frac{\partial}{\partial r}\left[J_n(k_\ell r)\right]+B\frac{\partial}{\partial r} J_n(k_t r)+n\frac{J_n(k_t r)}{r}\right\} \qquad (6.70)$$

$$V = C\left\{A \frac{n}{r} J_n(k_\ell r) - \frac{Bn}{r} J_n(k_t r) - \frac{\partial}{\partial r}\left[J_n(k_t r)\right]\right\} \qquad (6.71)$$

$$W = C\left\{iAk_0 J_n(k_\ell r) + iB\frac{k_t^2}{k_0^2} J_n(k_t r)\right\} \qquad (6.72)$$

The stresses are related to the displacements by equations (6.19) and (6.20) plus a further equation in terms of θ :

$$T_{r\theta} = \mu\left[\frac{1}{r}\frac{\partial u_r}{\partial \theta} + r\frac{\partial}{\partial r}\left(\frac{u_\theta}{r}\right)\right] \quad \ldots\ldots \qquad (6.73)$$

Substituting for these stresses in the displacement equations and putting $T_{rr} = T_{rz} = T_{r\theta} = 0$ at $r = a$ givesthree homogeneous linear equations in A, B and C.

Eliminating the constants and expanding leads to an equation dependent on the elastic constants λ and μ, the density ρ, the radius a and the wavelength Λ. This may be written in a non-dimensional form using the variables $\frac{c_p}{c_0}$ and $\frac{a}{\Lambda}$, with Poisson's ratio as a parameter. The results may then be plotted on a dispersion diagram as before. (fig. 6.6, curve 2).

The phase velocity of the first mode is zero at $\frac{a}{\Lambda} = 0$ and tends to c_R as $\frac{a}{\Lambda} \to \infty$.[105] As in the case

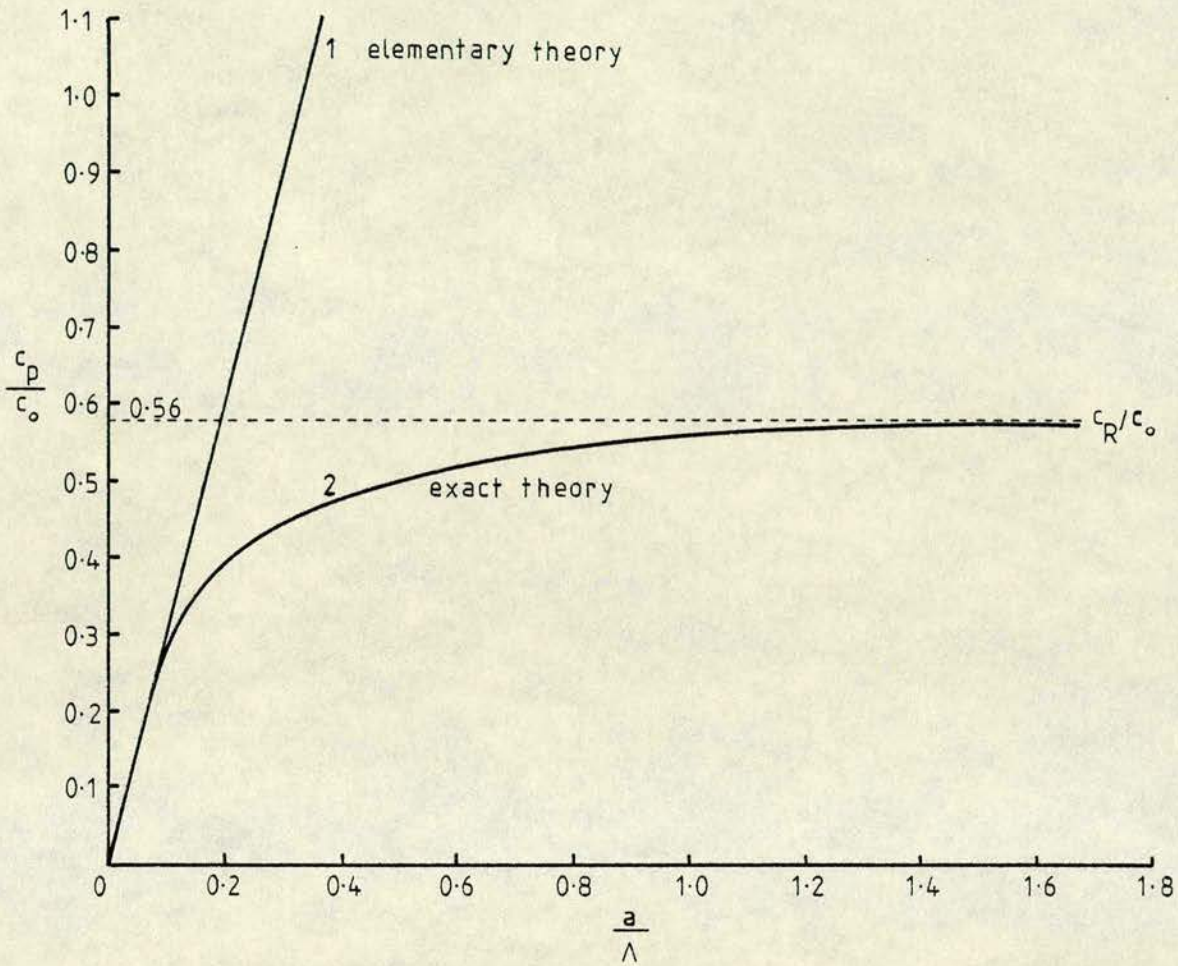

Fig. 6.6 Phase velocity of flexural elastic waves in a cylinder. (After Abramson[123]).

of longitudinal waves higher modes are unlikely to be sustained for a significant time in concrete. At low frequencies modes other than the fundamental will usually be evanescent in any material.[94]

In a dispersive medium, energy is transmitted not at the phase velocity but at the group velocity as defined earlier (equation 6.26). Fig. 6.7 shows the

group velocity curve for transverse waves.

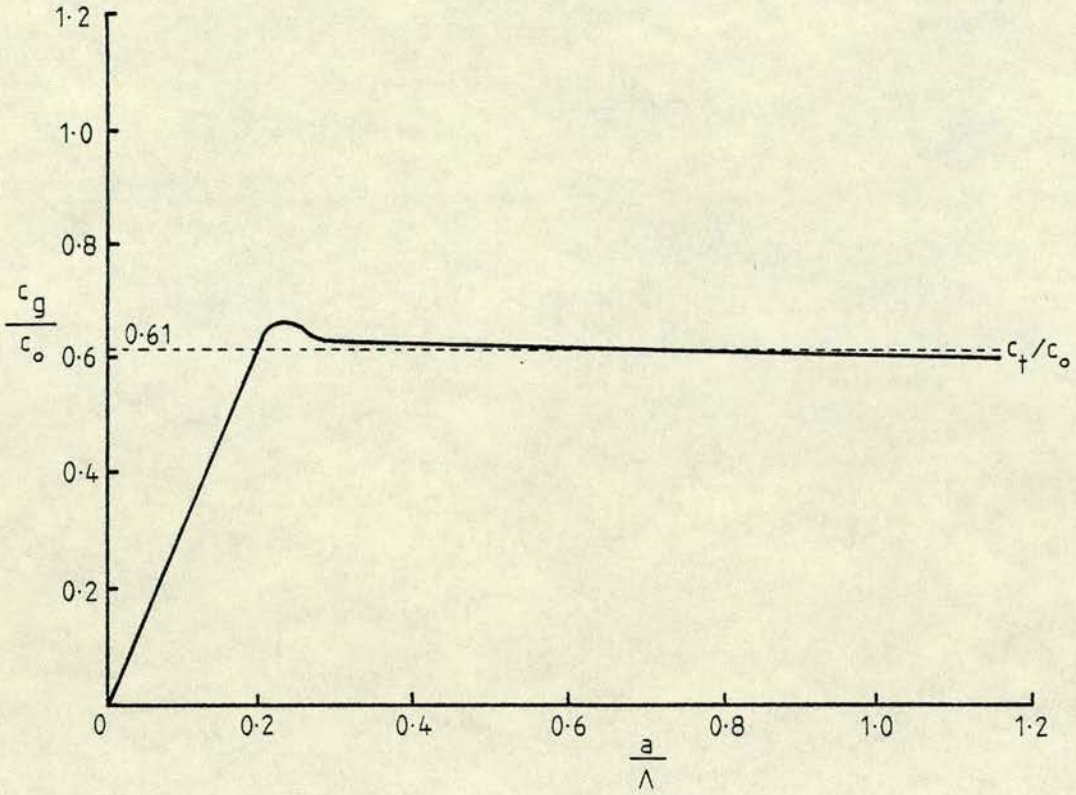

Fig. 6.7 Group velocity curve for flexural elastic waves in a cylinder (After Abramson[123]).

It should be noted that transverse waves are dispersive at low frequencies even according to the elementary theory. Thus any transverse wave-form of sufficiently low frequency to travel more than a few diameters through a concrete pile could not be propagated without change of form. Such is not the case with longitudinal waves as shown earlier in section 6.2.

6.2.2 (c) Approximate theories

A better approximation than the elementary theory may be obtained if the effect of rotary inertia is considered by writing:[121]

$$\left(F + \frac{\partial M}{\partial z}\right)\delta z = \rho I \frac{\partial^2 \alpha}{\partial t^2}\delta z \quad \ldots\ldots \quad (6.74)$$

where,

α = the angle through which the section has rotated

$$\alpha = \frac{\partial u_z}{\partial z} \quad \ldots\ldots \quad (6.75)$$

$$F = -\frac{\partial M}{\partial z} + \rho I \frac{\partial^3 u_z}{\partial z \partial t^2} \quad \ldots\ldots \quad (6.76)$$

$$\frac{\partial F}{\partial z} = -\frac{\partial^2 M}{\partial z^2} + \rho I \frac{\partial^4 u_z}{\partial z^2 \partial t^2} \quad \ldots\ldots \quad (6.77)$$

By substitution:

$$\rho A \frac{\partial^2 u_z}{\partial t^2} = -EI\frac{\partial^4 u_z}{\partial z^4} + \rho I \frac{\partial^4 u_z}{\partial z^2 \partial t^2} = 0 \quad (6.78)$$

or

$$c_0{}^2 K^2 \frac{\partial^4 u_z}{\partial z^4} - K^2 \frac{\partial^4 u_z}{\partial z^2 \partial t^2} + \frac{\partial^2 u_z}{\partial t^2} = 0 \quad (6.79)$$

The term additional to equation (6.64) represents the effect of rotational inertia.

From the above equation:

$$c_p = \frac{c_0}{\sqrt{1 + \frac{\Lambda^2}{4\pi^2 K^2}}} \qquad \ldots\ldots \qquad (6.80)$$

This equation is shown in fig. 6.8 curve 3 .

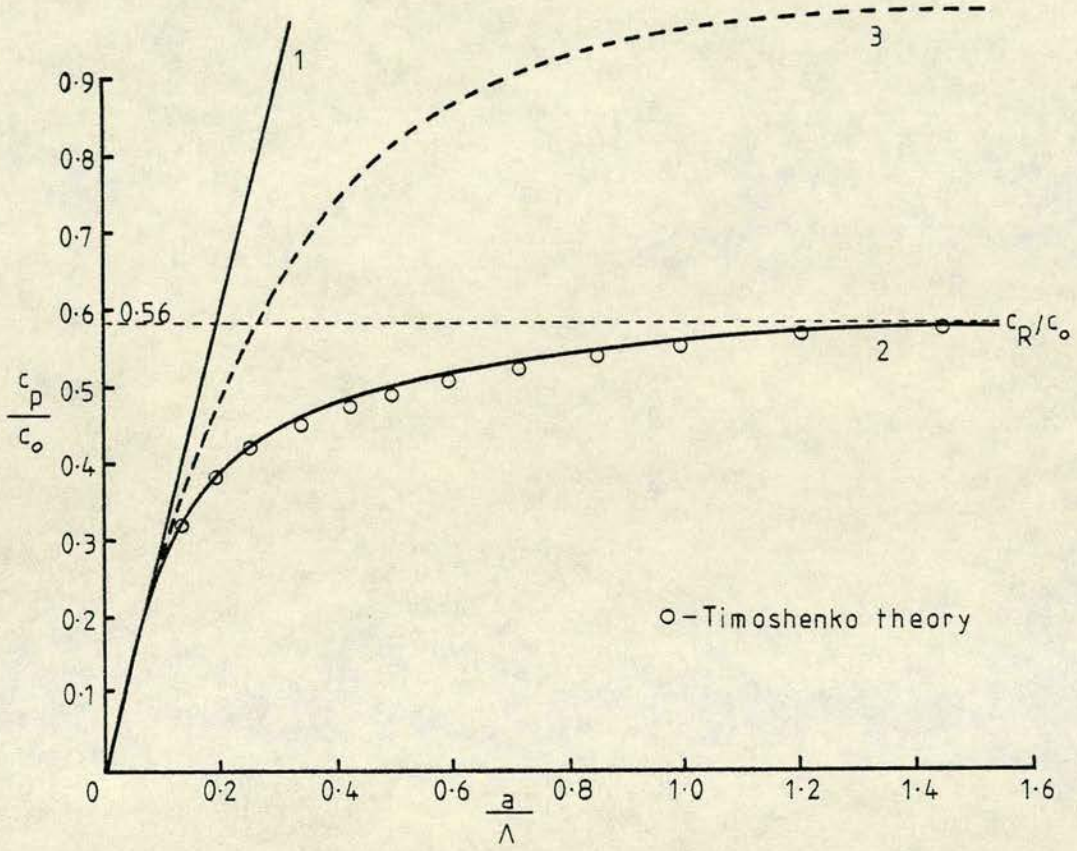

Fig. 6.8 Approximate theories of flexural waves in a cylinder. (After Abramson[123]).

An important approximate theory is that due to Timoshenko.[69,70] This theory includes the effect of the rotation of elements of the cylinder. (see p. 113).

The characteristic equation may be written:

$$c_0^2 K^2 \frac{\partial^4 u_z}{\partial z^4} - K^2(1+\varepsilon)\frac{\partial^4 u_z}{\partial z^2 \partial t^2} + \frac{\varepsilon K^2}{c_0^2}\frac{\partial^4 u_z}{\partial t^4} + \frac{\partial^2 u_z}{\partial t^2} = 0 \qquad (6.81)$$

where,

$$\varepsilon = \frac{2R}{1+\sigma}$$

R depends on the cross section shape,

10/9 for circular cross section.

The Timoshenko equation gives an excellent approximation to the exact theory (see fig. 6.8), and is frequently used in analysis of transverse vibrations since the exact theory equations are very difficult to work with.

Several other approximate theories of flexural wave propagation in cylinders have been given. Theories by Volterra[124] and Mindlin[125,126] give very accurate dispersion curves although the equations are complex.

Further mathematical treatments of continuous flexural waves in cylinders are contained in papers by Mason,[67] Thomson[68] and Kynch.[127]

6.2.3 Torsional waves

A further type of wave propagation in cylindrical rods is possible where $u_r = 0$, $u_z = 0$ and u_θ is finite and independent of θ.[93]

The angular displacement is:

$$u_\theta = u(r)e^{-ik_0 z}\, e^{i\omega t} \quad \ldots\ldots \quad (6.82)$$

Only one equation of motion remains:

$$\frac{\partial^2 u(r)}{\partial r^2} + \frac{1}{r}\frac{\partial u(r)}{\partial r} - \frac{1}{r^2}u(r) + \left\{\left(\frac{\omega}{c_t}\right)^2 - k_0^2\right\}u(r) = 0 \quad (6.83)$$

The solution to this equation may be written:

$$u(r) = A.J_1(k_t r) \quad (6.84)$$

where,

$$k_t^2 = \left(\frac{\omega}{c_t}\right) - k_0^2 \qquad \ldots\ldots \qquad (6.85)$$

The boundary conditions which must be satisfied are $T_{rr} = T_{rz} = 0$, and $T_{r\theta} = 0$ at $r = a$ if:

$$\left[\frac{\partial}{\partial r}\left(\frac{u_\theta}{r}\right)\right]_{r=a} = 0 \qquad \ldots\ldots \qquad (6.86)$$

This may be written as:

$$\left[\frac{\partial}{\partial r}\left(\frac{J_1(k_t r)}{r}\right)\right]_{r=a} = 0 \qquad (6.87)$$

or

$$\frac{J_0(k_t a)}{J_1(k_t a)} = \frac{2}{k_t a} \qquad \ldots\ldots \qquad (6.88)$$

Owen[128] has obtained roots to equation (6.88). The solution $k_t a = 0$ is of importance since $u(r) = 0$. The differential equation (6.84) may be written:

$$\frac{\partial^2 u(r)}{\partial r^2} + \frac{1}{r}\frac{\partial u(r)}{\partial r} - \frac{1}{r^2}u(r) = 0 \qquad (6.89)$$

The solution of this is:

$$u(r) = B.r \qquad \ldots\ldots \qquad (6.90)$$

Solutions to equation (6.83) then are:

$$u_\theta = B.r\, e^{-i\frac{\omega}{c_t}z}\, e^{i\omega t} \quad \text{when} \quad k_t = 0 \qquad (6.91)$$

$$u_\theta = B.J_1(k_t r) e^{-ik_0 z}\, e^{i\omega t} \quad \text{when} \quad k_t \neq 0 \qquad (6.92)$$

Equation (6.91) represents a non-dispersive wave since $c_p = c_g = c_t$ at all frequencies.[93,128]

Torsional waves have been studied by Owen[128] and Davies.[129] Experimental confirmation of the non-dispersive behaviour of the first mode has been obtained by Shear and Focke,[101] Owen[128] and Sittig[122]

The non-dispersive mode of torsion wave propagation is made use of in delay lines where undistorted pulse propagation is required.[130] The mode requires a special kind of excitation with the amplitude of the displacement proportional to the radius. A longitudinal impact is thus unlikely to produce torsional waves of any great magnitude.

Kolsky[121] has shown a very simple approximate theory which gives the exact dispersion curve of the first torsional mode of propagation in a cylinder. Suppose there are couples, C and $\left[C + \frac{\partial C}{\partial z}\,\delta z\right]$ acting on the end faces of a cylindrical element of length δz. The moment of inertia of the element is I, and relative angular motion $\delta\theta$ is produced by the couple. Then, in the limit:

$$C = \frac{\pi \mu r^4}{2} \frac{\partial \theta}{\partial z} \qquad \ldots\ldots \qquad (6.93)$$

$$\frac{\partial C}{\partial z}\,\delta z = I \frac{\partial^2 \theta}{\partial t^2} \qquad \ldots\ldots \qquad (6.94)$$

$$I = \frac{\pi \rho r^4 \delta z}{2} \qquad \ldots\ldots \qquad (6.95)$$

Combining these equations:

$$\mu \frac{\partial^2 \theta}{\partial z^2} = \rho \frac{\partial^2 \theta}{\partial t^2} \quad \ldots\ldots \quad (6.96)$$

This equation predicts the correct velocity of the first mode, $\sqrt{\left(\frac{\mu}{\rho}\right)}$.

6.2.4 Surface waves

Rayleigh[65] has shown that a wave existing near a free surface may carry energy (p. 63). These waves are similar to the skin effect found in electromagnetic waves in electrically conducting media.[131] Surface particle motion is elliptical with the major axis normal to the surface and its centre at the undisturbed surface.[132] The zone of influence of surface waves is generally confined to a layer of thickness of one wavelength. Both longitudinal and transverse components are present.[133]

A simple harmonic wave train travelling in the z direction may be described by:[93,65]

$$\phi = D\, e^{-ik_\ell x}\, e^{-ik_0 z}\, e^{i\omega t} \quad \ldots\ldots \quad (6.97)$$

$$\psi_y = T\, e^{-ik_t x}\, e^{-ik_0 z}\, e^{i\omega t} \quad \ldots\ldots \quad (6.98)$$

where,

D and T are constants.

Inserting the boundary conditions $T_{xx} = T_{xy} = T_{xz} = 0$ at $x = 0$ gives:

$$\left[2 - \left(\frac{c_R}{c_t}\right)^2\right] D \pm 2\sqrt{\left[\left(\frac{c_R}{c_t}\right)^2 - 1\right]}\ T = 0 \qquad (6.99)$$

$$\pm 2\sqrt{\left[\left(\frac{c_R}{c_\ell}\right)^2 - 1\right]} D + \left[2 - \left(\frac{c_R}{c_t}\right)^2\right] T = 0 \qquad (6.100)$$

The solution of these equations leads to the frequency equation:

$$\left(\frac{c_R}{c_t}\right)^2 \left[\frac{c_R^6}{c_t^6} - \frac{8c_R^4}{c_t^4} + c_R^2\left(\frac{24}{c_t^2} - \frac{16}{c_\ell^2}\right) - 16\left(1 - \frac{c_t^2}{c_\ell^2}\right)\right] = 0 \qquad (6.101)$$

If $c_R < c_t < c_\ell$ then surface waves will exist since the cubic equation has a real root. This root is usually close to c_t, but varies slightly with Poisson's ratio such that:[133]

$$c_R = \alpha c_t \quad . \qquad \ldots\ldots \qquad (6.102)$$

For $\sigma = 0.25$ (steel) α has a value of 0.92 .

The other two roots to the equation represent the reflection of longitudinal and transverse waves. Since surface waves diverge only in two directions they are less attenuated than internal waves.[132] Typically surface waves decay relative to surface area while internal waves decay according to volume. The velocity of propagation of surface waves depends only on the elastic constants of the medium. There is thus no dispersion of these waves and a plane surface wave will travel without change in form.[121]

The energy of surface waves is found to diminish with distance away from the boundary according to an approximately exponential law. This decay depends on frequency. The higher the frequency the less is the zone of penetration of the wave.

Surface, or Rayleigh waves are very sensitive to surface loading which will produce massive damping of the wave.[133] If some other medium is in contact with the surface, such as soil surrounding a pile, then energy will be lost to that medium. Longitudinal and transverse wave components will form in the adjoining medium with the direction of propagation angled according to the relative acoustic velocities in the two media.[134] Note that only the longitudinal component will exist in an adjacent liquid medium.

In the case of wave propagation along a beam or rod the problem is complicated by the proximity of the enclosing boundaries.[135,136] If the wavelength is large in relation to the beam cross section then surface waves will extend into the longitudinal axis from all sides. This accounts for the difference between the longitudinal velocity in an unbounded medium and the bar velocity.[132] Redwood,[93] when dealing with the fundamental longitudinal mode in a rod, states: "At low frequencies, while $c_p > c_t$, the displacement is mainly due to the set of plane transverse waves, since the set of dilatational waves exists only as a surface disturbance. At high

frequencies the total displacement becomes increasingly like a pure surface disturbance."

When a beam receives some disturbance at an end, then surface waves will travel across the end surface and reflect from the sides. This motion will be picked up by any receiving device and so will complicate the reception of axial signals. This behaviour of the end of a beam after an applied pulse is extremely complex and little work has been attempted on the subject. The problem is examined later in section 6.4.4, (p. 136).

A third appearance of surface disturbances on a cylinder is found in azimuthal waves which propagate around the curved surface. These waves have been examined by Elliott.[137] This form of wave is unlikely to be produced to any great extent by an axial end impact. Similarly these waves would not be detected by a receiver on the end surface of a cylinder and hence no interference of the axial waves would occur.

6.3 Other cross sections

Two other rod forms of practical value are the rectangular cross section and the cylindrical shell. Exact analysis of the rectangular case is not possible, and an exact analysis of the shell is difficult,[93] so approximate theories have been developed.

6.3.1 Rectangular solid rod

Dispersion curves for rods of square and rectangular cross section have been examined experimentally by Morse.[138,139] For a rod in which the dimensions of the sides are in the ratio 8 : 1 the experimental phase and group velocities are within a few per cent of the values given by the theory for a solid plate. For a rod of square cross section the values are within a few per cent of the theoretical dispersion curves for an analogous cylinder. In this instance the length of the side of the square and the cylinder radius are related by:

$$a = 0.565b \quad \ldots\ldots \quad (6.103)$$

where,

b = length of the side of the square.

The cross sectional areas of the two rods are then equal.

In a theoretical examination Morse obtained a characteristic equation very similar to that of the plate. The theory is based on the exact wave equations, but the boundary conditions of zero stress were approximated since no exact solution is possible for this case.

Kynch and Green[140] have compared Morse's results with another theory in which they interpret the dispersion curves for a rod as the interaction between a longitudinal mode and a screw mode. This theory also shows a close relation between square and cylindrical rods of equal cross sectional area. Chree[96] developed an approximate

theory to describe the propagation of longitudinal waves along rectangular rods. The following expression was obtained:

$$c_p = c_0\left(1 - \frac{\sigma^2 k_0^2 I}{2}\right) \quad \ldots\ldots \quad (6.104)$$

This equation is valuable only over a limited range of low frequencies.

6.3.2 Cylindrical shells

The cylindrical shell problem may be encountered in the case of shell piles as described in chapter 2 (p. 3). Several approximate theories have been used to describe the propagation of longitudinal waves in shells.

An exact theory has been derived by Mirsky and Herrmann.[141,142] The frequency equation is obtained by applying the appropriate boundary conditions to equations (6.11) and (6.12), including both the Bessel and Neumann functions. If the internal radius of the shell is set equal to zero the characteristic equation reduces to that of a solid cylinder. At very low frequencies $c_p \rightarrow c_0$ exactly as for a cylinder. At high frequencies $c_p \rightarrow c_R$, the velocity of Rayleigh surface waves.

Junger and Rosato[143] have given an approximate theory which shows close agreement to the exact theory at low frequencies. The theory shows progressive error at

higher frequencies. Other similar approximations have been produced by Lin and Morgan,[144] Naghdi and Cooper,[145] and Smith.[146]

In a later paper, Heimann and Kolsky[147] have shown that where the wavelength is small compared to the thickness of the shell wall the cylinder walls behave as a thin plate.

Shell piles are generally built up from precast sections of about 1m in length. Once in position in the ground the centre space is filled with fresh concrete and when this has hardened the composite structure acts as a solid pile. Although the acoustic velocities in the two concretes might differ, the propagation characteristics of the shell are similar to those of the solid pile especially at low frequencies. The presence of the shell is thus unlikely to modify the passage of a longitudinal pulse to any significant extent. Small reductions in cross sectional area at a joint between precast sections might give a small reduction in signal amplitude. This aspect is examined in the experimental work (chapter 7).

6.4 Pulsed Propagation in Cylinders

The Pochhammer-Chree solutions for propagation of sound waves in cylindrical rods apply strictly to infinite trains of sinusoidal waves. Several writers have shown both theoretically and by experiment that this theory is

inadequate in accounting for the behaviour of stress wave fronts or pulses.[148-159]

The essential departure of pulsed propagation from that of the continuous wave case appears to result from the advance of the wave front into previously undisturbed parts of the wave guide. In the case of continuous waves an oscillatory particle motion is induced, generally sinusoidal in character. A disturbance propagating into an undisturbed elastic medium, however, will reflect from the boundaries in a very complex manner.[160] If an attempt is made to apply the appropriate boundary conditions to this transient motion, the classical wave equations become mathematically intractable.[161] If a pulse is more than just a few cycles in length the behaviour of the central part can frequently be accounted for by reference to the case of continuous sinusoidal propagation, but the transient behaviour of the wave front requires some other approach.

6.4.1 Pulse bandwidth

The departure of pulse behaviour from that of the continuous wave case is further complicated by the form which the pulse takes. In particular the range of frequencies in the frequency spectrum must be considered.[93] Any pulse may be synthesized from a number of sinusoidal waves of different frequencies. This range of frequencies is known as the Fourier or frequency spectrum.[162] The interval between the highest and lowest

frequencies in the spectrum is a measure of the bandwidth of the pulse.

The characteristic behaviour of a pulse travelling along a rod will show a marked difference depending on whether the frequency spectrum is wide band or narrow band.[93]

6.4.2 Narrow bandwidth pulses

Narrow band pulses are generally produced by a pulse modulated carrier, the pulse length being such that the envelope contains some hundred or more cycles of the carrier. For example, if the carrier frequency is 10 MHz and the pulse duration is 10.10^{-6}s, then the pulse envelope will contain 100 cycles of the carrier signal. Its bandwidth relative to the carrier frequency is then narrow. Such narrow bandwidth pulses may be produced, for example, by electrical modulation of an acoustic transducer mounted on the surface of a specimen.

In many cases a narrow bandwidth pulse of longitudinal waves applied to one end of a solid wave guide is found to arrive at a point further along the axis considerably attenuated. The main pulse may frequently be followed by secondary or trailing pulses.[93] A sinusoidal variation launched into a wave guide may be regarded as an infinite set of plane longitudinal waves making angles with the axis of the guide.[163] On reflection at the walls of the guide each of these plane waves will generate a transverse wave which in turn will generate a

longitudinal wave when it strikes the wall diametrically opposite. Interference between the reflected components results in the formation of a series of pulses trailing the main pulse. Experimental evidence for this theory exists. The trailing pulses have been observed at the predicted time delays both when the applied pulse contains many hundred cycles of the carrier[105] and when it contains only a few cycles.[150]

The existence of the trailing pulses depends very much on the frequency. At low frequencies, corresponding to values of a/Λ less than 1, they may not appear at all.[164] At higher frequencies they will almost certainly be present. The significance of the trailing pulses lies in the energy loss from the main signal which must accompany their generation. This may cause large errors if the main signal is being used for the measurement of absorption in the solid. Experiments have shown that the phase velocity, c_p, changes only slightly as the carrier frequency is altered by as much as 10^6 Hz and does not show the rapid variation predicted by the classical theory.[157] In addition the theory fails to predict both the trailing pulses and the attenuation of the main pulse.

At lower frequencies, corresponding to values of a/Λ less than about 1.5, the Pochhammer-Chree solutions are more successful in describing the propagation of pulses. The experimental evidence gathered at these lower frequencies indicates that the fundamental longitudinal

mode is predominately excited. A pair of plane transverse waves are excited, with a surface disturbance representing the degenerate longitudinal waves and there are no trailing pulses.[93] If trailing pulses are found at low frequencies they can only come from higher order modes where $c_p > c_\ell$. There is some evidence for the excitation of these modes in practice, but their amplitudes are usually small.[103]

Tu, Brennan and Sauer[102] have measured the group velocities of pulses propagated in a cylindrical bar with values of a/Λ varying from 1 to 3. The variation of velocity over this range followed no known theoretical curve, being close to the fundamental mode value at $a/\Lambda = 1$, but increasing rapidly until $c_g \simeq c_\ell$ at $a/\Lambda = 3$. It would appear that at the higher frequencies the pulse behaved as if it were travelling in an unbounded medium with the dilatational velocity.

6.4.3 Wide bandwidth pulses

An impact to the end of a long rod, such as a hammer blow to the top of a pile, will generally result in a pulse of fairly wide frequency spectrum.[161] Pulses of this nature were produced as part of the experimental work undertaken by the author (see chapter 7). A typical pulse was analysed, using a fast Fourier transform on a mini computer, and the resulting frequency spectrum is given in fig. 6.9. The pulse as shown in fig. 6.10 was recorded after travelling one complete length of a 10m beam.

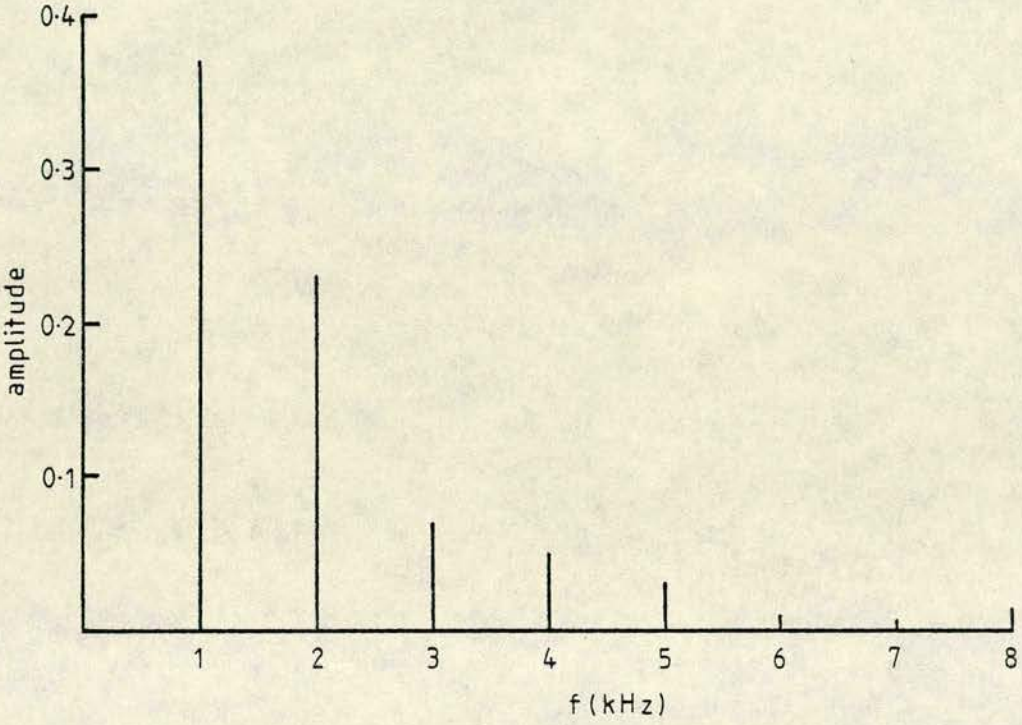

Fig. 6.9 Fourier transform of pulse used in the experimental study of impacts on a 10m concrete beam.

The fundamental frequency of approximately 1 kHz represents one cycle of the basic pulse. The higher frequencies are harmonics required to build up the pulse from component sine waves. The highest frequencies stem mainly from the sharp rise at the leading edge of the pulse.

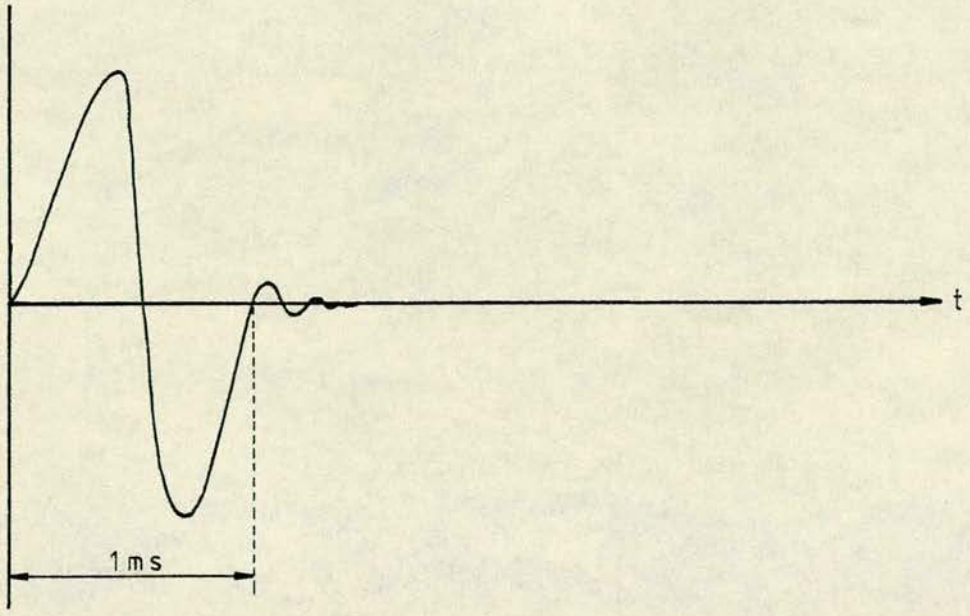

Fig. 6.10 Shape of a typical pulse obtained from an impact on a 10m concrete beam.

Several analyses of the propagation of such pulses are possible with varying degrees of complexity. Theories which attempt to give a complete quantative description are exceedingly complex. Most of the complexities arise in trying to account for the transient behaviour of the first few cycles of the pulse. If a pulse is more than just a few cycles in length the behaviour of the central part can frequently be accounted for by reference to the continuous wave equations.

The Pochhammer-Chree theory has shown that for longitudinal waves the velocity of propagation is not constant but varies with frequency (figs. 6.2, 6.3). Therefore a pulse containing a wide range of frequencies might be expected to behave in a dispersive fashion. Using Fourier analysis the applied pulse may be split into its continuous wave components. Continuous wave theory may be employed to find the relative phases of these

components at some point further along the wave guide. The new pulse shape may then be found by adding the component parts together again. Such an analysis based on continuous wave theory still fails to predict the transient behaviour accurately, but it can give a very close description of the later parts of the pulse arrival, especially at some distance from the source.[93]

Theoretical work by Davies[99] and by Kolsky[155,166] provide examples of this method. The most difficult task lies in choosing a mathematical function which describes the pulse at the source fairly closely but which has a simple Fourier series representation. Davies assumes a trapezoidal displacement in the longitudinal direction at the source, which corresponds approximately to a rectangular pressure pulse. Several features of distortion are indicated by the analysis. Sudden changes of shape are smoothed, while linear parts of the original pulse become oscillatory curves. The rise and fall remain approximately linear but with a reduction in slope of as much as 60 per cent. This reduction in slope must be due to widening of the pulse as the higher and lower frequencies disperse.

Kolsky has used a similar analysis to derive the distortion of a pulse of different shape. The results show similar characteristics to that seen in Davie's work. The initial rise of the pulse is slowed and oscillations appear along the top of the pulse. (fig. 6.11).

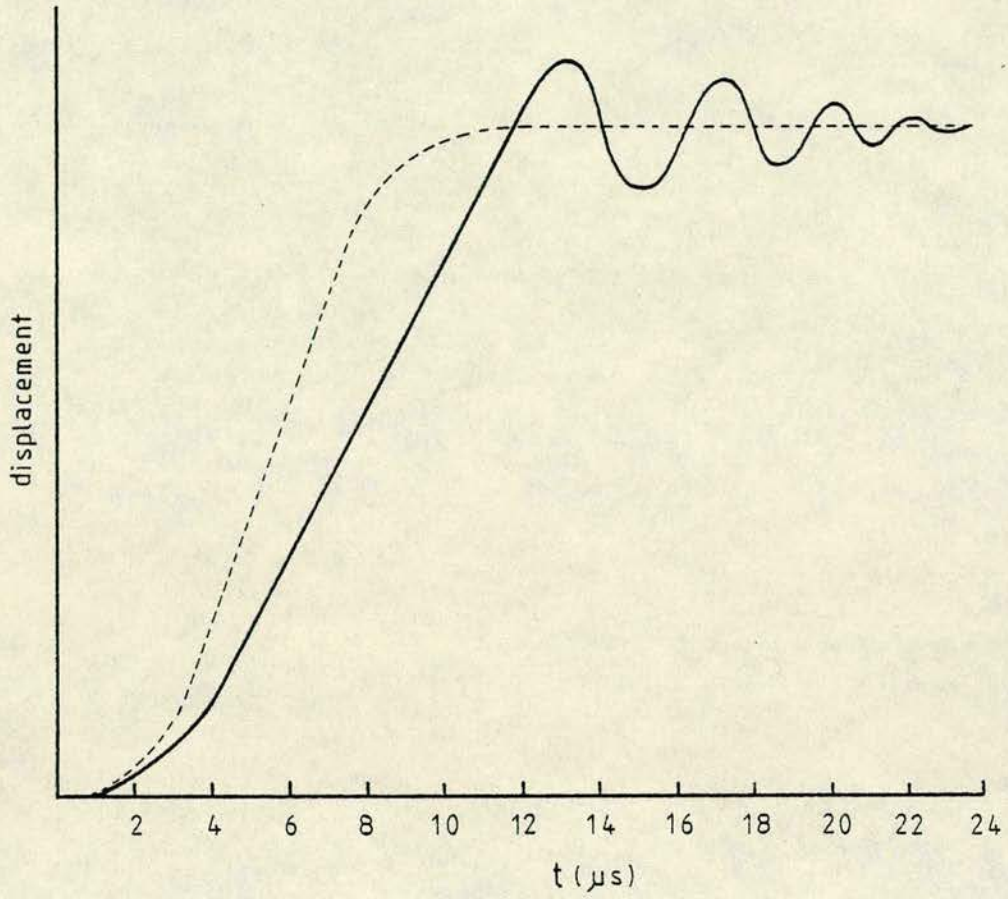

Fig. 6.11 Distortion of a pulse applied to a cylinder (After Hsieh and Kolsky[166]).

Experimental work by Kolsky[161] has shown close agreement with this theoretical approach. Such an analysis is useful in predicting the behaviour of a pulse at large distances from the source, or at points far from the front of the pulse. It does not predict any arrival with a velocity greater than the bar velocity (c_0), and is therefore of little use in describing the received signal at points close to the source where the direct arrival of the spherical wave front travelling at c_ℓ will be strong.

A method of describing pulse propagation in special

circumstances has been described by Shalak.[159] The pulse is assumed to be produced by the impact of two identical cylinders moving in opposite directions. Initially the problem is solved under conditions of radial restraint thus allowing a plane longitudinal wave to propagate. Next the behaviour of an infinite cylinder subjected to a radial stress is examined. If this stress is set equal to the radial restraint applied initially, then a combination of the two problems will give the response of the system to the original pulse. The shape of the distorted pulse is similar to that obtained by Kolsky (fig. 6.11). Folk et al[104] have described a similar method of analysis which is more generally applicable. Several other papers describe approximate analyses of pulse propagation which show sufficiently close agreement with experimental work.[94,110,114]

The complexities of the theoretical analyses arise from basic uncertainties concerning the nature of the pulse and the difficulties of applying the continuous wave equations for an infinite cylinder to the case of a pulse governed by the unsolvable end boundary conditions. The more significant features of pulse propagation are, however, indicated by the theory. Initially a spherical wave will radiate from the source and travel into the beam at the longitudinal velocity in an unbounded medium, (dilatational velocity, c_ℓ). This wave front may propagate for some distance down the beam axis depending

on the frequency and the rate of absorption in the medium. When the spherical wave strikes the sides of the wave guide reflections will take place and propagation down the wave guide will be a complex combination of longitudinal, transverse and surface waves. In addition any eccentricity in the applied pulse will produce a strong transverse or bending wave.

The bulk of the energy will travel in the form of a longitudinal pulse at the bar velocity, c_0. In a long rod this pulse will be the first arrival at the far end. This pulse will be a grouping of the dominant waves excited by the source. The extent to which this pulse is dispersed will depend on the frequencies composing the pulse, the pulse length and the lateral dimensions of the wave guide. Where the pulse length is long compared to the width of the rod, the pulse will travel with little distortion for a considerable distance. Higher frequencies will always be dispersed and trail behind the main pulse where they may form trailing pulses as described earlier (p. 126).

The main theoretical aspects of the propagation of a pulse in a rod due to a longitudinal impact have been verified by experimental work. Almost all of the investigations have been conducted with pulses centred upon some low frequency for which a/Λ was generally less than 1.

An important study was conducted by Ripperger.[152]

Pulses were generated by allowing small steel balls to strike the end of a cylindrical bar. Measurements at various points along the bar allowed the pulse to be studied during its travel. Thus distortion of the pulse due to dispersion could be observed directly. A systematic study was made of the relationship between pulse durations and rod diameters. This revealed that the shortest pulse which could be transmitted through a given cylindrical bar without appreciable distortion by dispersion has a duration of the time required to travel a distance of 7 to 8 times the bar diameter. This corresponds to a value of about 0.13 for the ratio a/Λ.

Measurements of the velocity of propagation of pulses of various durations in bars of different diameters indicated that the peak of the pulse is invariably propagated at the bar velocity, ($c_0 = \sqrt{E/\rho}$). No part of the disturbance could be detected at any velocity greater than the bar velocity.

Changes in pulse shape which Ripperger observed were a reduction in amplitude, a widening of the base of the pulse and a decrease in the slope of the leading edge. These effects were all reduced as the pulse duration was increased. The shorter the pulse the more noticeable was the disturbance following it. For the shortest pulses the disturbance became quite large and complex.

Some experiments by Davies[99] have shown that a pulse will travel at the velocity due to the dominant wavelength in the pulse. This velocity may vary from a maximum of

the bar velocity, c_0 to a minimum of about $0.38\ c_0$.

Using similar methods Oliver[103] found that the first part of a pulsed signal arrived with a velocity of c_0. Some time after the first arrival some longer waves appeared which were found to belong to a flexural mode. These were followed immediately by the onset of very short waves. During the rest of the pulse the signal consisted of two superimposed waves of different frequencies. At a time corresponding to the minimum group velocity (fig. 6.3), the two frequencies became nearly equal and the signals were of large amplitude. Further oscillations were attributed to surface waves on the end of the specimen which stored energy and released it for some time after the cessation of the applied pulse. This latter effect has great significance in the detection of echo signals arriving at the end from which the original pulse was generated.

6.4.4 End resonance effects

A noticeable feature of a pulse produced in a bar by rapid loading of the end is the appearance of oscillations which have no counterpart in the time variation of the applied load. Some of these oscillations result from the dispersion effect as described earlier, but in addition to this effect, a receiver mounted on or near the struck end will show further oscillations generally of high frequency. These waves of a resonant nature are associated with the end of the rod. They may be thought of as the result of

constructive interference of surface waves on the end surface.

When a pulse is applied to one end of a rod most of the energy will go into propagation of the several waveforms discussed earlier. A small fraction in a narrow frequency band will remain at the end near the source. This end resonance will be gradually leaked down the rod as one of the normal propagating modes. A similar end resonance will be set up at the far end on arrival of the main pulse.

A theoretical description which accounts for all details of the observed behaviour near the end of a rod after the application of a pulse does not exist at present. Exact theoretical solutions for elastic waves in terminated cylindrical rods are not known because of the difficulty in solving the wave equations subject to the boundary conditions at two intersecting surfaces. Bishop[118] commented on the terminated rod problem and suggested the possible existence of a wave system confined to the end of the rod.

Oliver[103] has studied the problem and suggests that waveforms attributed by other researchers to higher modes of propagation are in fact due to end resonance. He applied absorbent material to the source end of a long rod. A receiver at the far end showed marked decrease in amplitude of the components considered to derive from the end effects. The transmitted parts of the main pulse were

unaffected.

Particle motion at the end of a rod during resonance is indicated by fig. 6.12. The motion in this case is symmetrical about the axis of the rod.

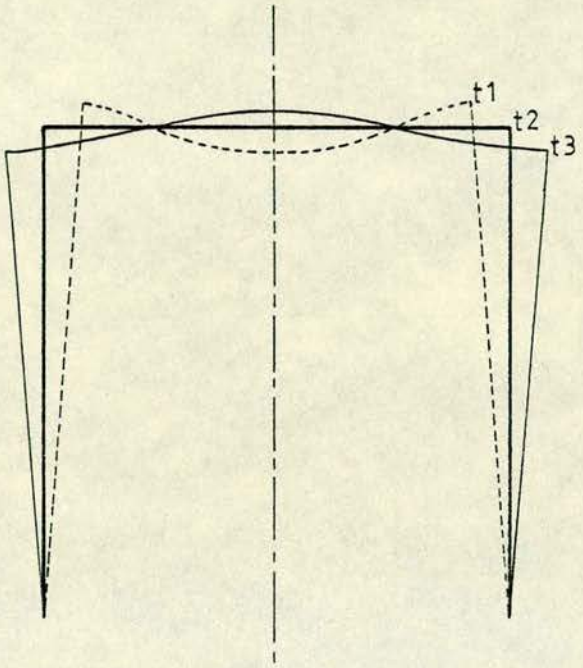

Fig. 6.12 Particle motion during end resonances (After Oliver[103]).

Oliver also detected additional modes of resonance which were not symmetrical about the axis by using the source and receiver at the same end. These were not studied in detail. Shaw[169] has studied surface wave resonances on the cylindrical surface of a flat disc. From these and other experiments unusual effects are known to occur when surface waves are in the vicinity of a corner.

6.5 Reflection of pulses in rods

In examinations of the reflection of longitudinal pulses at beam extremities, reference is frequently made

to the elementary theory of longitudinal propagation. (Section 6.2.1 (a), p. 89). The theory is useful because it predicts plane fronted waves which are comparatively simple to deal with. Despite the complexity of the exact theory and the attendant complications of pulsed propagation the approximation is valid at low frequencies.

Davies[170] has investigated the distribution of stress over the cross section of a bar at the head of a longitudinal pulse. To determine experimentally the non uniformity of the stress distribution small steel balls were lined up on the upper end surface of a 2½ inch diameter bar. When a bullet was fired against the lower end of the bar the balls flew off and their trajectories were photographed. An analysis of these trajectories showed that the stress at the head of a pulse is uniformly distributed over the cross section after the pulse has travelled four to five diameters from the point of impact.

The amplitude and form of a pulse reflected from the end of a beam will depend on the nature of the reflecting end and on the medium with which the end is in contact. A flat end is relatively simple to deal with and the amplitude and phase of the reflected pulse may be determined. In the cases of an angled or broken end, or where an abrupt change in cross section occurs, the analysis is complex. Theories exist for angular incidence of plane waves at a boundary, but the problem

of reflection from the angled end of a wave guide has received little attention.

6.5.1 Reflection at a perpendicular end

A stress pulse whose operative Fourier components have wavelengths long compared with the diameter of the bar in which it travels will propagate without dispersion. At the end of the bar the nature of the reflected pulse will depend on the boundary conditions. The bar is initially considered in a vacuum.

The displacement due to the incident pulse may be given by:

$$u_i = F(c_0 t + z) \qquad \ldots\ldots \qquad (6.105)$$

and that due to the reflected pulse by:

$$u_r = f(c_0 t - z) \qquad \ldots\ldots \qquad (6.106)$$

The stresses produced by the two pulses will be:

$$T_i = E\frac{\partial u_i}{\partial z} \quad \text{and} \quad T_r = E\frac{\partial u_r}{\partial z} \qquad \ldots\ldots \qquad (6.107)$$

and the resultant stress will be:

$$E\left(\frac{\partial u_i}{\partial z} + \frac{\partial u_r}{\partial z}\right) = E\left(F'(c_0 t+z) - f'(c_0 t-z)\right) \qquad (6.108)$$

If z is measured from the end of the bar, the condition that the end is free from stress is:

$$F'(c_0 t) - f'(c_0 t) = 0 \qquad \ldots\ldots \qquad (6.109)$$

Thus the shape of the reflected pulse is the same as that

of the incident pulse but is opposite in sign. A compression pulse will be reflected as a tension pulse and vice versa.

The displacement at any point in the bar is given by $u_i + u_r$, and at the free end of the bar where $z = 0$ this will be $2F(c_0 t)$. Therefore displacements and hence particle velocities will be twice their corresponding values as when the pulse is travelling through the bar.

When a pulse is reflected from a fixed boundary at the end of a bar, the boundary condition is that the displacement is zero at $z = 0$. From equations (6.105) and (6.106) the total displacement is given by:

$$u_i + u_r = F(c_0 t+z) + f(c_0 t-z) \quad \ldots\ldots \qquad (6.110)$$

and this is zero at $z = 0$. Therefore $f(c_0 t)$ is equal to $-F(c_0 t)$ and the displacement u_r of the reflected pulse is equal and opposite to that of the incident pulse. The stress set up by the reflected pulse is given by $E\frac{\partial u_r}{\partial z}$ and this is now found to be equal to $E\frac{\partial u_i}{\partial z}$, the stress for the incident pulse. A compression pulse is thus reflected at a fixed boundary unchanged but the displacement is reversed. The stresses produced by the incident and reflected pulses thus add up on a fixed boundary and the value of the resultant stress is double the corresponding values as when the pulse is travelling along the bar.

When a pulse of plane waves strikes a boundary separating two materials some of the energy is trans-

mitted and the remainder reflected. The transmitted and reflected intensities may be expressed by the reflection and transmission coefficients, the values of which will depend on the acoustic impedance of each medium.

Specific acoustic impedance is defined as the ratio of acoustic pressure to particle velocity:

$$Z = \frac{p}{v} \qquad \ldots\ldots \qquad (6.111)$$

where,

Z = specific acoustic impedance

p = acoustic pressure

v = particle velocity

This is analogous to electrical impedance and is equal to the mechanical impedance per unit area of cross section of the medium.

Z is complex and can be expressed as:

$$Z = R + iX \qquad \ldots\ldots \qquad (6.112)$$

where,

R = resistive component

X = reactive component

For plane progressive waves the imaginary component disappears leaving a real quantity which is analogous to electrical resistance. This real quantity is known as the characteristic acoustic impedance of the material and is equal to the product of the density and velocity

of sound in the material, i.e.:

$$R = \rho c \quad \ldots\ldots \quad (6.113)$$

It can be seen from equation (6.113) that the characterestic impedance depends only on the physical properties of the medium and is independent of the wave characteristics or frequency.

For a wave incident normally on a boundary between two media, the acoustic pressure ratios of incident, transmitted and reflected waves maybe expressed in terms of the acoustic impedancies as follows[39]:

$$\frac{p_t}{p_i} = \frac{2R_2}{R_1+R_2} \quad \ldots\ldots \quad (6.114)$$

$$\frac{p_r}{p_i} = \frac{R_2-R_1}{R_1+R_2} \quad \ldots\ldots \quad (6.115)$$

where,

subscripts i, t and r refer to incident, transmitted and reflected waves

subscripts 1 and 2 refer to the first and second media in the direction of propagation

Particle velocity ratios may be similarly expressed:

$$\frac{v_t}{v_i} = \frac{2R_1}{R_1+R_2} \quad \ldots\ldots \quad (6.116)$$

$$\frac{v_r}{v_i} = \frac{R_1-R_2}{R_1+R_2} \quad \ldots\ldots \quad (6.117)$$

Where R_2 is less than R_1, sound is travelling from an acoustically dense medium into an acoustically less dense medium. Equation (6.115) shows that reflection will take place with a phase change of 180° in acoustic pressure. Equation (6.117) shows that there will be no change in particle velocity and hence particle displacement.

Where R_2 is greater than R_1 it can be seen that no phase change in acoustic pressure will occur but that particle velocity will change phase by 180°. These are partial cases of the fixed and free ends described above in section 6.5.1, (p. 140).

The power at any point in an acoustic field may be expressed in terms of the acoustic intensity, which is defined as the rate of flow of acoustical energy through unit area of an imaginary plane surface drawn about the point and orientated at right angles to the direction of wave motion. The intensity, I, may be expressed as:

$$I = pv \quad \ldots\ldots \quad (6.118)$$

where p and v are r.m.s. quantities.

At the boundary between two media the ratio of the acoustic intensity of the reflected wave to that of the incident wave defines the reflection coefficient, while the ratio of the intensity of the transmitted wave to that of the incident wave is the transmission coefficient.

From equations (6.114), (6.115), (6.116), (6.117) and

(6.118), it can be seen that:

$$m_r = \frac{I_r}{I_t} = \left[\frac{R_2 - R_1}{R_1 + R_2}\right]^2 \quad \ldots\ldots \quad (6.119)$$

$$m_t = \frac{I_t}{I_r} = \frac{4R_1R_2}{(R_1 + R_2)^2} \quad \ldots\ldots \quad (6.120)$$

where,

m_r = reflection coefficient

m_t = transmission coefficient

also,

$$m_r + m_t = 1 \quad \ldots\ldots \quad (6.121)$$

Where R_1 and R_2 are equal, m_t has a maximum value of one, and m_r becomes zero. This is an ideal case, but in practice good acoustic coupling occurs where R_1 and R_2 have values of the same order of magnitude, i.e. $0.1 \leq m_t \leq 1$.

Typical values of R for concrete, water and air are given in table 6.1.

Medium	ρ	c	R
	(kg/m^3)	(m/s)	$(kg/m^2/s)$
air	1.3	330	430
water	1000	1500	1.5×10^6
concrete	2300	4000	9.2×10^6

Table 6.1 Characteristic impedence values

A few simple calculations using the above impedence values will yield the following results.

1. A sound wave propagated through concrete will be almost totally reflected by a dry crack or void.
2. Approximately 70-80% of the sound energy will be reflected if the same discontinuity is filled with water.

In the calculations it is assumed that no diffraction takes place around the edges of the discontinuity.

6.5.2 Change in cross section

This problem has been studied by Ripperger and Abramson[171] and by Fischer.[172] A mathematical theory of pulse reflection at a change in cross section of a rod according to the exact theory has not been produced. A convenient and workable relationship between incident and reflected longitudinal waves has been derived by Rayleigh.[65] This may be readily extended to give the relationship between the incident and transmitted waves. The bending wave problem is somewhat more complicated but has been treated by Mugiono.[173]

The solutions are based on the assumptions of an infinitely long bar and steady state wave propagation. Propagation is represented by the familiar elementary wave equations (6.3) and (6.63). Where the frequency spectrum of a pulse is such that its form is not seriously altered by dispersion as it progresses along the bar, it

is not unreasonable to expect that reflection and transmission coefficients based on steady state theory can represent the behaviour of a pulse at a change in cross section. This condition is easily met in the case of longitudinal propagation,[171] but as shown earlier in section 6.2.2, bending wave pulses are always distorted by dispersion regardless of the wavelength.[149]

For plane longitudinal waves incident on a change in cross section in a rod the conditions of continuity are:

$$F_1 = F_2 \quad \ldots\ldots \quad (6.122)$$

$$v_1 = v_2 \quad \ldots\ldots \quad (6.123)$$

where,

F is the force acting over the cross section.

From condition (6.122):

$$(T_i + T_r)A_1 = T_t A_2 \quad \ldots\ldots \quad (6.124)$$

and from condition (6.123):

$$v_i - v_r = v_t \quad \ldots\ldots \quad (6.125)$$

Note that if the reflected pulse has a stress of the same sign as the incident pulse, the particle velocity must have the opposite sign.

From the elementary theory of longitudinal wave propagation (section 6.2.1 (a) p. 89):

$$T = \rho c_0 v \quad \ldots\ldots \quad (6.126)$$

Solving equations (6.124), (6.125) and (6.126) gives:

$$T_r = \frac{\rho_2 A_2 c_{02} - \rho_1 A_1 c_{01}}{\rho_2 A_2 c_{02} + \rho_1 A_1 c_{01}} Ti \quad \ldots\ldots \quad (6.127)$$

$$T_t = \frac{2\rho_2 A_1 c_{02}}{\rho_2 A_2 c_{02} + \rho_1 A_1 c_{01}} T_i \quad \ldots\ldots \quad (6.128)$$

If the discontinuity involves only a change in area, these equations reduce to:

$$T_r = \frac{A_2 - A_1}{A_2 + A_1} T_i \quad \ldots\ldots \quad (6.129)$$

$$T_t = \frac{2A_1}{A_2 + A_1} T_i \quad \ldots\ldots \quad (6.130)$$

From these results it may be seen that if the discontinuity represents an increase in cross section, the incident wave is reflected without change in sign. A decrease in cross section causes the reflected wave to be changed in sign. Again, the analogy with the cases of fixed and free end are seen. It should also be noted in the general equation (6.128) that if $\rho_2 A_2$ is very small, as in the case of air, very little stress can be transmitted past the discontinuity. Rayleigh[65] pointed this out as the explanation of why very little energy can be lost from a vibrating bar to the atmosphere. The corollary of a bar in substantial contact with an acoustically dense medium is obvious.

Experimental work by Ripperger and Abramson[171] showed general agreement with values calculated from the theory.

Fischer[172] has investigated the transmission and reflection of an elastic rectangular stress pulse in a cylindrical bar with a neck or swell of varying length. A graphical method was used to plot the form of the reflected and transmitted pulses. The method, known as graphodynamics, is also used in plotting electrical waves, flow in pipes and open channels, and torsional disturbances in elastic rods. In a series of experimental and graphical investigations it was demonstrated that the transmitted pulse is the same after a neck and a swell of the same length if the area ratios are inversely the same. This accords with the theory previously described.

Transverse or bending waves have been examined by Ripperger and Abramson[171] and by Mugiono.[173] A similar form of behaviour to that of the longitudinal case was noted, but the dispersive nature of the waves made prediction more difficult.

6.5.3 Reflection at an angled end

The theory of angular reflection and refraction at an interface between two media is fully established with substantial verification by experimental work, particularly in the field of seismology. Although little attention has been paid to reflection from a non-perpendicular end to a wave guide, the theory appropriate to the unbounded case is significant. Reflections from the angled end of a concrete beam have

been studied experimentally by the author. (see chapter 7.)

The simpler case of reflection at a solid/vacuum interface is examined first. This case approximates closely to that of a solid in air. It is found that when either a longitudinal or a transverse wave impinges on a boundary between two media, both reflection and refraction take place.[121] In the most general case four separate waves are generated, a wave of each type forming in each medium.

When a plane longitudinal wave is incident on a free surface (i.e. boundary with a vacuum) there can be no refracted waves. The boundary conditions cannot be satisfied by assuming that only a longitudinal wave is reflected, and it may be shown that a transverse wave will also be generated.[93]

The angles of incidence and reflection of the longitudinal waves will be equal. The angle of reflection of the transverse wave is given by:

$$\frac{\sin a_t}{c_t} = \frac{\sin a_\ell}{c_\ell} \qquad \ldots\ldots \qquad (6.131)$$

where,

a_t and a_ℓ are the angles of incidence and reflection of transverse and longitudinal waves.

This last result may be obtained by consideration of the phase velocities of the longitudinal and transverse

waves along the surface. Since one wave is generated from the other, the phase velocities must be equal. But:

$$c_p = \frac{c_\ell}{\sin a_\ell} \quad \ldots\ldots \quad (6.132)$$

and:

$$c_p = \frac{c_t}{\sin a_t} \quad \ldots\ldots \quad (6.133)$$

hence the relationship (6.131). More rigorous proofs exist elsewhere,[121] but the above illustrates the physical significance of the process.

It is obvious that the amplitudes of the incident and reflected longitudinal waves cannot be equal since some energy is transferred to the generated transverse wave. The following relationships connecting the amplitudes of the three waves may be derived:[130]

$$\frac{\ell_r}{\ell_i} = \frac{\left(c_t/c_\ell\right)^2 \sin 2a_\ell \sin 2a_t - \cos^2 2a_t}{\left(c_t/c_\ell\right)^2 \sin 2a_\ell \sin 2a_t + \cos^2 2a_t} \quad (6.134)$$

$$\frac{t_r}{\ell_i} = \frac{2\left(c_t/c_\ell\right)\sin 2a_\ell \cos 2a_t}{\left(c_t/c_\ell\right)^2 \sin 2a_\ell \sin 2a_t + \cos^2 2a_t} \quad (6.135)$$

where,

ℓ = longitudinal wave amplitude

t = transverse wave amplitude

i and r refer to incident and reflected components

These equations give the relative amplitudes of the reflected

longitudinal and transverse waves as a function of the angle of incidence a_ℓ . Arenberg[130] has drawn curves showing ℓ_r/ℓ_i as a function of the angle of incidence a_ℓ over the full range of Poisson's ratio. These are reproduced in fig. 6.13.

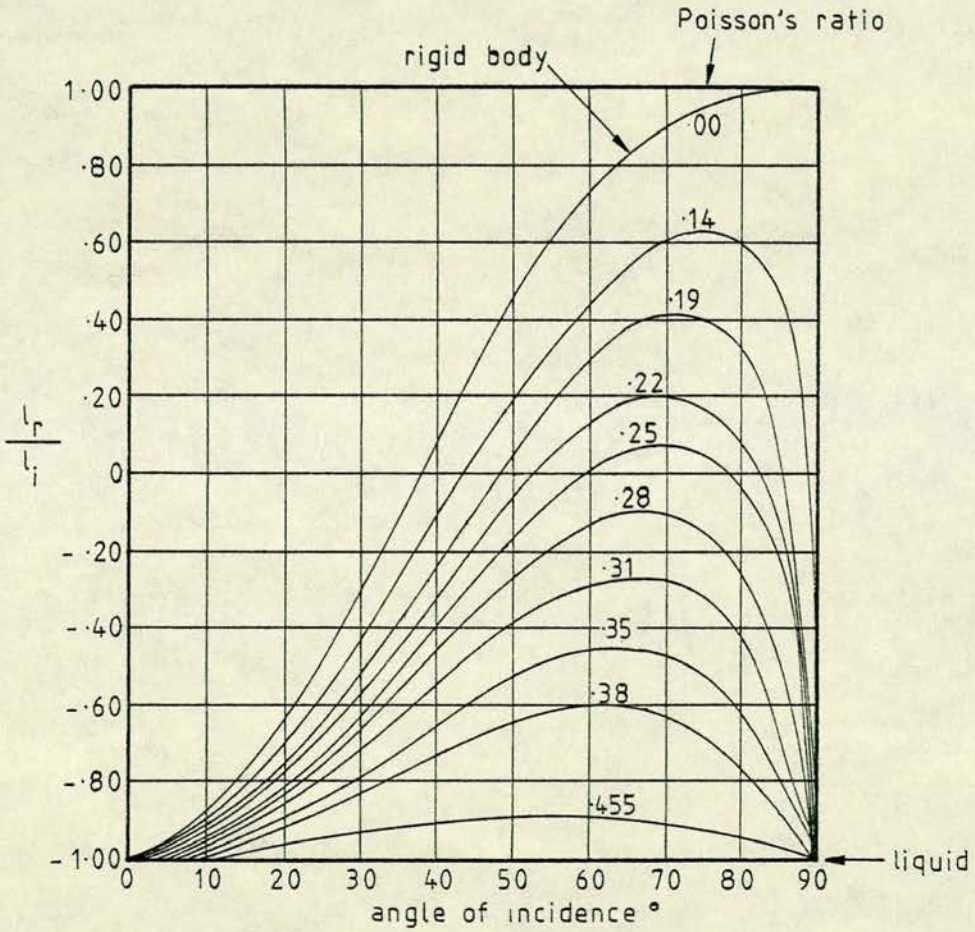

Fig. 6.13 Reflection of a longitudinal wave at a solid/vacuum interface. (After Arenberg[130]).

Some important features of these curves are:[93,174,175,176]

(1) The phase change of the longitudinal wave on reflection at the boundary is π radians if $0.26 < \sigma \leq 0.5$. For $\sigma < 0.26$ the phase change is zero for some values of a_ℓ. The displacement corresponding to the transverse wave which is generated is always in phase with the incident longitudinal wave.

(2) For $\sigma < 0.26$ there are two angles of incidence at which $\ell_r/\ell_i = 0$. Here the incident longitudinal wave is totally converted to a transverse wave.

(3) At grazing incidence ($a_\ell = 90^\circ$) and at normal incidence ($a_\ell = 0^\circ$), $\ell_r/\ell_i = -1$ and no transverse wave is formed.

The case of incident transverse waves is complicated by the orientation of the wave motion with respect to the reflecting boundary. The waves may be horizontally polarised where the transverse displacement of the wave is in the y direction, or vertically polarised in the xz plane. (see fig. 6.14).

It is found that a plane transverse wave whose displacement is wholly in the y direction is reflected without phase change or loss of amplitude.[93]

The case of vertical polarisation is more complex. It is not possible to satisfy the boundary conditions at all angles of incidence with a reflected transverse wave

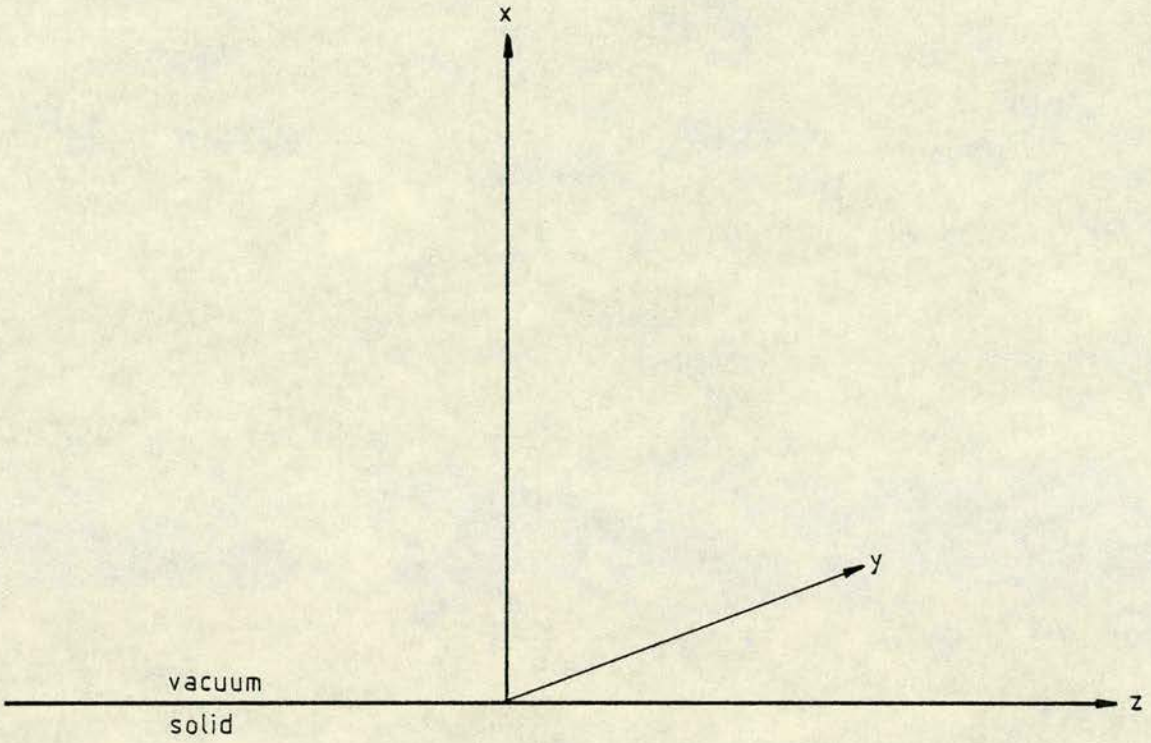

Fig. 6.14 Polarisation planes of incident transverse wav

alone, and a longitudinal wave is therefore generated.[121] By applying the boundary conditions the relative amplitudes of the incident and reflected waves may be found. The characteristics are similar to those seen in the reflection of plane longitudinal waves. There is a critical angle beyond which the transverse wave is reflected without loss of amplitude. This angle is reached when the angle of the generated longitudinal wave is 90°. Angles greater than 90° have no meaning and the longitudinal wave no longer merits this description. The motion becomes a surface disturbance decreasing exponentially with distance from the surface and carries no energy.

More complicated cases occur when angular reflection takes place at a solid/fluid or solid/solid interface. The problems may be tackled in the way used for the solid/vacuum interface. The boundary conditions in the solid/fluid case, are that the pressure in the fluid is equal to the normal stress in the solid and that the transverse stress is zero. At the solid/solid interface there must be continuity of all stresses.

The equations describing reflections at a solid/fluid interface may be obtained from the equations of a solid/solid interface if the modulus of rigidity of one material is put equal to zero. A wave travelling through a solid and incident on a fluid boundary may be longitudinal or transverse. The number of variables is large and full treatment is contained in the references.[177,178]

The boundary conditions for the solid/solid interface require that both the displacements and the stresses shall be continuous.[179] As before, (p.151) it is found that:

$$c_p = \frac{c_\ell}{\sin a_\ell} = \frac{c_t}{\sin a_t} = \frac{c'_\ell}{\sin a'_\ell} = \frac{c'_t}{\sin a'_t} \qquad (6.136)$$

where the prime symbols refer to waves travelling in the second medium.

Other than in seismic work an interface between two semi-infinite solids is rare. Many curves are required to give a good description of all the components

of reflection. Published tables and curves are contained in the references.[93,177-184]

In general, critical angles are found, beyond which total internal reflection takes place with change of phase but without loss of amplitude, while a surface disturbance appears in the second medium.

6.5.4 Reflection at a broken end

Reflection from a rough surface has been paid little attention in the scientific literature, from either a theoretical or a practical viewpoint. Some scattering of the incident wave must occur, but there appears to be no way of predicting to what extent, since the exact nature of the reflecting surface is unknown. It is expected that higher frequency waves or components of a pulse will be scattered to a greater extent than those of lower frequency. A longitudinal pulse should retain some degree of its original form but with a reduction in amplitude and extension of period.

Some researchers have studied reflection from regular, non-planar surfaces such as a sinusoidal corrugation.[185,186] The mathematics involved is extremely complex and lengthy and only simple cases of plane waves with a harmonic variation are considered.

Parker[185] has shown that if the reflecting surface is not absolutely flat, the character of the reflection is changed according to the relative roughness of the surface. Although part of the reflection will be

specular, some scattering is bound to occur. The degree of scattering is influenced by the angle of incidence of the primary wave and its frequency.

At the broken end of a concrete beam reflection will be influenced by the small scale irregularity of the surface and the larger scale configuration of the broken section.

6.6 Pulse generation by impact

In work to date on research and development of the sonic echo test, stress wave generation has been achieved by a hammer blow to the pile head.[34-41] Little attention has been paid to this aspect of the testing method. Since many of the propagation characteristics of a stress pulse are dependent on its form, an understanding of how this is influenced by the impact process is important.

The transfer of energy under impact conditions is complicated and complete mathematical analysis is difficult. Complete solutions have been obtained only for simple geometrical models utilising the laws of conservation of mass and momentum, and a mechanical energy balance. Many different approaches to the problem have been made but no general impact theory has been developed to date.

A good approximation of impact behaviour may sometimes be obtained if boundary conditions involving force or velocity are prescribed. Analyses designed for cases

of equivalent static loading frequently show wide discrepancies from the experimental evidence.[188]

6.6.1 Present approach

The approach adopted here is similar to that employed by Ripperger[152] in a study of the impact of ball bearings on long metal rods. The impact of the hammer produces stress in both the pile head and the hammer tip during the period of contact. These stresses travel away from the impact region in the form of stress pulses. The wavelength of any stress pulse so developed is then considered as a function of the contact time.

The contact problem is treated in two stages. Initially the impact of a hammer on an assumed rigid surface is examined. The influence of the hammer geometry on the dimensions of the pulse are studied, particularly with regard to the relationship between the hammer length and the wavelength of the generated signal. Secondly, the Hertz[189] theory of impact is applied to the problem to determine the contribution of elastic deformation in the contact region.

6.6.2 Impact of a rod on a rigid mass

For the purposes of the analysis the pile is considered as a rigid static mass and its vibrational behaviour is ignored. The hammer is treated as a rod in which wave propagation is considered as one dimensional, and the contact surfaces are assumed perfectly plane. These

assumptions are not realised in practice, hence the necessary further consideration in terms of the Hertz theory.

On impact, a stress wave will be generated in the hammer tip and travel back through the hammer at the bar velocity.

If the hammer velocity is v_0, then for continuity:[190]

$$v_2 = v_0 - v_1 \quad \ldots\ldots \quad (6.137)$$

where,

v_1 and v_2 are stress wave particle velocities in the hammer and the pile.

The same force acts on each of the impact surfaces and this may be equated approximately by:[190]

$$F = A_1 \rho_1 c_1 v_1 = A_2 \rho_2 c_2 v_2 \quad \ldots\ldots \quad (6.138)$$

where,

A = cross sectional area

ρ = density

Solving the above two equations simultaneously gives:

$$\frac{v_1}{v_0} = \frac{A_2 \rho_2 c_2}{A_1 \rho_1 c_1 + A_2 \rho_2 c_2} \quad \ldots\ldots \quad (6.139)$$

$$\frac{v_2}{v_0} = \frac{A_1 \rho_1 c_1}{A_1 \rho_1 c_1 + A_2 \rho_2 c_2} \quad \ldots\ldots \quad (6.140)$$

For the case of a high impedance ($A_2 \rho_2 c_2$) pile head, $v_1 \rightarrow v_0$. The tip of the hammer is therefore stationary

and a step fronted compression wave travels back through the hammer at velocity c_1 . When this compression wave reaches the free end of the hammer it is reflected as a tension wave which travels with velocity c_1 back towards the hammer tip. Particle velocity in the tension wave will be equal and of opposite sense to that in the compression wave (v_1) and the entire hammer will move with this velocity when the tension wave reaches the hammer tip. The hammer thus rebounds at its approach velocity. The hammer head develops a force on the pile head with a limiting value of $A_1\rho_1 c_1 v_0$ during the time $\frac{2L_1}{c_1}$, which the pulse takes to travel twice the length of the hammer. The stress in the pile due to this force is $\frac{A_1\rho_1 c_1 v_0}{A_2}$. Thus the stress developed in a given pile is proportional to the impact velocity and the hammer mass, i.e. the momentum.

Provided that the hammer is shorter than the pile the minimum contact time is determined by the return of the stress pulse in the hammer, and so cannot be less than $\frac{2L_1}{c_1}$.

In practice there will be energy losses associated with the stress wave travelling in the hammer and local deformation of the impact region. In addition the pile will not be perfectly rigid and static. The contact time will therefore be longer than the minimum time for the ideal case described above. Only if the hammer is of a similar length to the pile will the contact time be

affected by the returning pile stress wave.

Although the contact time may be extended by various effects the influence of the minimum time due to the hammer stress wave is strong, and there is generally a linear relationship between hammer length and contact time.[188] (Fig. 6.15).

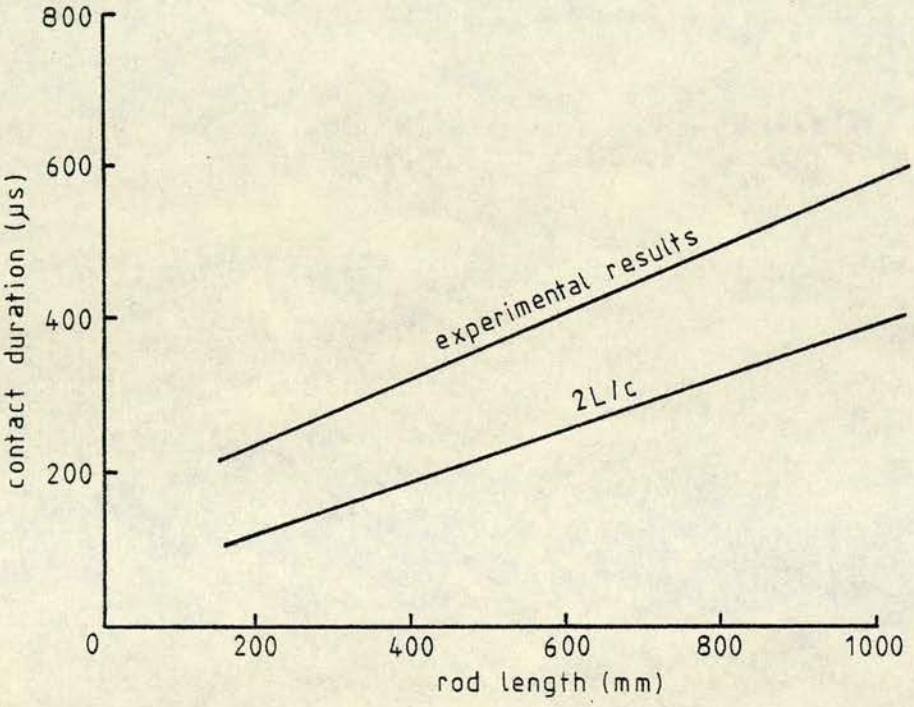

Fig. 6.15 Contact duration as a function of rod length for the longitudinal impact of a steel rod. (after Sears [191]).

6.6.3 Hertz impact theory

The above analysis is based on the assumption of instantaneous contact and uniform pressure distribution across the surfaces of the colliding bodies. This requirement demands that the surfaces are ideally smooth planes located exactly normal to the direction of relative

velocity. Such conditions are hard to achieve even under laboratory conditions. The practical difficulties inherent in achieving perfectly normal impact of plane ended rods are responsible for the almost universal use in impact experiments of bars with hemispherical ends.

A flat contact, however, means less energy loss due to plastic deformation and material degeneration. This has particular relevance in the case of pile testing where generation of the maximum amplitude stress wave is sought.

Hertz[189] developed a force-deformation relationship which describes the impact of two elastic bodies whose contact surfaces can be approximated by paraboloids in the vicinity of the impact. Such a representation encompasses a wide variety of bodies and is inapplicable only for discontinuous surfaces such as the apex of a cone or wedge.

The theory treats the contact of two bodies as an equivalent problem in electrostatics. A solution is obtained in the form of a potential which describes the stresses and deformations near the contact point as a function of the geometrical and elastic properties of the bodies. The result, though both static and elastic in nature, has been applied widely to impact situations where deformation results. The use of the theory beyond the limits of its validity has been justified on the basis that it appears to predict accurately most of the impact parameters that can be verified experimentally. The

theory is covered extensively in the references.[188,189] Only the derived formulae are included here.

From Newton's second law of motion:

$$F = -m_1\frac{d^2w_1}{dt^2} = -m_2\frac{d^2w_2}{dt^2} = -\frac{m_1 m_2}{m_1+m_2}\frac{d^2\alpha}{dt^2} \quad \ldots\ldots \quad (6.141)$$

where,

m = mass

w_1, w_2 = displacement of the two bodies along the axis of impact

$\alpha = w_1 + w_2$

The term α, called the approach, represents the relative compression of the two bodies. It is assumed that motion occurs only along the line joining the centres of gravity and that these are sufficiently far from the contact area that compression at these points is negligible.

The initial conditions are $\alpha = 0$ and $\frac{d\alpha}{dt} = v_0$, where v_0 is the impact velocity.

By integration it may be shown that:[188,189]

$$\frac{1}{2}\left[\left(\frac{d\alpha}{dt}\right)^2 - v_0^2\right] = -\frac{2}{5}k_1 k_2 \alpha^{\frac{5}{2}} \quad \ldots\ldots \quad (6.142)$$

where,

$$k_1 = \frac{m_1+m_2}{m_1 m_2}$$

k_2 is a constant representing the elastic constants E and σ and the radii of curvature of the contact surfaces

The maximum compression α_m, occurs at the instant of zero relative velocity $\frac{d\alpha}{dt} = 0$, giving:

$$\alpha_m = \left[\frac{5v_0^2}{4k_1k_2}\right]^{\frac{2}{5}} \quad \ldots\ldots \quad (6.143)$$

If the process is considered as elastic reversible deformation, then the maximum compression occurs at half the total duration of contact. Integrating equation (6.142) with change of variable $z = \frac{\alpha}{\alpha_m}$, gives the contact time:

$$t_c = \int_0^{\frac{1}{2}t} dt = 2\int_0^{\alpha_m} \frac{d\alpha}{\sqrt{(v_0^2 - \frac{4}{5}k_1k_2\alpha^{\frac{5}{2}})}}$$

$$= \frac{2\alpha_m}{v_0}\int_0^1 \frac{dz}{\sqrt{(1-z^{\frac{5}{2}})}} = \frac{4}{5}\pi^{\frac{1}{2}} - \frac{\Gamma\left(\frac{2}{5}\right)}{\Gamma\left(\frac{9}{10}\right)}\frac{\alpha_m}{v_0} \quad \ldots \quad (6.144)$$

where,

Γ = gamma function.

This reduces to:

$$t_c = 2.9432\,\frac{\alpha_m}{v_0} = \frac{2.9432}{v_0^{\frac{1}{5}}}\left[\frac{5}{4}\,k_1k_2\right]^{\frac{2}{5}} \quad \ldots\ldots \quad (6.145)$$

The general relation between α and t is represented by the elliptical integral:

$$t = \int_0^{\alpha} \frac{d\alpha}{\sqrt{(v_0^2 - \frac{4}{5}\,k_1k_2\alpha^{\frac{5}{2}})}} \quad \ldots\ldots \quad (6.146)$$

It may be seen from equation (6.145) that the total contact time varies with $v_0^{-\frac{1}{5}}$. This time is also a

function of the masses of the two bodies, represented by the constants k_1 and of the curvature of the contact surfaces as represented by the constant k_2. Fig.6.16 shows measured values of the contact duration as a function of impact velocity for the collision of two steel bars with hemispherical ends.

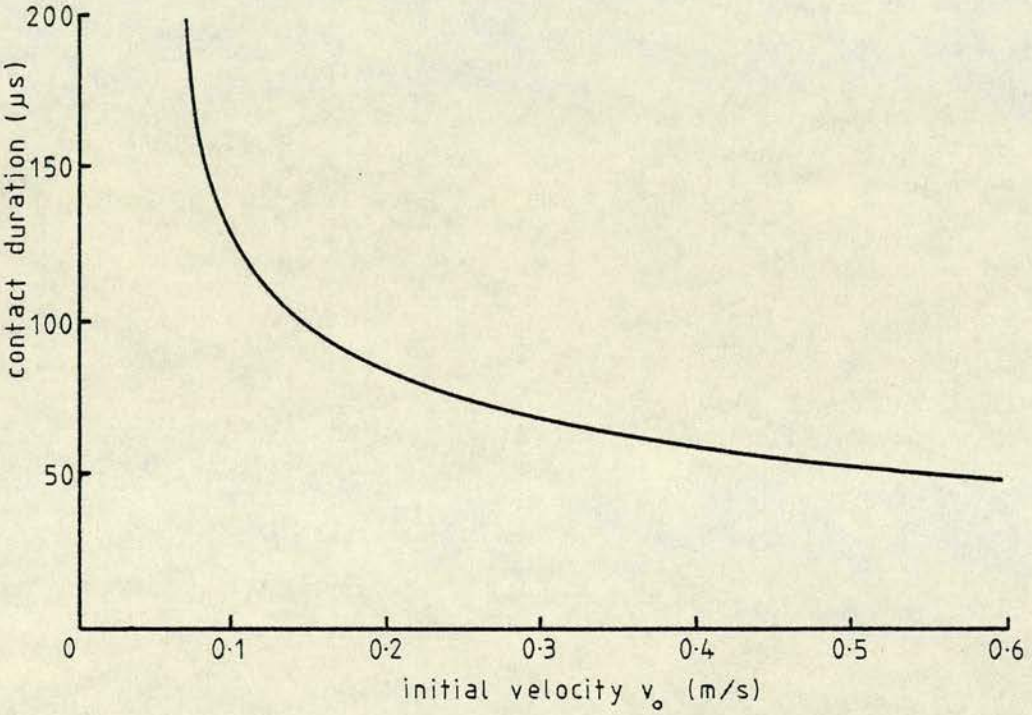

Fig. 6.16 Contact duration as a function of impact velocity for the collision of two steel bars. (After Sears[191]).

An appropriximation to equation 6.146 is:[192]

$$\alpha = \alpha_m \sin\left(\frac{1.068\, v_0\, t}{\alpha_m}\right) \qquad \ldots\ldots \qquad (6.147)$$

and the force time relation is then approximated by:

$$\left.\begin{aligned} F &= \frac{1.14\ v_0^{\,2}}{k_1\ \alpha_m} \sin \frac{1.068\ v_0 t}{\alpha_m} \quad , \quad 0 \leqslant t \leqslant \frac{\pi\ \alpha_m}{1.068\ v_0} \\ F &= 0 \quad , \quad t > \frac{\pi\ \alpha_m}{1.068\ v_0} \end{aligned}\right\} \qquad (6.148$$

A stress pulse generated by an impact, as analysed above, is thus sinusoidal in form, rising to a maximum value at time $t_c/2$. At time t_c the displacement has returned to zero, and the impacted surface is rebounding elastically free of constraint by the hammer.

For the impact of a ball bearing on the plane end of a steel rod, Ripperger[152] has used a modified form of the Hertz theory. In this instance:

$$\alpha_m = \left[\frac{5}{4} \frac{v_0^{\,2} m}{k}\right]^{\frac{2}{5}} \qquad \ldots\ldots \qquad (6.149)$$

where,

m = mass of the ball bearing

$$k = \frac{2\ E\ R^{\frac{1}{2}}}{3(1-\sigma^2)}$$

R = radius of the ball bearing.

The elastic constants were taken as identical for the two bodies. The approximation for materials with similar values of E and σ is close.[66]

Application of the theory to collisions between two rods or a rod and a semi-infinite body must have regard to the returning stress waves as discussed in section

6.6.2 (p. 158).[188] Returning tension stress waves will reduce or eliminate the contact force as shown in fig. 6.17. The degree by which the contact force is reduced by these

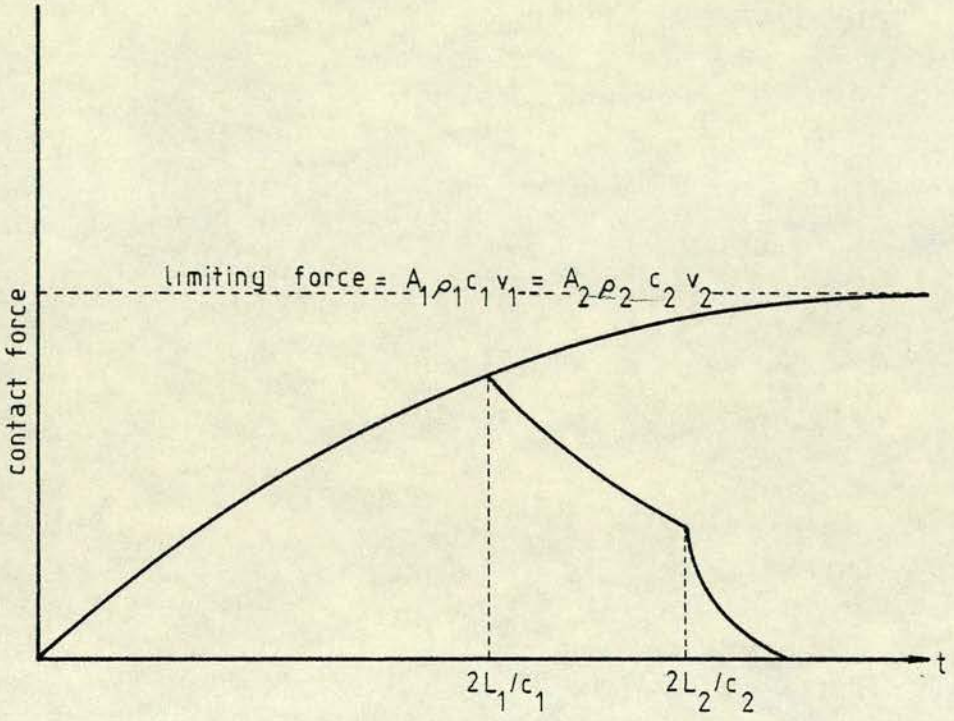

Fig. 6.17 Qualitative force history for the longitudinal impact of two circular rods. (After Goldsmith[188])

stress waves depends upon the character of the boundary conditions existing at the contact surface, and this has so far escaped precise definition.[193] Experimental work has shown that the simple assumption of perfect pulse transmission may have serious defects. The problem of contact between two plane ended bars does not appear to have been investigated.

For elastic collisions the solution is bounded by the predictions of the theory of wave propagation for

plane ended rods, and the Hertz theory in the form of equations 6.141 to 6.146.[188]

Experimental evidence indicates that plastic flow at the contact point will diminish the maximum force and prolong the duration of contact relative to a completely elastic impact which produces the same maximum indentation.[194-196]

When an impact is so severe that plastic flow occurs outwith the local contact deformation regions in the bodies, the process must be analysed by theories accounting for plastic flow and plastic wave propagation. This aspect is not considered here since for practical purposes impacts do not extend into this region.

6.7 Discussion

The many aspects of acoustic propagation in rods, dealt with in the foregoing sections, have important implications for the application of acoustic echo sounding to foundation piles. The physical characteristics of a stress wave travelling along a beam, composed of a material such as concrete, impose certain restraints on the design and application of testing equipment. A thorough knowledge and understanding of the physics of pulsed propagation through a concrete beam will contribute to successful analysis and interpretation of waveforms.

The elementary theory of longitudinal waves in bars predicts that such waves travel with a constant velocity,

$c_0 = \sqrt{E/\rho}$, known as the bar velocity. The exact Pochhammer-Chree theory shows this to be true only for wavelengths large compared to the diameter of the bar. Shorter waves travel more slowly, the limiting value being that of Rayleigh surface waves. This variation of velocity with frequency, known as dispersion, is of crucial importance in any measurement of the length of foundation piles by the use of sound transmission.

If a disturbance is started at a point on one end face of a pile, spherical waves will travel out with the dilatational velocity, c_ℓ . These waves will move along the pile and be reflected from the surface of the concrete in a complex manner. Transverse and surface waves will be generated and the transmission will become dispersive.

Elastic materials are not inherently dispersive. The dispersion effect in rods arises solely as a result of wave reflections from the boundaries, and is an interface phenomenon, not a physical property of the material.

In addition to the transverse and surface waves produced through reflection, the initial impact may generate primary transverse, surface and torsional waves. Any stress wave motion along a pile is therefore likely to involve a complex train with the bulk of the energy leading at the bar velocity.

Transverse waves display dispersion at any frequency.

Torsional waves propagate without dispersion, but at a velocity substantially less than the bar velocity. Pure torsional waves are difficult to excite. A longitudinal pulse of wavelength at least several times the diameter, thus appears to be the most suitable to obtain a measure of the length of a pile. The use of a low frequency not only ensures that propagation is at a constant and precisely known velocity, but that the pulse shape is maintained and may be recognised in a complex waveform.

Stress wave transmission may easily be employed to measure the length of a bar of regular cross section. Where the far end of a pile is flat and perpendicular a measurement may be made from the arrival time of the returning echo signal. The fixity of the pile base may be judged from the sense of the reflected signal. Where the cross section is irregular or where the end face is broken or angled some modification of the echo signal is to be expected. A reduction in amplitude will most likely occur and the period of the signal may be extended. A pile with a substantial defect such as a completely voided section is likely to produce a recognisably different waveform from that of an intact specimen.

Oscillations due to end resonance effects may be expected to some degree in the waveform as received at the pile head. In certain cases this interference may be strong enough to obscure the returning echo, and the possibility of misinterpretation exists. This problem

may require treatment by electronic signal processing.

Generation of stress waves by hammer impact has been considered satisfactory in practical application, but there has been little or no systematic study of the most appropriate form of pulse or how this may best be achieved. Although impact theory is complex and incomplete, particularly for the collision of two plane surfaces, hammer length and the impact velocity appear to be the most important parameters for consideration in equipment design.

It should be noted that most of the established theoretical and experimental treatment of impact theory and wave motion in rods has involved metals such as brass and steel. In the case of wave propagation, a variation in dynamic modulus of the material merely changes the value of the bar velocity. Poisson's ratio, which governs dispersion, has similar values for steel and concrete. Steel typically has a value of around 0.29, while a dynamic determination of Poisson's ratio for concrete yields an average value of 0.24.[187]

The elastic behaviour of concrete under impact should accord with that of metals with respect to the controlling elastic constants. As the elastic limit is approached, however, the considerable difference in behaviour will become more apparent.

6.8 Conclusions

1: A longitudinal pulse stress wave is the best form of acoustic propagation for the echo sounding of concrete foundation piles.

2: The velocity of propagation will be at the bar velocity, $\sqrt{E/\rho}$.

3: Dispersion effects will intensify with increase in pile diameter and reduction in pulse wavelength.

4: A pulse of sufficiently large wavelength will travel through the pile without significant change of form due to dispersion.

5: The wavelength of the pulse should be an order of magnitude larger than the diameter of the pile.

6: Such a pulse may conveniently be generated by an impact to the head of the pile.

7: The pulse wavelength will be governed by the impact variables, particularly those of impact velocity and hammer length.

8: Reflection from a free end, such as the base of a friction pile, will be characterised by a reflected signal display of the same sense as the impact pulse.

9: In the case of a fixed end, such as the base of a pile founded in rock, the reflected signal display will be inverted.

10: Any change in cross section along the pile will produce a partial reflection which will arrive before the bottom echo.

11: A complete discontinuity, such as a voided section or layer of soil, will produce an earlier reflection and no base echo will be present.

12: Reflection from an angled or broken end may cause a reduction in amplitude and some change of form of the reflected signal.

13: Surface waves and end resonance effects may interfere with the main signal leading to misinterpretation of the waveform.

14: Interference might be controlled by electronic signal processing.

15: Interpretation of waveforms should be conducted with reference to the theoretical and experimental analyses contained in this chapter.

7. EXPERIMENTAL WORK

7.1 Introduction

It became apparent from a study of other workers' results,[13,15,31,32,34,37,40,41] and from early field testing conducted by the author (section 4.4, p.45) that signal waveforms were frequently obscure and difficult to interpret. Three principal contributory factors were recognised:

1: Signal attenuation by the surrounding soil. Several researchers[13,15,31,32,40] had obtained substantial echo signals from piles in air, but when the piles were placed in the ground reflections became very weak or were lost.

2: Multiple reflections coming from irregular cross sections of cast in situ piles. Precast piles of regular cross section generally would produce clearer traces with stronger reflected signals than cast in situ piles of similar dimensions.[13,15,31,32,34,37,40,41]

3: Reflected signal obscured by other modulations at the pile head.[13,15,31,32,34,37,40,41] In the case of short piles the base reflection could merge with the later part of the impact signal. In longer piles while this effect was not present the reflected signal was weak and could be obscured by noise due to interference from surface oscillations at the pile head.

An experimental programme was evolved to study other relevant variables in isolation from the above interfering effects.

7.2 Experimental programme

The series of experiments described in this chapter was designed to investigate two important and distinct aspects of the testing technique:

1: Variation in the composition and operation of testing equipment.

2: Variation in pile geometry, including the nature and location of reflecting surfaces.

The first part was concerned with the generation of the acoustic pulse and its reception after one reflection.

In the second part the influence of the pile on the configuration of the received waveforms was studied.

7.2.1 Variation of equipment and the operating mode

The following variables were studied on a 10 m beam:

1: Hammer

- (a) Mass/length
- (b) Height of fall
- (c) Shape of the striking surface
  - (i) Flat
  - (ii) Pointed
  - (iii) Round
- (d) Impact location
  - (i) On the pile head
  - (ii) Relevant to transducer.

2: Transducer

(a) Type

(b) Location

(i) On the pile head

(ii) Relevant to hammer impact.

7.2.2 Influence of pile geometry

The following reflecting surfaces were investigated on a 10 m beam:

1: At the pile base.

(a) Perpendicular free end.

(b) 5 tonne end reaction on soil.

(c) Angled end

(i) 30° cut

(ii) 50° cut

(iii) 70° cut

(d) Broken end

(e) Fixed end.

2: Along the pile body

(a) Progressive cut 0.5m from fixed end

(b) Progressive cut 0.5m from free end

(c) Protrusion at mid point

(d) Protrusion at 1/4 point and at mid point.

Variation in pile diameter was studied using four 1m model piles.

Effects due to extensive cracking were examined on a 5m long model pile.

7.3 Apparatus

The testing equipment consisted of:

(a) 6 steel reinforcing rods used as hammers.

(1)	226 g	92 mm
(2)	464 g	190 mm
(3)	713 g	291 mm
(4)	961 g	393 mm
(5)	1211 g	495 mm
(6)	4455 g	905 mm

(b) Acoustic transducers:

(1) 50 kHz, 50 mm diameter piezo-electric transducers (3)

(2) 50 kHz, 30 mm diameter piezo-electric transducer

(3) exponential probe transducer

(4) geophone

(c) 75 ohm screened coaxial cable

(d) Tektronix 7632 storage oscilloscope.

(e) Telequipment DM63 storage oscilloscope

(f) Polaroid camera.

(g) Scaffold testing rig to support the equipment and provide suspension points for the hammers.

The steel rod hammers are identified by the above numbering. The rods are shown in plate 1 (appendix 1), and details of rounded and pointed tips in Plate 2.

The acoustic transducers are displayed in plate 3.

The following reinforced concrete test pieces were used:

(a) 10 m × 200 mm × 200 mm

(b) 1 m × 50 mm diameter

(c) 1 m × 75 mm diameter

(d) 1 m × 100 mm diameter

(e) 1 m × 150 mm diameter

(f) 5 m × 100 mm diameter

Each specimen was cast from a typical pile mix of 1:1½:3 and water-cement ratio of 0.5. Test cubes were cast for pulse velocity and crushing strength measurement. The 10 m beam is shown in plate 4.

7.4 Experimental technique

7.4.1 Signal generation

For convenience, the piles were tested in a horizontal position while resting on acoustically insulated supports. The steel rods were suspended from the mobile testing rig and swung in the manner of a pendulum to strike the pile. (Fig. 7.1, Plate 5).

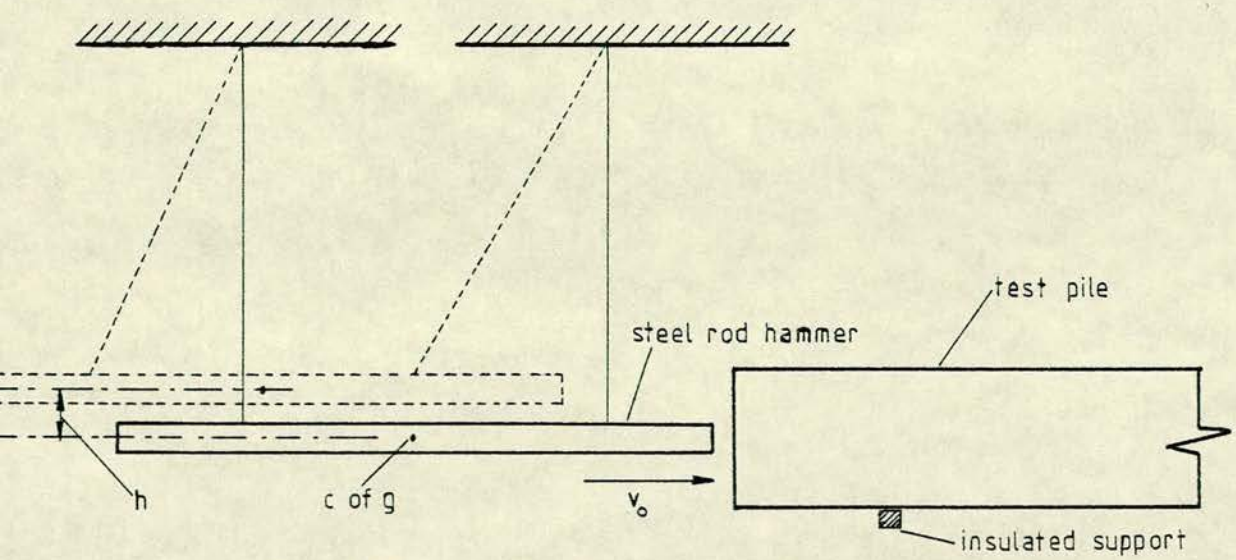

Fig. 7.1 Hammer operation

The vertical distance (h) through which the centre of gravity of the rod dropped to the rest position was measured. The impact velocity (v_0) could then be calculated from:

$$mgh = \tfrac{1}{2} mv_0^2 \quad \ldots\ldots \quad (7.1)$$

where,

m = mass of the hammer.

7.4.2 Signal reception and display

An acoustic transducer (1) was attached to the impact end of a pile under test. This transducer monitored the movement of the pile head following a blow from the hammer. When possible a second transducer (2) was attached to the other end of the pile to record the motion of the pile base.

The signals from these two transducers were displayed with respect to time on separate channels of the oscilloscope. The oscilloscope sweep was triggered either directly from the impact end transducer (1) or from a third transducer (3) placed close to the hammer impact point, (Fig. 7.2, Plate 6).

When the hammer struck the pile the modulations from transducers (1) and (2) were recorded by a single scan of the oscilloscope beam. The display was stored on the screen and a permanent record could be retained on polaroid film.

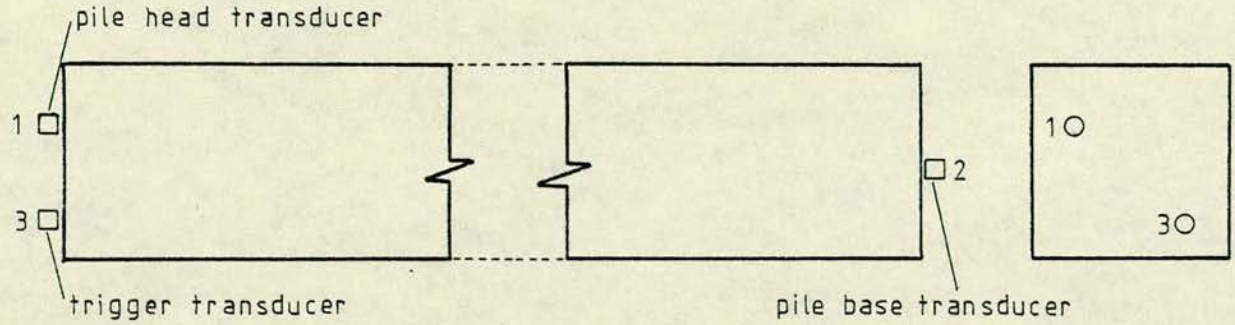

Fig. 7.2 Location of transducers

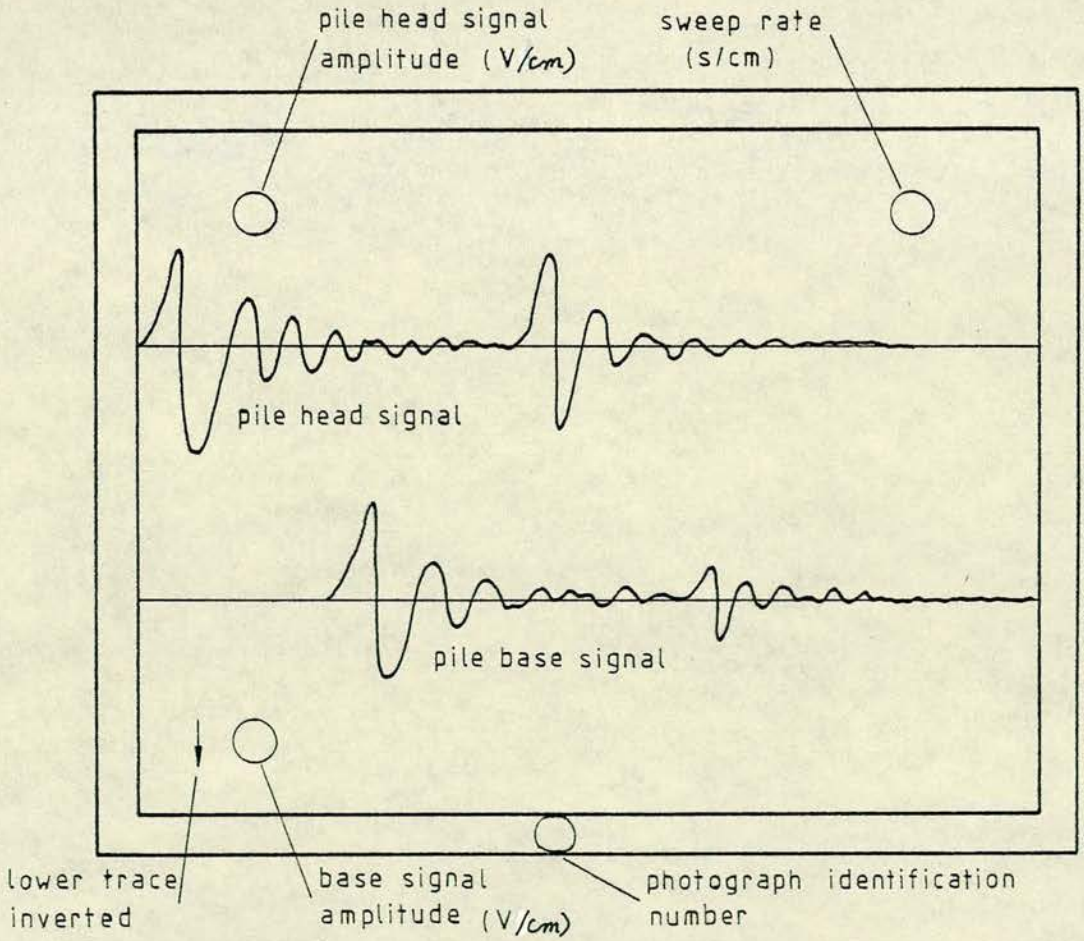

Fig. 7.3 Signal display photograph

7.4.3 Photographic records

After several hammer blows to ensure consistency of the signals, the result of each test was photographed for later interpretation. The features of the signal display photographs are shown in Fig. 7.3.

Modulation of the pile head transducer appears in the upper trace and that of the pile base transducer in the lower trace. Print outs show the vertical scales (top and bottom left) and the time base scanning rate (top right). An arrow displayed at bottom left indicates reversed polarity of the lower trace. Each photograph is identified by a number on the lower white surround. The complete series of photographic records is contained in appendix 2.

7.4.4 Transducer polarity

The polarity of each transducer connection was determined so that the direction of displacement could be related to trace movement on the vertical axis of the oscilloscope screen. An example is shown in photograph 74. This response was obtained from a light finger tap on the face of a 50 mm diameter transducer. An increase in pressure on the transducer face corresponds to a negative movement of the trace (downwards). This is followed by a positive gradient as the transducer face rebounds elastically after which the motion is quickly damped. Except in the case of some early field work, the above polarity was adopted for all transducers throughout the testing programme.

7.4.5 Interpretation of waveforms

When the transducer polarity is known, the waveforms may be interpreted in terms of the direction of displacement of the pile surface. A longitudinal compression wave arriving at the end of a pile produces a pressure increase at the transducer face and hence an initial negative displacement in the signal, (as in photograph 74). The arrival of a tension wave has the opposite effect. The signal polarities for the four possible combinations of wave type and direction of propagation relative to the transducer face are shown in fig. 7.4.

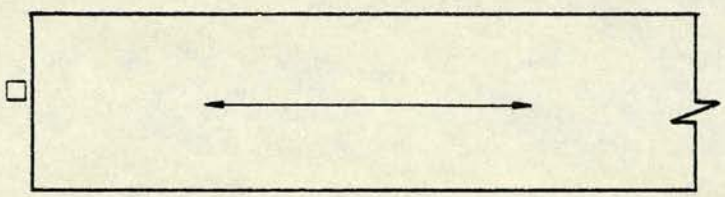

WAVE & DIRECTION	SIGNAL POLARITY
← compression	-
← tension	+
→ compression	+
→ tension	-

Fig. 7.4 Signal polarity due to wave type and direction

It is evident that the pile base transducer faces in the opposite direction to the one on the pile head. Thus a compression wave leaving the pile head after a hammer blow (compression wave away from transducer face, +ve signal)

has the opposite effect on arrival at the pile base (compression wave towards transducer face, -ve signal).

To facilitate visual comparison of the two traces, the lower trace (pile base transducer) was always used in the inverted polarity mode. This is indicated by the downwards pointing arrow on the print out, immediately adjacent to the lower trace scale reading.

7.4.6 Transducer contact check

Before commencing a series of tests, involving both pile head and pile base transducers, a simple procedure was adopted to verify a balanced response. The upper and lower traces were merged on the centre line of the display with a suitable time scale. (photograph 75). If the two transducers were responding equally a smooth exponential decay curve would be obtained. A weak irregular signal from any transducer indicated a poor contact with the concrete surface and this could be corrected before testing.

Signal peaks alternate between the head and base transducers. The weaker initial response from the pile head transducer (first signal peak) stems from a shear wave component on the pile head, whereas the later peaks are due to the fully developed longitudinal wave front.

7.5 Results and analysis

The reasoning behind the experimental programme, as outlined in section 7.2 (p.175), was based on parallel considerations of fundamental research of the physics,

and the establishment of criteria for equipment design.

The method of analysing the results was dictated partly by the above considerations and partly by the complex interdependent sequence of events between a hammer impact and the arrival of the first reflected signal. This pattern of influence governing the amplitude and period of the echo signal is shown schematically in fig. 7.5

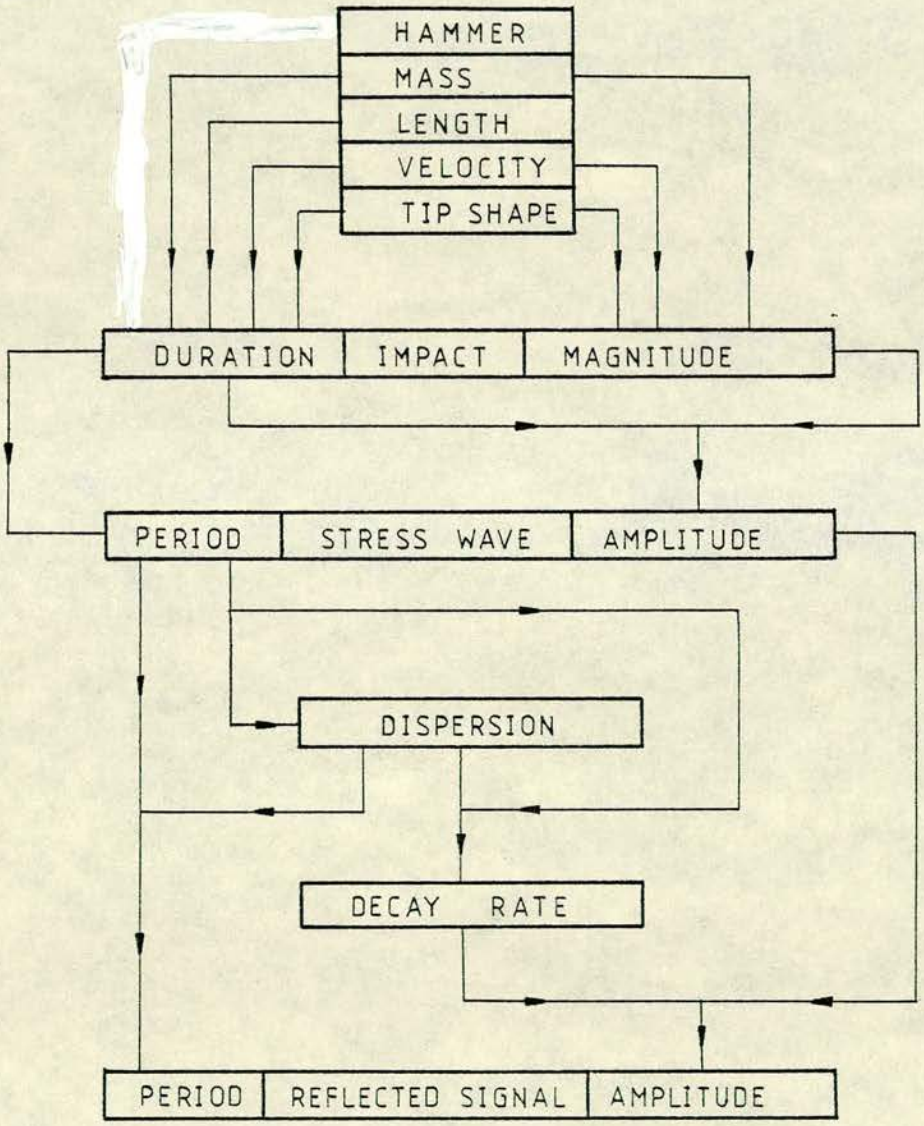

Fig. 7.5 Schematic representation of impact-echo event sequence

The first reflected signal is the one upon which the sonic echo test is based. The influence of variables on the form and magnitude of this signal is therefore of primary interest for the purposes of equipment design.

Measurements for the analysis were taken from the photographic records contained in appendix 2. Tables of results are shown in appendix 3, and graphs in appendix 4.

The main characteristics of the waveforms and the measurements taken from them are shown in fig. 7.6.

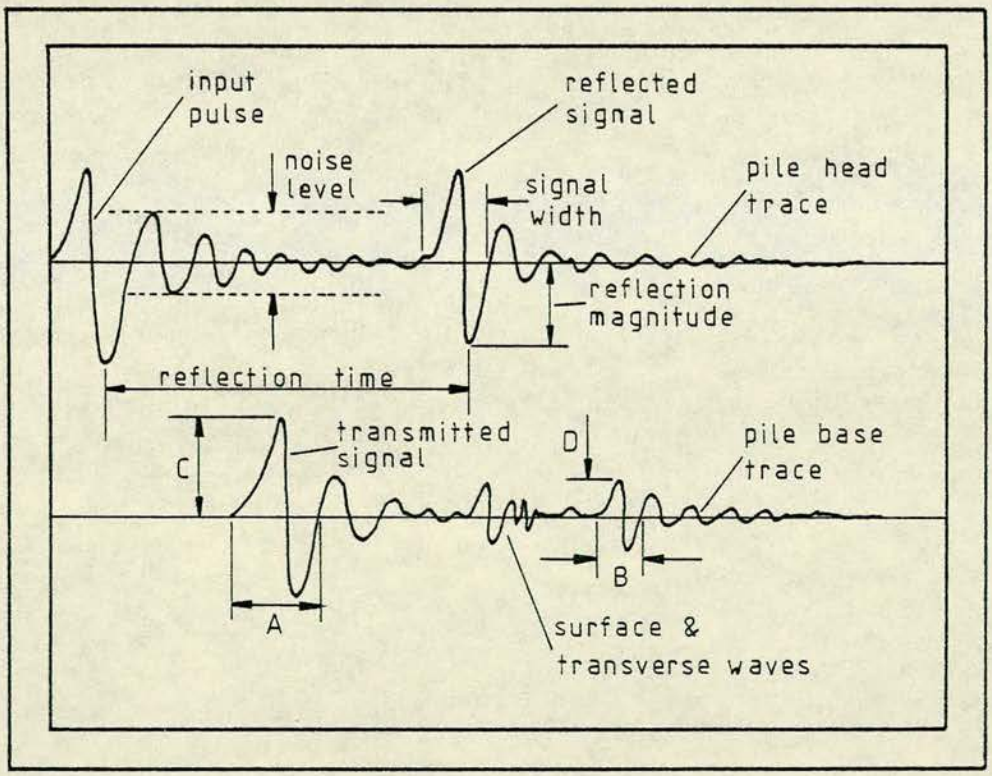

Fig. 7.6 Waveform characteristics and measurements taken.

7.5.1 Hammer variables

7.5.1 (a) Hammer mass/length and drop height

Bars 1, 5 and 6 were dropped from heights varying between 1 mm and 400 mm onto the 10 m beam. (Photographs 76-129). Large transducers (50 mm dia.) were used at both ends of the beam. The following measurements were taken.

(i) Reflection time (Table 4)

Measured between the impact signal and the first reflection at the pile head transducer, upper trace, (fig. 7.6). The time interval was constant within the limits of measurement (1 scale division = 0.2 ms). The average value for the 54 tests was 5.25 ms, giving a velocity over the 20 m path length of c_0 = 3810 m/s.

Measurements on test cubes (Table 3) at 28 days gave an average value of c_ℓ = 4222 m/s.

$$\rightarrow \quad \frac{c_0}{c_\ell} = 0.9 \ .$$

Measurements across the beam cross section (Table 3) gave an average value of c_ℓ = 4201 m/s

$$\rightarrow \quad \frac{c_0}{c_\ell} = 0.91 \ .$$

For 28 day old concrete of a typical pile mix (1:1½:3, w/c = 0.5) pulse velocity lies between 3800 m/s and 4200 m/s (section 3.2.4). The bar velocity c_0 is typically 0.9 c_ℓ (section 5.2.2 (a)). At the

frequencies generated in the tests, propagation was within the region of the dispersion curve where $c_g/c_0 = 1$, (fig. 6.3).

(ii) Reflected signal magnitude (Table 5)

The measurement was taken from the rebound peak of the reflected pulse since this part of the signal was the most consistent, (see photograph 75). Graphs 1-3 show variation of reflected signal amplitude with drop height for the three bars.

It should be noticed that the reflected signal amplitude does not increase linearly with drop height, whereas the kinetic energy of the hammer does. Thus there is a diminishing return in terms of signal strength with increasing energy in the hammer blow.

From equation 6.143 it may be seen that the maximum relative compression (α_m) between two colliding bodies is determined by $v_0^{\frac{4}{5}}$. If it is assumed that displacement in one body forms a fixed proportion of the compression term, then that displacement will also vary with $v_0^{\frac{4}{5}}$. Displacement at one end of a body propagates through the material in the form of a stress pulse whose amplitude and period are determined by the initial surface displacement. Thus signal amplitude must vary in proportion to α and hence to $v_0^{\frac{4}{5}}$. Graph 4 shows reflected signal amplitude as a function of $v_0^{\frac{4}{5}}$ for the three bars.

It should be observed that there is a signal loss due to attenuation in the concrete between the input signal

and the first reflection, during which the pulse has travelled 20 m. This signal loss is not at a constant rate because of signal period variation (see below), and so this variation forms part of the impact-reflected signal sequence. (fig. 7.5).

The echo signal is controlled primarily by the impact variables, however, and the connection between these variables and the form of the stress wave is persistent.

With this consideration, the measurements were taken from the reflected signal since the impact signal magnitude was found to vary in an apparently random manner. Additionally, the direct link between the impact variables and the reflected signal is of interest for practical application of the method, as mentioned above.

In equation 6.143 , $k_1 = \frac{m_1+m_2}{m_1 m_2}$.

If m_1 is the mass of the hammer and m_2 that of the pile, then, when m_2 is constant and $m_2 >> m_1$ the constant k_1 will be determined by $\frac{1}{m_1}$. Thus, from equation 6.143 α_m and therefore reflected signal amplitude, will vary with $m_1^{\frac{2}{5}}$.

In Graph 5 reflected signal amplitude is plotted as a function of (bar mass)$^{\frac{2}{5}}$, with drop height (or impact velocity) as a parameter. The relationship is apparent except towards the higher end of the velocity range. At this level of energy input from bar 6,

plastic deformation in the steel bar and degredation of the concrete was detected. This implies a consequential reduction of amplitude of the generated stress wave.

Graph 6 shows reflected signal amplitude as a function of $m^{\frac{2}{5}} v_0^{\frac{4}{5}}$. The values for the three bars generally follow the same line. The relationship therefore holds for all bars.

(iii) Reflected signal period (Table 6)

The period of one complete cycle of the reflected signal was measured (fig. 7.6). This is a measure of the signal wavelength which may be computed from:

$$\Lambda = P c_0 \qquad \ldots\ldots \qquad (7.2)$$

where,

P = period of signal cycle.

Graph 7 shows the reflected signal period plotted against drop height for the three hammers.

The initial signal period is determined by the impact duration, itself a function of the impact velocity, as examined in section 6.6.

Reflected signal period as a function of impact velocity is shown in Graph 8. The trend of decreasing period with increasing velocity displays a similarity to the contact duration/impact velocity curve in fig. 6.16. Impact contact duration and thus the initial stress wave period have been shown to vary with $v_0^{-\frac{1}{5}}$, equation

6.145 (section 6.6.3). Reflected signal period as a function of $v_0^{-\frac{1}{5}}$ is shown in Graph 9. It may be seen from this graph that the reflected signal period is heavily dependent on the impact velocity according to the same ratio. Therefore the rate of widening of the pulse between the impact and the reflected signal must be constant.

Measurements of the rate of increase in signal period were taken between the first and second signals at the pile base (lower trace fig. 7.6, A and B). The results, as given in table 7, indicate a constant rate of signal period increase (dispersion) through the range of impact velocity.

From the examination in section 6.6.2 it is evident that the contact period is dependent on the lengths of the colliding bodies, according to the stress wave reflection time of $\frac{2L}{c}$. In the case of a short hammer and long pile the returning pile stress wave may be disregarded. By the identical argument applied to the reflected signal amplitude, equation 6.145 predicts a variation of contact time according to the function $m^{\frac{2}{5}}$. The stress wave period is thus related to hammer length and mass.

Within the range of bars used as hammers during the tests mass and length varied as integral quantities. In the absence of discrete variation of these quantities, the relationship was analysed according to:

$$P = f\left[v_0^{-\frac{1}{5}}, (Lm)^x\right] \quad \ldots\ldots \quad (7.3)$$

with x to be determined.

The standard method was employed with:

$$\log P = x \log(Lm) + \log(v_0^{-\frac{1}{5}}) \quad \ldots \quad (7.4)$$

Values of signal period were plotted against the product Lm on log scales, (graph 10). Several lines were drawn at constant velocity. Averaging the gradients yielded a value for the exponent of 0.1. Graph 11 shows variation of reflected signal period with $(Lm)^{0.1}$. In graph 12 signal period is shown as a function of $(Lm)^{0.1}\ v_0^{-\frac{1}{5}}$. It may be seen that the relationship extends across the range of length and mass represented by the three bars.

An extended study of the reflected signal period was conducted using bars 1 - 6, (photographs 130-153). Four different energy inputs to the beam were adopted and the hammers were swung from heights according to their mass where:

$$\text{Energy} = m\ g\ h$$

The results are given in table 8. Graph 13 shows that the above relationship applies independently of individual hammer values of length, mass and velocity.

(iv) Attenuation (Table 9)

The attenuation or rate of decay of the propagating pulse was measured between the positive half cycle

amplitudes of the transmitted signal and the pile head reflection, as displayed on the lower trace, (fig. 7.6, C and D). The random amplitude of the impact signal precluded a measurement from the upper trace. Over the time interval t , the change in amplitude level is given by:

$$\Delta = \frac{20 \log_{10}\left[\frac{C}{D}\right]}{t} \quad \ldots\ldots \quad (7.5)$$

The measurements taken and the calculated attenuation rates are given in table 9. In graphs 14 - 16 the calculated attenuation rates are plotted as a function of the hammer drop.

Signal attenuation is due to diffraction, scattering and absorption, (section 5.2.3). At the low frequencies generated in the tests (section 6.4.3) most of the attenuation would be caused by absorption. In general the attenuation due to absorption is proportional to the frequency of the transmitted wave, (section 5.2.3 (c)). Graphs 17 - 19 show decay rate as a function of the reflected signal period reciprocal, i.e. the frequency. The attenuation rate increases with frequency and a linear trend is discernable within the scatter of the points.

(v) Signal/noise ratio (Table 10)

The reflected signal amplitude was compared to the noise level over the period from the impact to the first

reflection. Peak to peak noise was measured since the oscillations were evenly distributed on either side of the zero axis, e.g. photograph 108 . The measurements and the calculated signal to noise ratios are given in table 10.

In graphs 20 - 22, signal to noise ratio is plotted as a function of the hammer drop height. The ratio decreases with the height of fall but the relationship is not linear. The trend follows that of the signal period variation with drop height, (graph 7). This suggests that the generated noise is related in some way to the signal frequency.

The noise preceding the reflected pulse is probably due to surface oscillations of the pile head (sections 6.2.4, and 6.4.4). The velocity of surface waves is approximately 0.5 c_ℓ (sections 3.2.3, 5.2.2 (c), and 6.2.4). From the beam cross section measurement of c_ℓ = 4201 m/s (table 1), the period of travel of a surface wave across the pile head, (200 mm) is:

$$\frac{0.2}{0.5 \times 4201} = 95.2\ \mu s$$

and therefore the frequency of oscillation is:

$$\frac{1}{95.2 \times 10^{-6}} = 10.5\ kHz \quad .$$

If the square section beam is considered as an equivalent cylinder, then from equation (6.103), the equivalent

diameter is:

$$1.13 \times 200 = 226 \text{ mm},$$

giving a frequency of end oscillation of 9.3 kHz. Measurements of this surface noise frequency may be taken from the photographs by counting signal peaks across a time interval. For example:

Photograph 81, bar 1, 21 cycles in 2.1 ms → 10 kHz

" 108, bar 5, 18 " " 2.7 ms → 6.7 kHz

" 125, bar 6, 16 " " 1.8 ms → 8.9 kHz

As the hammer drop is increased the generated signal frequency increases (graph 7). As this frequency approaches that of the natural end oscillation frequency a resonance effect is likely to occur. This would result in a reduced signal/noise ratio with rise in frequency as obtained in the tests.

Signal/noise ratio for the period from impact to 1.5 times the reflection time was measured (table 11). The variation with hammer drop is shown in graphs 23-25. For practical purposes this covers the range of noise amplitude which could interfere with the reflected signal.

7.5.1 (b) Hammer tip variation (Table 12)

Hammer tip configurations of a 45° conical end and a hemispherical end were compared to the results for a flat ended bar, (photographs 81-90). Bar 5 was used from drop heights of 20 mm and 200 mm, with large (50 mm dia) transducers at either end of the beam. The pointed end results were taken after the first blow and again after

several blows by which time the hammer point had bedded into concrete at the impact point.

From table 12 it may be seen that the reflection time was again constant throughout the tests. Reflected signal amplitude was substantially better for the flat ended impact. The reflected signal period was extended in the case of the hemispherical tip. This follows the reasoning of the Hertz impact theory (section 6.6.3), where greater elastic penetration by the rounded surface results in an extended impact time.

The attenuation rates and signal to noise ratios were not significantly different within the experimental error bounds.

7.5.1 (c) Impact location (Table 13)

The location of the hammer impact on the pile head was varied through several different transducer positions, (photographs 164-195). Bar 5 was used from drop heights of 20 mm and 200 mm, with large (50 mm dia) transducers at either end of the beam. The reflection time was constant. Reflected signal amplitude and period, attenuation rate and signal/noise ratio did not show any related variation. The amplitude of the input pulse (1st signal on upper trace) displayed a marked fluctuation. This fluctuation was in general random, with a trend of lower amplitude with greater transducer-hammer separation. Graphs 26-27 show the variation of input signal amplitude with transducer-hammer distance. The input pulse arrives

at the transducer as a surface wave radiating out from the impact point. Increased attenuation with distance travelled concurs with the experimental results.

Measurements were also taken of the impact/rebound ratio (I/Rb) of the input signal, (section 3.2.4). The values fluctuated by a factor of three.

The random nature of the input signal obtained from one pile appears to invalidate any measurements from this part of the trace for a comparison between different piles. This applies to the impact/rebound ratio (I/Rb) and the system decay rate (SDR) as suggested in section 3.2.4.

7.5.2 Transducer variables

7.5.2 (a) Transducer type (Table 14)

Four transducer types were compared over a range of measured parameters. Bar 5 was used from drop heights of 20 mm and 200 mm. A large (50 mm dia) transducer was used to monitor the signals at the pile base (lower trace). The results are shown in photographs 196-203.

The reflection time was constant across the range of transducers. The exponential probe transducer showed the maximum reflected signal amplitude. Measurements of reflected signal period and signal/noise ratio, however, indicated the large (50 mm dia) transducer to be the most suitable of the devices tested in this instance.

7.5.2 (b) Location (Table 13)

The transducer location experiments were conducted in conjunction with those of the impact location, (section 7.5.1 (c), photographs 164-195).

The reflection time, reflected signal amplitude and period, attenuation rate, and signal/noise ratio were independent of transducer location. Input signal amplitude varied with hammer-transducer distance as measured in section 7.5.1 (c).

When the transducer was remote from the centre of the pile head, reflected surface and transverse waves appeared on the trace, (e.g. photograph 188, upper trace). From section 5.2.2:

$$c_t = 0.55\ c_\ell$$
$$c_R = 0.5\ c_\ell$$
$$c_0 = 0.9\ c_\ell$$
$$\therefore\ c_t = 0.61\ c_0$$
$$\text{and}\quad c_R = 0.56\ c_0$$

Measuring the reflection times from the upper trace of photograph 188 :

reflection time at c_0 = 5.1 ms

" " " c_t = 8.6 ms

$\rightarrow$ $c_t = 0.59\ c_0$

reflection time at c_R = 9.1 ms

$\rightarrow$ $c_R = 0.56\ c_0$

To detect the transverse and surface waves after a single

transmission through the beam, the pile base transducer was moved off centre, (e.g. photograph 165, lower trace). Measuring the transmission times from the lower trace:

transmission time at c_0 = 2.5 ms

" " " c_t = 4.1 ms

→ c_t = 0.61 c_0

transmission time at c_R = 4.7 ms

→ c_R = 0.53 c_0

In general the transverse waves were generated by an off centre impact (e.g. photograph 172). However, the transducer would not pick up these waves when it was placed centrally, (e.g. photograph 178).

7.5.3 Pile base variables (Table 15)

Bar 5 was used from drop heights of 20 mm and 200 mm. One large transducer (50 mm dia) was placed at the pile head, and another at the pile base when the particular experimental conditions permitted.

To aid comparison of values between the tests the results are grouped in two series corresponding to the 20 mm and 200 mm drop heights, (photographs 204-218 and 219-232).

7.5.3 (a) End reaction on soil

To examine the reflected signal from a pile base founded on soil, the 10 m beam was jacked hydraulically against a soil bank, (plate 7). Records of the

reflected signal were taken with zero reaction and with the load cell reading 5 tonnes, (plate 8).

The measurements, (table 15) showed the reflection time unchanged by the base reaction. Reflected signal amplitude was reduced and the signal period lengthened slightly. Signal/noise ratio was unaffected. The results agree with the theory of reflection from an acoustically less dense medium, displaying partial refraction and a reflection at reduced amplitude without change of phase, (section 6.5.1).

7.5.3 (b) Angled end

The base end of the 10 m beam was cut at angles of 30°, 50° and 70°, (plate 9 (30°), plate 10 (50°). Measurements from trace records of the tests showed:

(i) Increased reflection time

(ii) Reduced reflected signal amplitude

(iii) Extended reflected signal period

(iv) Increased attenuation

(v) Less favourable signal/noise ratio.

The increased reflection time of between 10% - 13% introduces a corresponding error into the calculation of pile length based on the bar velocity, and this has important implications for practical application of the method.

The reduction in reflected signal amplitude stems from partial conversion of the incident longitudinal wave into a reflected transverse wave, (section 6.5.3). The

results do not follow the predictions of Arenberg's curves, however, (fig. 6.13) of variation of reflected signal amplitude with angle of incidence. In addition, on an extended time scale (photographs 208,210,212,223,225, and 227) there was no evidence of transverse wave generation. The reasons for this are not clear but it should be noted that previous theoretical and experimental work has dealt with reflection at an infinite boundary between two surfaces (half space) and not at the extremity of a waveguide.

7.5.3 (c) Broken end

The beam end was broken to simulate reflection from a cast in situ pile base, or discontinuity, or from a break in a precast pile, (plate 11).

Results were similar to those obtained with the angled ends. The extended reflection times of 5.9 ms - 6.1 ms were measured over a shorter pile length of 9.6 m to the broken surface, giving an error in estimation of the pile length of 18% - 22%. The double reflection probably originated from the protruding steel reinforcement, (photographs 213,228).

On an extended time scale it can be seen that subsequent reflections were weak and would be difficult to detect outwith the ideal laboratory conditions, (photographs 214, 229).

The extended signal period confirms the thesis of section 6.5.3 that higher frequency components of the pulse

are more readily scattered by a non specular surface.

7.5.3 (d) Fixed end

The base of the 10 m beam was cast into a large mass of concrete, (plate 12 and plate 13). The length of beam up to the mass was 9 m, and the measured reflection times of 5.2 ms - 5.4 ms gave an error in the calculated pile length of 11% - 15%.

The reflected signal amplitude, attenuation rate and signal/noise ratio were comparable to those obtained from the broken end. The signal period was greatly extended, this possibly resulting from the ill-defined boundary of the concrete mass.

The expected inversion of the reflected signal phase was evident. With extended time scale and amplitude magnification (photograph 217) the inversion of alternate reflections can be seen.

7.5.4 Change of cross section (Table 16)

Bar 5 was used from a drop height of 200 mm. A large (50 mm dia) transducer recorded signals at the pile head. A base transducer was precluded by the nature of the experiments.

7.5.4 (a) Progressive cut 0.5 m from fixed end

The beam cross section was cut progressively at 8.5 m, i.e. 0.5 m in advance of the fixed end at 9.0 m. Measurements were taken of the fixed end reflected signal until it was attenuated to zero, (photographs 230, 233-240).

Likewise, the reflected signal from the cut was measured from the point of its appearance. Graph 28 shows the amplitudes of the two reflected signals as a function of the percentage cut through the cross section. The decay of one signal and the rise of the other are approximately linear with change in the cut area. It can also be seen that the free-end reflection is of considerably larger amplitude than the fixed end reflection in this instance, with similar amplitudes at 50% cut area. A completely fixed end, where the holding device has no dimension in the longitudinal direction, is difficult to achieve. Thus the signals obtained in the tests were of lengthened period and reduced amplitude compared to the perfect free end case. The signals may reasonably be expected to improve with increased efficiency of the fixity.

Graph 29 shows the variation of signal attenuation with increase in cut area. The attenuation rate was measured between the input signal and the reflected signals. The input signal displays some random variation and is not due to a plane fronted longitudinal wave (sections 7.5.1 (c) and 7.4.6). However, this was the only means of determining the attenuation in this series of tests, and the measurements serve to show relative loss in amplitude between the fixed and free end reflected signals.

From the graph it may be seen that the cross over in attenuation of the two signals occurs at approximately 50% cut area.

In graph 30 the signal/noise ratios of the two reflections are shown as functions of the cut area. The cross over point is near to the 50% cut area point.

It is apparent from the three graphs that the amplitude, attenuation rate and signal/noise ratio of the reflection from a discontinuity, show improvement with increase in area of reflecting surface. Conversely, reflections from points beyond the point become progressively weaker.

7.5.4 (b) Progressive cut 0.5 m from free end

The beam cross section was cut progressively at 8.0 m, 0.5 m in advance of the free end at 8.5 m. Measurements were taken of the reflected signal from each surface, (photographs 240-245).

Graph 31 shows the rise and fall of the respective signal amplitudes as the cut area is increased. The variations are approximately linear. The cross over point is in the region of 65% cut area, and the base echo generally displays a proportionately stronger signal. This may be explained by diffraction of the signal around the partially cut section. At the free end base, however, total reflection must occur across the surface.

Graphs 32 and 33 show the variation of attenuation rates and signal/noise ratios. The trend is similar to the above case with the base reflection displaying slightly more favourable ratios.

Plate 14 shows the beam after the complete cuts

at 8.5 m and 8.0 m.

7.5.4 (c) Protrusion at mid point

A large obstruction was cast around the mid point of the beam (4 m), with dimensions of 500 mm × 200 mm, (plate 15). Bar 5 was used at a drop height of 200 mm.

From photograph 246 the following signals may be seen:

A - Base reflection at reflection time of 4.8 ms

B - Inverted reflection from protrusion

C - In phase secondary reflection from protrusion

D - In phase transmitted signal

E - In phase secondary transmitted signal.

The base reflection time may be compared to the reflection time in the unobstructed 8.0 m beam of 4.6 ms., (table 16). The error in length estimation is therefore in the region of 4%. Signal amplitude, attenuation rate and signal/ noise ratio are likewise adversely affected.

The inverted reflection from the obstruction occurs at 2.3 ms, corresponding to a path length to the reflection point of:

$$\frac{2.3}{4.8} \times 8 \quad = \quad 3.83 \text{ m} \quad .$$

This is approximately in line with the front of the obstruction at 4 - 0.1 = 3.9 m, (fig. 7.7).

The secondary reflected and transmitted signals stem from a transverse wave which travels to the lateral extremities of the obstruction and reflects to the beam, (fig. 7.7). When this reflected transverse wave encounters

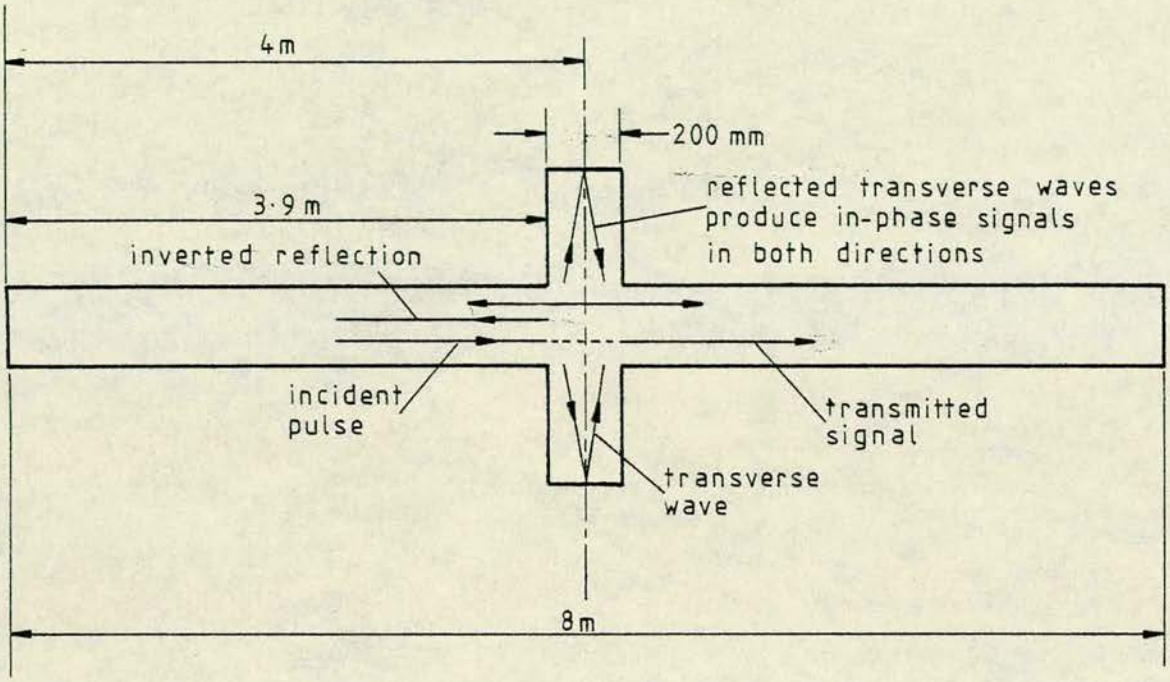

Fig. 7.7 Reflection and transmission at an obstruction

the beam it generates a longitudinal pulse which propagates in either direction along the beam away from the obstruction. These pulses give rise to the secondary in phase reflected and transmitted signals.

The amplitude of the base reflection (A) is reduced by the intervening obstruction. The decay rate is little changed, but the signal to noise ratio is extremely poor. In addition to the above reflections, multiple reflections are set up between the obstruction and the ends of the pile, resulting in a complex waveform.

7.5.4 (d) Protrusions at the mid point and quarter point

A second identical obstruction to the above was cast at the quarter point of the beam, 2 m from the head, (plate 16).

Photograph 247 shows the signal received at the pile head transducer (upper trace) and at the base transducer (lower trace). No base echo is detectable from among the multiplicity of reflections. Only the out of phase first reflection from the first obstruction may be identified with any certainty (A). On the lower trace it may be seen that a secondary in phase signal (B) has greater amplitude than the initial pulse (C). Thus even if this signal were returned unmodified to the pile head, the wrong echo signal would be identified in the absence of a base transducer.

Photographs 248 and 249 show respectively, on the lower traces, the arrival of the signals at the extremities of the first and second obstructions. Note that these traces are not inverted. The relative amplitudes of these signals indicate that much of the signal energy does not pass the first obstruction.

With the multiplicity of reflections between obstructions and the beam ends, and the fact that the initial pulse is not the strongest arrival at the base, it is clear that detection of and measurement from a base echo is impossible in this instance.

7.5.5 Variation in pile diameter (Table 17)

The influence of pile diameter was studied on four 1 m test piles of different diameters. Bar 1 was used from a drop height of 10 mm, and bar 5 from a height of 5 mm, (photographs 250-253 and 254-257).

From equations (6.143) and (6.145) it may be seen that both the generated signal amplitude and period vary according to $(k_1)^{\frac{2}{5}}$,

where,

$$k_1 = \frac{m_1 + m_2}{m_1 m_2}$$

m_1 = mass of the hammer

m_2 = mass of the pile.

Graphs 34-37 show variation of the reflected signal amplitude and period with $(k_1)^{-\frac{2}{5}} = \left(\frac{m_1 m_2}{m_1 + m_2}\right)^{\frac{2}{5}}$. The trend indicates an increase in the measured parameters with rise in the value of $(k_1)^{-\frac{2}{5}}$. This series of tests was by no means exhaustive, and further examination is warranted.

When $m_2 >> m_1$, the constant k_1 alters little with large change in pile diameter. Thus, for practical purposes, control of the measurable parameters may be attained by attention to the hammer variables.

7.5.6 Effects due to cracking (Table 18)

Cracking in a pile was studied using a 5 m × 100 m

diameter model pile. The pile was extensively cracked throughout its length with complete cracks through the cross section at approximately one metre intervals. Bar 5 was used through a range of drop heights of 5 - 300 mm.

Measurements from the photograph records (photographs 258-288)showed the reflection time gradually increasing from 4.2 ms to 5.0 ms in the course of testing. Repeated blows from the hammer increased the concrete degradation, reducing the pulse velocity and increasing the propagation time. The reflection times correspond to a bar velocity c_0 of 2000 - 2381 m/s, which is substantially lower than the velocity obtained on the 10 m beam of 3810 m/s.

The reflected signal magnitude was erratic but approximately followed the variation of $v_0^{\frac{4}{5}}$ (graph 38) as previously established in section 7.5.1 (a).

The signal period did not change with the drop height as previously but oscillated about a mean value of 1.0 ms.

Signal attenuation was generally a little higher than observed on the 10 m beam, but did not show any increase with drop height as before. Signal to noise ratio was very poor and became worse during the course of the tests. Towards the higher range of drop height large reflections were received from cracks near to the head of the pile (photographs 275-288).

7.6 Discussion

Most practical research carried out on the acoustic echo method of pile integrity testing has been undertaken

on piles in situ, or on small laboratory test specimens of metal or concrete.

The value of work on piles has been limited by soil attenuation of the test signal, and by the ill-defined or unknown boundary conditions along the pile body and at the base. Earlier work on metal specimens has been valuable in establishing the theory of stress-wave propagation in cylinders. However, in direct application to concrete piles much of the theory must be considered with reference to the widely different rates of attenuation in these materials and the very low frequencies which are consequently imposed on testing of large concrete members.

The use of short laboratory specimens of metal or concrete has been of limited value because of the small time separation between the input and reflected signals. Additionally there has been a lack of experience with full size testing apparatus under laboratory conditions to determine equipment design and establish operation procedure.

The experimental work described above has attempted to provide a systematic analysis under closely controlled conditions, while retaining some of the realities of full size operation. In this respect the exercise has sought to bridge the gap between laboratory work and site investigations on construction piles.

The salient points arising from the experimental work are discussed under the headings of equipment and pile variables.

7.6.1 Equipment

One of the most important conclusions from the testing programme is that for the conditions studied no variation in the signal generation or receiving apparatus has any influence over the velocity of pulse propagation. Within the range of frequencies required for pile testing, stress wave pulses travel at the predicted bar velocity, $c_0 = 0.91\, c_\ell$. Thus the reflection time is constant and estimation of pile length is not affected by the form or operational mode of equipment.

The reflected signal amplitude has been shown to conform with the Hertz impact theory, varying with $m^{\frac{2}{5}}$ and $v_0^{\frac{4}{5}}$. Thus the primary variable controlling signal amplitude is the impact velocity. It should be noted, however, that the signal wavelength decreases with increasing velocity $(v_0^{-\frac{1}{5}})$ in accordance with the Hertz theory. Therefore when increased impact velocity has resulted in an unacceptably short signal, recourse must be made to a heavier hammer in order to improve the signal amplitude.

The reflected signal period, while varying with $v_0^{-\frac{1}{5}}$ as predicted, did not appear to follow the theoretical variation with hammer mass and length. Nevertheless, the derived empirical relation has demonstrated an increase of signal period with hammer length and mass. Further treatment of this aspect is required to identify separate relationships.

The signal wavelength should be considered from the

point of view of attenuation, which increases linearly with rise in frequency. Likewise the signal/noise ratio becomes less favourable with increased impact velocity.

Thus a compromise must be sought between the best signal amplitude and a signal period commensurate with an acceptable attenuation rate and signal/noise level. The limiting factor for increased velocity is obvious visible degradation of the concrete surface, at which point there is a marked fall off of energy transfer from the hammer to the pile stress wave.

A pointed hammer tip is ruled out because of this last effect. A flat hammer tip achieves the best signal amplitude and is therefore to be preferred. The slight increase in signal period with a hemispherical tip does not seem to be a worthwhile compromise in view of the ensuing decrease in amplitude.

Variable nature of the input signal under identical conditions on one pile precludes any useful measurements from this parameter. As mentioned above, this renders of questionable value any measurement of the impact/rebound ratio or system decay rate, as used by presently available commercial systems.

The form and amplitude of the reflected signals obtained in the tests varied quite markedly with the type of transducer. The reflection time was unaffected. The study was of limited extent, but served to indicate the importance of this item of equipment. The most suitable

of the devices tested was the large (50 mm diameter) piezo-electric transducer. This achieved the best signal amplitude and signal/noise ratio. The surface area of the transducer face may be of importance since the incident signal is essentially a plane fronted wave extending across the pile cross-section. A large contact area, though, can generate the problem of attaining satisfactory contact on the rough surface of a pile head. Selection of the most suitable type of transducer may be aided by discussion with manufacturers.

The location of the receiving device should be considered in the elimination of interference from transverse and surface waves. Transverse waves of a bending nature involve rotation about the central axis, (section 6.2.2 (a)). A receiver placed centrally on the pile head is thus best able to minimise this effect. Conversely, end surface oscillations may involve an off-centre nodal point where the amplitude of detected surface waves would be at a minimum, (fig. 6.12).

7.6.2 Pile variables

As demonstrated in the test programme, changes in the pile boundary conditions can greatly alter the signal waveforms. The pile base configuration affects the reflection time and the amplitude and period of the reflected signal. Changes in cross-section along the pile body produce additional signals between the input and base reflection.

Soil pressure on the pile base reduced the signal amplitude and extended the period. Such an effect would be increased on a pile in situ by the soil contact along the pile body. The reflection time was unaffected by the soil reaction.

The angled and broken ends resulted in a similar reduction in amplitude and an extended signal period. The most significant factor was the extended reflection time. The implications for site testing are important since estimation of pile length is obtained from the reflection time. In this instance the error was up to 22% over estimation. In practice, however, cast in situ piles are unlikely to possess perfectly flat and perpendicular ends, and the discrepancy between similarly cast piles on a site would not be large. For friction piles the achieved pile length would not be critical within the range of error introduced by the base conditions.

The fixed end test produced the characteristic inverted signal in accordance with the theoretical prediction. For an end bearing pile founded in acoustically dense rock, such an inverted echo would be certain confirmation that a foundation in rock had been achieved. In the case of weaker rock such as shales or mudstone the absence of an inverted echo need not necessarily mean that a bearing stratum had not been penetrated. In such circumstances correlation between the estimated length based on a free end echo and the predicted depth of the bearing stratum

would be appropriate.

The experiments conducted on the variation in cross-section indicate that to a reasonable approximation the amplitude of the reflected signal is linked to the area of the reflecting surface. Therefore, with appropriate allowance for signal attenuation the pile base or any complete discontinuity must produce the maximum amplitude reflection.

Increases in cross-sectional area as modelled by the protrusion experiments have the most serious implications for practical application of the method. A large discontinuity or a large swell along the pile body both reduce or eliminate the prospect of receiving and identifying a base echo. In the case of a discontinuity this would correctly identify a faulty pile. With one or several protrusions, however, the condition of the pile beyond the section producing the first inverted signal might be difficult to assess. Real piles are unlikely to have such regularly defined protrusions as cast in the tests, but any variable cross-section must inevitably lead to a multiplicity of reflections and a confused signal waveform.

The conclusions from the tests on different pile diameters are somewhat obscured by the limited extent of the experiment and the short length of test piles which could be cast. The trend appears to be one of small alteration of stress pulse dimensions with large change in pile diameter. The effect, if present, cannot be

regulated since piles are only present as constructed. The problem is thus one of equipment design and operation.

Extensive cracking in a pile was shown to reduce substantially the propagation velocity. A pile constructed from a weak mix for any reason would have the same effect, (section 5.3). In such circumstances the possibility exists of confusion between a short pile of cracked or poor quality concrete and a full length pile of the required concrete quality. In case of doubt, partial excavation of the upper part of the pile might be of use.

7.7 Conclusions

Equipment

1: The reflection time is unaffected by any variation in equipment design or operation.

2: Signal amplitude can be increased by use of a heavier hammer or increase of the impact velocity up to the point of concrete degredation.

3: Signal period can be increased by reduction of the impact velocity or by use of a longer or heavier hammer.

4: Signal attenuation is approximately proportional to the signal frequency.

5: Signal to noise ratio becomes less favourable with increased impact velocity.

6: A flat hammer tip is the best compromise for maximum signal amplitude and acceptable signal period.

7: The variable nature of the input signal invalidates measurements based on this parameter.

8: Use of the correct type of receiving device is crucial for the successful reception and interpretation of waveforms. Manufacturers' advice is recommended.

9: The selection of the location of the receiving device affects the degree of noise picked up from transverse waves and pile head oscillations.

Pile

1: Pile base conditions can affect signal amplitude and period and change the reflection time.

2: Soil pressure on the pile base reduces signal amplitude and extends the period.

3: An angled or broken pile base can reduce the reflection time by up to 22%.

4: A fixed end produces an inverted echo signal display.

5: A reduction in cross-section produces a reflected signal of amplitude approximately proportional to the area of the reflecting surface.

6: An increase in cross-sectional area produces multiple reflections along the pile body and a confusing waveform. Such protrusions may be recognised by the characteristic fixed end inverted signals.

7: Stress pulse dimensions do not appear to alter rapidly with change in pile diameter.

8: An extensively cracked pile or one composed of weak concrete displays a substantially reduced propagation velocity. The possibility exists for confusion between short piles of good concrete and long piles of poor concrete.

8. ASSESSMENT OF THE METHOD WITH IMPLICATIONS FOR DEVELOPMENT

8.1 Current status of pile testing by sonic echo

The requirement of establishing satisfactory construction of cast in situ concrete foundation piles has proved extremely troublesome to the civil engineering industry. The many types of destructive and non-destructive test techniques which have been investigated, with only limited success, indicate the difficulty of the problem.

With perception of this fact it should be appreciated that the most profitable area for improvement lies in better pile design and more successful methods of construction. The realities of the situation, however, dictate that integrity testing will continue to be demanded.

Within this context, the various techniques presently available have no obvious overall advantages, and individual circumstances must determine the suitability for the adoption of a particular method.

The sonic echo test has express advantages in portability and ease of use without prior preparation of the pile. The method is particularly suited to the testing of precast piles driven into relatively weak soils. Such is the position in Holland where the T.N.O. system[34] is frequently specified for inclusion in piling contracts. Signal processing in this system includes simple bandpass

filters to remove unwanted frequencies, and an exponential gain amplifier to compensate for exponential signal attenuation.

The French system, developed by C.E.B.T.P.[13,15,17], and operated in the UK by their British subsidiary, Testconsult Ltd., is recommended for use on steel piles and on precast piles up to a length of 15m. Signal processing equipment, similar to that of the Dutch system, includes a low pass filter to remove high frequency pile head oscillations and an exponential gain amplifier. In addition the system incorporates a circuit to combine the signals from several receivers. The purpose of this circuit is to enhance in-phase pile base reflections in the presence of random noise.

Application of the technique to cast in situ piles has been attempted by the above organisations. No additional signal processing equipment has been developed specifically for this purpose. Steinbach[31,32] in the USA, has applied the method to steel piles and precast and cast in situ concrete piles. A simple low pass filter was employed to reduce the level of high frequency components which were generated mainly by pile head surface oscillations.

Preliminary evaluation of prototype equipment has been conducted in the UK by C.N.S. Electronics Ltd.[40] The developed system is intended for use on all types of piles. No signal processing is employed at present.

Trials and commercial testing with the above systems

have shown acceptable results with steel piles and precast piles. A base echo is identifiable on a sound pile and interference is usually confined to pile head oscillations. Piles with serious defects generally display recognisably different waveforms from those of intact specimens. On long thin piles where the pile head oscillation frequency is much higher than that of the base echo, the filtering and amplification equipment shows a distinct advantage in enhancement of the reflected signal. With large diameter piles where the surface oscillations are of a lower frequency, signal enhancement has been less successful. Apparently, no attempt has been made by any researchers to generate stress wave pulses of a much lower frequency in order to differentiate from pile head noise.

Application of the method to cast in situ piles has been less successful. In all trials the proportion of interpretable information has been low. Results are characterised by complicated waveforms in which any base echo is difficult to detect. In addition to noise from surface waves, irregular signals often appear on the trace. These are presumed to stem from reflections at irregularities of cross section along the pile body. In some cases clear traces with little noise have been obtained, but without the appearance of any base reflection.

Testing personnel frequently have difficulty with the interpretation of such waveforms. There is often the temptation to look for, and identify, a convenient

signal peak as a base reflection, from a knowledge of the pulse velocity and the nominal length of the pile. The procedure should ideally be operated in reverse. One researcher[41] has cited the absence of any reflection as evidence of a sound pile. There are several circumstances in which a defective pile could produce the same type of signal, as examined further below.

Some fifteen years of development and trial of the method have shown little or no improvement in the successful application to cast in situ piles. The technique of characteristic similarity[40,41], in which several measured parameters are compared between piles, has some advantage with large numbers of nominally identical piles. This can be used as an aid to selection of suspicious piles for load testing.

The above systems are described in greater detail in chapter 3.

8.2 Implications of acoustic theory

The sonic echo technique is based on an estimation of pile length from the measured reflection time and a knowledge of the propagation velocity along the pile body. Velocity measurements are generally taken from test cubes or from a pulse transmitted through the pile cross section near to the head. Steinbach[31,32] has used the surface wave velocity on the pile head, with an appropriate conversion factor to obtain the longitudinal wave velocity, (equation 3.1).

None of these measurements allows for the difference between the velocity of longitudinal waves in an unbounded medium, and the longitudinal velocity in a component with the shape of a long rod or bar, (section 6.2.1). Foundation piles come within this category, and therefore the bar velocity must be used to determine pile length.

The bar velocity is related to the unbounded longitudinal wave velocity by:

$$c_o = 0.9\, c_\ell \qquad \ldots\ldots \qquad (8.1)$$

where,

c_o = bar velocity

c_ℓ = longitudinal wave velocity

This conversion should be applied to test cubes or pile head measurements before establishing a pile length from the reflection time.

Only the French researchers[13,15,17] appear to have been aware of the significance of these different velocities. Steinbach[31,32] correctly identified the bar velocity equation but then neglected to include it when obtaining the longitudinal velocity from the surface wave velocity.

Other researchers and operators[34,40,41] are either unaware of the bar velocity or have decided that to use it is inappropriate. Frequently measurements to find the pulse velocity are not made, and a figure of 4000 m/s is assumed.

For 28 days old concrete of a typical pile mix (1:1½:3, w/c = 0.5) the longitudinal pulse velocity

lies between 3800 m/s and 4200 m/s (section 3.2.4). This converts to a bar velocity of between 3420 m/s and 3780 m/s. The assumption of a velocity of propagation along the pile axis of 4000 m/s is thus too high by a factor of 11%. An appropriate assumed velocity would be 3600 m/s.

The pulse velocity is affected by variables such as type of aggregate, mix proportions, water/cement ratio,curing environment and age, (section 5.3). The range of variation has been found to lie approximately between 1500 m/s to 5000 m/s for extremely poor quality concrete with little strength up to good quality concrete with a crushing strength in excess of 50 N/mm^2.[46,54,187] Thus, if at all possible, a value for the pulse velocity should be obtained from cube or pile head measurements, since an incorrectly assumed velocity could introduce a substantial error.

It should be appreciated, though, that pulse velocity in the lower regions of a pile may not concur with that in the pile head or in test cubes. The curing conditions are different, but more importantly, foreign matter in the form of ground water or soil can mix with the concrete.

If this were to take the form of a well defined break in the continuity of a pile of otherwise good quality concrete, the incident pulse would be reflected at the boundary. The indication would be a substantial reflected signal at a time interval too short to correspond to a base reflection. If the concrete quality

gradually deteriorated down the length of the pile there would be no such signal, since a reflection will only occur at the boundary between two media of differing acoustic impedance, (section 6.5.1). Under these conditions the pulse would travel more slowly in the regions of weaker concrete and thus give a false indication of the pile length.

There thus exists the possibility for confusion between a correct length pile, of good quality concrete, and a short pile, or intact section of pile, of poorer quality concrete. The over estimation of length could be up to 100%. Extensive cracking in a precast pile would produce the same effect, but the condition would likely be detected from multiple reflections at the cracked sections appearing on the signal trace.

The amplitude and form of a base reflection is totally dependent on the nature of the pile base. Theoretical considerations predict the maximum amplitude reflection from a perpendicular boundary between two media of very different acoustic impedances, (section 6.5.1). A pile base which presents an angled or rough broken surface to an incident beam will thus reduce the amplitude of the reflection and lead to more difficult detection by the receiving equipment. This would apply to broken or angled precast pile bases or the conical shoe used in some shell pile designs.

The base of a cast in situ pile can be cast in an ill defined bore in the presence of ground water and mud.

The condition of the base is unimportant for the efficiency of a friction pile, but is crucial for the satisfactory production of an echo signal. A pile extremity which gradually changes from good quality concrete to a poorer quality, and then into a weak mixture of concrete and soil, will not present a good reflecting surface to an incident pulse. The conditions described are in fact an excellent means of transferring the acoustic energy into the soil, where it would be quickly attenuated.

Therefore a perfectly sound cast in situ pile, of the correct length, might well produce no detectable base echo, because of the nature of the base. Equally, the same reasoning applies to a pile of any quality of concrete and of virtually any length. The absence of a base reflection thus yields no information whatever to the operator.

No signal processing can overcome this condition since the reflected signal is simply not produced. Casting of an efficient reflector into the pile base is a possibility, but defeats the objective of operation from the pile head without prior preparation.

A reflection will occur at any abrupt change in cross section of a rod. (section 6.5.2) Precast piles without defects are free from this condition, but cast in situ piles can vary markedly in cross section while retaining a perfectly adequate bearing capacity. The reflections generated by an irregular cross section would be of similar period and form to any base echo, thus

leading to a confused waveform of multiple reflections, any one of which could be the base echo.

Filtering of the signal would be ineffective since the unwanted reflections must be of similar frequency to the base echo. A signal addition technique, based on the reinforcement of the in-phase base echo would likewise fail, since reflections from changes in cross section would also arrive in phase.

The end of a rod is known to oscillate at a resonant surface wave frequency after excitation by an impact, (section 6.4.4). A pile head transducer cannot avoid this motion and so the signal trace is complicated by the additional modulation, and a reflected signal is obscured.

Filtering has proved effective where the surface oscillation frequency is different from that of the stress wave pulse. With increase of pile diameter the frequency of the end oscillation approaches that of the pulse, and filtering becomes ineffective. However, the frequency of the pulse is dependent to some extent on the nature of the impact (section 6.6). It seems possible, therefore, by generating a pulse of suitable wavelength, to reduce confusion with surface waves. Filtering would then be effective.

In very short piles (<5m) the reflected signal returns during the impact time and thus becomes involved with the impact signal. To avoid this a

signal of much shorter wavelength might be used, again by control of the impact variables. The increased attenuation due to the higher frequency signal, (section 5.2.3) would not be too great a disadvantage in very short piles.

8.3 Implications of the experimental investigation

The programme of practical work has shown general agreement with the theory and with other researchers laboratory work on small specimens of concrete and metals. In a few cases the theory has not been exactly modelled by the experiments and some new considerations have been prompted.

Measurements of the velocity of propagation through a concrete beam have confirmed that the bar velocity and not the unbounded longitudinal velocity is applicable, (section 7.5.1).

The signal period and amplitude were found to depend on the hammer variables of mass/length and impact velocity. For example the signal period in the tests varied from 0.4 ms using a 0.2 kg bar at drop heights in excess of 250mm, to 2.0 ms using a 4.5 kg bar from a drop height of 1mm. These signal periods correspond to frequencies of 2500 Hz and 500 Hz. It is thus possible to alter the signal frequency where confusion with pile head oscillations might occur. The tests showed that such variation of the signal did not affect the reflection time, which remained constant. A higher frequency signal imposes a penalty of increased attenuation and dispersion of the

pulse. Therefore any alteration would best be to a lower frequency where possible.

The signal amplitude increases with increase in impact velocity, but the signal period decreases. Thus any increase in signal period with a given bar means a compromise of reduced amplitude level. To achieve a longer signal period with increased amplitude a larger hammer is necessary.

The impact location is important on piles of large diameter. The impact signal reaches the pile head transducer by way of a surface wave travelling at the Rayleigh wave velocity:

$$c_R = 0.5\ c_\ell = 0.55\ c_o \quad \ldots\ldots \qquad (8.2)$$

If the transducer is placed some distance from the impact then the delay results in a shorter and false reflection time. The estimation of pile length is then too short. The size of the error depends on the ratio of the transducer - hammer impact separation and the length of the pile, i.e.:

$$\text{error} = \frac{b/c_R}{RT + b/c_R} \quad \ldots\ldots \qquad (8.3)$$

where,

b = transducer - hammer separation

RT = the apparent reflection time

For example, on a pile of 1m diameter and 10m in length, with the transducer and impact point at either side of the pile head, the estimation of pile length was up to 10% too short, (section 4.4.3).

The experimental work also showed that the hammer tip shape can affect the input signal. A pointed tip broke up the pile head concrete, but produced a better signal once the point had bedded into a good contact area, after several blows. The 45^{o} conical end did not generate as high an amplitude signal as the flat end, (section 7.5.1 (b)). The less sharp the angle of the conical end, the more energy is likely to be propagated down the pile and not lost to surface and transverse wave generation.

This is similar in principle to the sliding weight and nose cone apparatus developed by C.N.S. Electronics,[40] (section 3.2.4). Although the conical nose cone may result in a reduced amplitude signal as above, the system does have the distinct advantage of easier operation on a rough pile head or one which is covered with mud or water.

The type of transducer was found to have a marked effect on the form of signal display (section 7.5.2(a)). The reflection time was unaffected. This study indicated that the type of receiving device is an important consideration in any testing system. A study of transducer characteristics was not included in this project. Selection of suitable transducers would be best achieved through consultation with specialist manufacturers.

The investigation of an angled pile end resulted in a reduction in reflected signal amplitude of up to 70%,

and an increased reflection time of 10% - 13%. The increased reflection time produces the same error in over estimation of pile length. The substantial amplitude loss was accompanied by a widening and general degeneration of the form of the pulse. The reflection from such a pile extremity would be more difficult to detect.

Study of a broken end showed a similar result. The error in the reflection time and therefore estimated pile length was up to 22%, and the reduction in amplitude was up to 70%.

If the results for the angled and broken ends are viewed in conjunction with the effect of the soil reaction, then it is possible that the incident pulse may be distorted and reduced in amplitude to a degree that would make the reflection difficult to detect. Similar conditions might be expected at the base of a cast in situ pile or the broken base of a precast pile.

The fixed end study produced an inverted signal display as predicted by the theory. (section 7.5.3(d)) There was some widening of the pulse and loss of amplitude (up to 70%), but the inverted signal was easily recognisable.

The reflecting mass was cast from an identical mix to that of the test beam. The reflection was therefore totally due to the fixity of the end and not to any difference in acoustic impedance. The implication for testing of end bearing piles is that only a weak inverted signal at best would be obtained at a pile base well

founded in a relatively weak rock of lower acoustic impedence such as shale or mudstone. A pile base founded in a strong rock of high acoustic impedance, such as granite, would produce a substantial inverted signal.

It should be noted that the acoustic pressure phase does not change at a fixed end reflection. A compression wave is reflected as a compression wave. A compression wave arriving at the transducer from the opposite direction, however, is displayed as an inverted signal. There appears to have been some confusion on this point in the research by Geophysical Prespection Services[41], and in the prototype operation manual prepared by them for C.N.S. Electronics[40]. The signals from fixed and free end piles are confused and wrongly identified.

The experiments with progressive cuts near to fixed and free ends demonstrated that the amplitude of the reflection increases approximately linearly with the area of the reflecting surface. The extent of a pile shaft discontinuity could thus be gauged very approximately from the amplitude of an early reflection. Additionally, small reductions in cross section, which would not substantially reduce the pile bearing capacity, can allow the incident pulse to pass and return after reflection from the base.

The experiments which investigated the effect of protrusions from the pile body have important implications for application of the method. A protrusion has the

ability to store some of the energy from a signal as it passes. This transient retention of energy is thought to be in the form of a transverse wave which travels to the extremities of the protrusion and is reflected back to the pile axis, (fig. 7.7). At this point it generates a secondary compression pulse which travels to the pile base, and a secondary tension wave which travels towards the pile head. (section 7.5.4).

The secondary signals occur in addition to the primary transmitted compression pulse, and a primary reflected compression pulse from the front of the obtrusion.

With two protrusions on the beam, the secondary signals and multiple reflections between them combined in a complicated waveform. The first signal to arrive at the base was of lower amplitude than a subsequent, and closely following signal peak.

Thus even if the signal combination was returned to the surface, the distinct possibility exists that the wrong signal would be identified as a base echo. In the tests no base echo was evident at the appropriate point on the signal trace.

Although cross section irregularities on a cast in situ pile would not be so regularily defined as in the experimental case, a similar effect must inevitably occur.

The waveforms obtained from the tests on the beam with two protrusions showed a close resemblance to many irregular and complex waveforms from tests on cast in situ piles by the author (section 4.4) and others.[13,14,31,32,34,37,40,41]

In these circumstances it is difficult to envisage how a reflection technique could prove useful.

A study of different diameters of model piles indicated that the generated signal period changes little with large change in pile diameter. This was endorsed by the experimental work on the beam and the field tests. The diameter of the piles and model piles tested varied from 50 mm to 1m , a factor of 20. The period of the stress pulses lay in the range of 0.4 ms to 2.0 ms, a factor of 5. Much of the signal period range was obtained from variation of the equipment and operation variables.

Thus a small variation in equipment would be required to test a wide range of pile diameters.

The experiments using the 5m cracked model pile confirmed that a reduction in concrete quality is accompanied by a reduction in pulse velocity. This factor leads to a substantial error in estimation of pile length as discussed above. In this case the average propagation velocity along the pile was 2200 m/s. If a bar velocity from the cube tests of 3800 m/s is used to calculate the pile length from the reflection time, a figure of 8.6m is obtained. This is an over estimation of 72%.

The photographs from these tests displayed large early reflected signal peaks from the cracked sections. In a pile this would be reason to suspect the integrity and the estimated length. A pile composed of a weaker concrete, due to other reasons such as the inclusion of

ground water, would not display these early signal peaks from cracks. Thus there would be no indication that the wrong pile length had been calculated.

8.4 Limitations of the technique

Pile testing by sonic echo has been applied successfully to steel and precast concrete piles for a number of years.[34,37] The test is frequently specified for inclusion in piling contracts in Holland, where precast piles driven into weak soils are common.

With piles such as these the test technique is useful. The regular cross section and well defined base result in a substantial echo signal which may be identified on the signal trace.

If a pile is broken during driving a short reflection time indicates the length of pile down to the break.

The bar velocity may be determined accurately from sample piles. Since precast piles are cast under favourable and closely controlled conditions, the concrete quality is good and the acoustic characteristics are uniform throughout. The velocity measurement may therefore be applied to piles in situ with confidence and an accurate estimation of length obtained.

In the case of most other types of piles the test has limited application depending upon the nature of the pile structure.

Precast piles which are assembled and driven in sections cannot be tested using the echo technique.[34] At the first join below ground level a large reflection

is produced and the signal oscillates back and forth in the first section of pile. Parts of the pulse which are transmitted into the second section of the pile behave similarily and so on. It is impossible to detect a base echo under these conditions.

Shell piles, in which a concrete shell is driven into place, and then filled with fresh concrete,are more suitable subjects.

The concrete core provides continuity for propagation of the pulse and the shoe at the pile base acts as a fairly efficient reflector, (section 4.4.2). The concrete quality may not be as uniform as that of precast piles, however, and the length estimation is not as accurate. The shell joints do not produce multiple echos as in the case of jointed precast piles. It is assumed that the pulse propagates through the core with internal reflection at the inner wall of the shell. The transducer and the hammer blow must be applied to the head of the core and not to the shell surround.

Application of the technique to precast piles is often limited by the considerations discussed above. The pile base may fail to act as a reflector and the variable cross section generates a complex and obscuring signal.

In such circumstances the test is of reduced value on individual piles. Comparison of measurements between a large number of nominally identical piles can be used to identify anomolous piles, with possible selection for load testing.[41]

Cast in situ piles in which the steel lining is left in place after casting provide better subjects for the technique. The lining imposes a regular cross section on the pile shape and results are similar to those from precast piles in respect of the simplicity of the signal waveforms. Step tapered piles with linings have been tested with some success, with each step identified by its own discrete echo signal.

The base of a steel lined pile is no different from that of any cast in situ pile, however, and the technique is limited by the degree to which the base acts as a reflector.

8.5 Future development of pile testing by sonic echo

There are two categories under which the technique may be considered for possible development.

1. Specific improvements in the apparatus and procedure for use on precast piles
2. Application to cast in situ piles

8.5.1 Improvements for testing precast piles

Specific improvements for the application to precast piles are considered possible in the design of signal processing equipment and in the control of the impact signal frequency.

The main interference in precast piles is due to surface waves on the pile head. The greater the difference between the input signal frequency and the noise frequency, the more effective is the use of filtering to remove the noise. The input signal frequency can be

controlled by varying the impact velocity, and the size and weight of the hammer. It would be preferable to lower the input signal frequency if possible, since this results in a reduced attenuation level.

A suggested procedure is as follows.

Increase the drop height from a low value with a given hammer. The most efficient height would be the point where the signal amplitude was of an acceptable level, and the signal frequency was still low enough to escape attenuation by the filter. If the signal frequency entered the range of the filter before the signal amplitude became satisfactory, then a heavier hammer would be selected, and the procedure repeated.

The surface wave frequency decreases with pile diameter. Therefore a variable filtering system would be required to accomodate a variety of pile diameters. Likewise, heavier hammers would be required for larger pile diameters to given signal frequencies of acceptable amplitude, and of lower frequency than the surface waves. For very large diameter piles with a low head oscillation frequency, it may prove necessary to use an input signal of higher frequency.

As an alternative to, or in combination with the above signal processing, a signal enhancement technique by addition and averaging of several hammer blows could be employed. By varying the impact point on the pile head, the surface wave noise would tend to become random

on average, whereas the base echo would always arrive in phase. This system could only be operated in the presence of random noise. Any in phase noise signals would be amplified together with the echo signal.

8.5.2 Application to cast in situ piles

There are three inherent problems to be overcome before the method can be improved for testing cast in situ piles.

1. Interference from surface waves
2. Very weak or non existant base echo
3. Interference from reflections at pile cross section irregularities.

The surface wave interference is identical to that on precast piles and may be handled in the same fashion.

A weak base reflection could be enhanced by using the signal averaging technique as described above, with addition of signals from blows to different parts of the pilehead. A reflection which was too weak to be detected on the first trace would grow with subsequent impacts until it could be recognised above the averaged noise level.

If there is no base echo because all of the sound is being transmitted into the soil, then no method of signal processing can improve the situation. In these circumstances a reflection technique cannot work. An optimistic view is that there may always be some reflection, however small, and that this could eventually be enhanced to a recognisable level.

The third problem, reflections from irregularities

along the pile, would be very difficult to overcome. There are two ways in which these noise signals could defeat signal processing.

1. The noise signals are of similar frequency to any base echo.
2. The arrival time of the unwanted signals cannot be varied.

In the first case any filtering technique would tend to reduce the base echo together with the unwanted reflections. Therefore filters of any kind would have limited application.

A signal averaging technique would likewise be of reduced benefit. The time of arrival of reflections from any cross section of a pile cannot be varied with respect to the base reflection time. Therefore signal enhancement by averaging over several impacts would amplify the noise signals in addition to the base reflection.

Developments of the method designed specifically for precast piles would also prove beneficial in the case of cast in situ piles in which some degree of base echo was present, and in which the cross section irregularity noise was not too high. Thus a development programme designed to improve the application to precast piles would be of direct benefit for extended use on cast in situ piles.

8.6 Conclusions

1. The sonic echo test at its present stage of development is a successful means of establishing the integrity of steel piles and precast concrete piles after driving.
2. Precast piles assembled in jointed sections cannot be tested by the method.
3. Shell piles with a continuous concrete core can be tested by the method, but not to the same accuracy as obtained on solid, single section precast piles.
4. Cast in situ piles show reduced accuracy and range of application of the test.
5. The method is particularly difficult to apply on piles with an irregular cross section and a poorly defined base.
6. Cast in situ piles in which the steel lining is left in place may be tested successfully by the method if all piles in a group have well-defined bases.
7. Improvement of the method for use on precast piles may be achieved by:
    1. Control of the input signal frequency with selective filtering of surface wave noise.
    2. Signal enhancement by averaging over successive impacts at different locations on the pile head.
8. Any improvements designed specifically for precast piles would prove beneficial on cast in situ piles which were amenable to the test.

9. CONCLUSIONS

9.1 Scope of the work

An acoustic reflection technique for the non-destructive in situ testing of foundation piles has been examined. Currently available non-destructive pile integrity tests have been reviewed with particular attention to systems based on the sonic echo principle. The relevant acoustic theory has been studied, and a practical examination conducted into the problems of equipment operation and the interpretation of results. Application of the system to various pile types has been evaluated and possibilities for future development considered.

The following specific conclusions have been drawn.

9.2 Integrity testing of foundation piles

1: To counter the problem of defective foundation piles the first considerations should be to improve design and construction practice.

2: Defects will inevitably occur, particularly in the case of cast in situ piles.

3: Faults which occur in piles during driving or casting in situ are difficult to detect.

4: Load testing or excavation and inspection are the only certain methods, at present, of proving pile integrity.

5: Load testing every pile on a large site is economically prohibitive; as an alternative load testing small numbers of piles at random is an inefficient way of detecting faulty piles.

6: None of the non-destructive pile test methods presently available has the overall advantage of an acceptable combination of accuracy and economy.

7: In general resources could be applied more effectively by blanket non-destructive testing followed by selective load testing.

9.3 Integrity testing by sonic echo

1: The several commercial systems presently available or under development have no significant differences in equipment or operation.

2: The main advantages of the sonic echo test are:

(i) Low cost, both in terms of equipment and operation.

(ii) Rapid test which can be applied to 50 or more piles per day.

(iii) No prior preparation of piles is required.

3: Disadvantages of the sonic echo method are:

(i) Requires experienced operation.

(ii) Specialist interpretation is necessary.

9.4 Applications of sonic echo testing

1: At its present stage of development the sonic echo test is a successful method for determining the structural integrity, and/or driven length, of steel piles and precast concrete piles.

2: Cast in situ piles may be tested by the method but with a reduced accuracy which is governed by the base conditions and the regularity of the cross section.

3: Cast in situ piles in which the steel lining is left in place show better results because of the constrained cross section. Step-tapered piles have been tested with correct identification of the cross section variations.

4: Shell piles with a solid concrete core have been tested successfully by the method. Results typically lie between those for precast piles and those for cast in situ piles.

5: Precast piles assembled in jointed sections cannot be tested by the method due to multiple reflections within the upper sections.

9.5 Theoretical considerations

1: A longitudinal pulsed stress wave is the best form of acoustic propagation for the sonic echo testing of piles.

2: Such a pulse may be generated by a vertical blow to the head of a pile.

3: Propagation of a longitudinal pulse in a pile occurs at the bar velocity, $\sqrt{E/\rho}$, equal to 0.9 times the longitudinal velocity in an unbounded medium.

4: The unbounded longitudinal velocity may be obtained from test cubes or from a measurement through the cross section at the head of a pile.

5: To limit dispersion of the pulse (i.e. increase in period and reduction in amplitude) the pulse wavelength should be at least an order of magnitude larger than the diameter of the pile.

6: Surface waves and end resonance effects generally occur at the pile head. Careful analysis is required to avoid confusion with reflections from defects or the pile base.

9.6 Operation and equipment

1: The reflection time is unaffected by any variation in equipment design or operation.

2: Signal amplitude can be increased by use of a heavier hammer or increase of the impact velocity up to the point of concrete degredation.

3: Signal attenuation is approximately proportional to the signal frequency.

4: The frequency of the input signal may be reduced by reduction of the impact velocity or use of a heavier hammer.

5: Signal to noise ratio becomes less favourable with increased impact velocity.

6. A flat hammer tip is the best compromise for maximum signal amplitude and acceptable signal period.

7: The correct type of receiving device is important for the successful reception and interpretation of waveforms. Manufacturer's advice is recommended.

8: The location of the receiving device on the pile head may affect the degree of noise received from transverse waves and pile head oscillations.

9.7 Signal interpretation

1: Reflection from a free end such as the base of a friction pile or an intermediate void will be characterised by a reflected signal display of the same sense as the input pulse.

2: In the case of a fixed end, such as the base of a pile founded in rock, the reflected signal display will be inverted.

3: A sharp reduction in cross section will produce a partial in phase reflection, which will arrive before the base echo.

4: The amplitude of the reflected signal at any depth is approximately proportional to the area of the reflecting surface.

5: A sharp increase in cross section will produce a partial in phase reflection which will arrive before the base echo.

6: A complete discontinuity, such as a void or layer of soil, will produce an early in phase reflection and no base echo will be present.

7: An extensively cracked pile or one composed of weak concrete will display a substantially reduced propagation velocity.

8: Accurate interpretation of waveforms requires a thorough understanding of the theoretical and experimental analyses contained in this thesis.

9.8 Development

1: The impact velocity and hammer mass/length may be optimised for application to specific pile types and dimensions.

2: Such control of the impact variables could achieve:

(a) Separation of the propagated signal and surface wave frequencies to give more effective use of filters.

(b) Improved signal/noise ratio and thus increased scope for exponential amplification of the signal.

(c) Reduced signal decay rate with a potentially increased range of pile length to which the test could be effective.

3: A signal enhancement system might be developed, based on addition and averaging of signals from successive impacts at several different locations on the pile head.

REFERENCES

1. BOBROWSKI, J., BARDMAN-ROY, B.K., MAGIERA, R.H. and LOWE, R.H.
The structural integrity of large diameter bored piles. Behaviour of piles: Proc. Conf. Inst. Civ. Engrs., London, September 1975.

2. MITCHELL, J.M.
Assessing large diameter piles.
The Consulting Engineer, December 1973, 37-39.

3. WHITAKER, T.
Structural integrity of piles.
Civil Engineer, June 1974, 20-23.

4. WELTMAN, A.J.
Integrity testing of piles: a review.
DOE and CIRIA Piling Development Group, report PG4, September 1977.

5. WEST'S PILES
Pile types, an examination of two systems of classifying piles, with reference to CP 2004 and CP110.
Civil Engineering and Public Works Review, January 1979, 42-47.

6. WELTMAN, A.J. and LITTLE, J.A.A.
A review of bearing pile types.
DOE and CIRIA Piling Development Group, report PG1, September 1977.

7. THORBURN, S. and THORBURN, J.Q.
Review of problems associated with the construction of cast-in-place piles.
DOE and CIRIA Piling Development Group, report PG2, January 1977.

8. NEW CIVIL ENGINEER
Esso's giant oil tanks - a question of more haste, less speed.
New Civil Engineer, 28th February 1974, 28-38.

9. DAVIS, A.G. and DUNN, C.S.
From theory to field experience with the non-destructive vibration testing of piles.
Proc. Inst. Civ. Engrs. Pt. 2, December 1974, 571-593.

10. DAVIS, A.G. and ROBERTSON, S.A.
Vibration testing of piles.
Structural Engineer, June 1976.

11. DAVIS, A.G. and ROBERTSON, S.A.
Economic pile testing.
Ground Engineering, May 1975, 40-43.

12. GARDNER, R.P.M. and MOSES, G.W.
Testing bored piles formed in laminated clays.
Civil Engineering and Public Works Review,
January 1973, 60-63.

13. PAQUET, J.
Etude vibratoire des pieux en béton résponse
harmonique et impulsionelle, application au controle.
Annls. Inst. Tech. Batim., 21st year, No. 245,
May 1968, 789-803.

14. BRIARD, M.
Controle des pieux par la methode des vibrations.
Annls. Inst. Tech. Batim., 23rd year, No. 270,
June 1970, 105-107.

15. PAQUET, J. and BRIARD, M.
Controle non destructif des pieux en béton.
Carottage sonique et méthode de l'impedance méchanique.
Annls. Inst. Tech. Batim, No. 337, March 1976, 50-80.

16. ROBERTSON, S.A.
Vibration testing.
The Consulting Engineer, January 1976, 36-39.

17. BAKER, C.N. and KHAN, F.
Caisson construction problems and correction in Chicago.
Proceedings of the American Society of Civil Engineers
Soil Mechanics and Foundations Division, February 1971,
417-440.

18. COHAS, H., CONVERT, M. and PROST, J.
Ausculatation dynamique de pieux par la méthode des
reservations parallèles.
Bull. Liaison Labo. P. et Ch. 77 May-June 1975, 9-10.

19. FRISTCH,D.
Auscultation des pieux et des parois moulées en béton.
Bull. Liaison Labo P. et Ch. 78 July-August 1975, 65-69.

20. LEVY, J.F.
Testing for soundness of cast-in-situ concrete piles.
Greater London Council, Bulletin No. 48 (2nd series)
August-September 1971, 1-6.

21. LEVY, J.F.
Sonic pulse method of testing cast-in-situ concrete piles
Ground Engineering, No. 3, 1970, 17-19.

22. ROBERT, A.
Exemple d'utilisation des méthodes d'auscultation de pieu
Bull. Liaison Labo. P. et Ch. 69, January-February 1974,
14-17.

23. VOLD, R.C. and HOPE, B.R.
Ultrasonic testing of deep concrete foundations.
British Journal of N.D.T., September 1978, 232-241.

24. MOON, M.R.
A test method for the structural integrity of bored piles.
Civil Engineering and Public Works Review, May 1972, 476-480.

25. ADIL, N.
The measurement of concrete density by back-scattered gamma radiation.
British Journal of N.D.T., March 1977, 72-77.

26. FORDE, M.C., WHITTINGTON, H.W. and McCARTER, J.W.
Application of electrical resistivity to integrity testing of concrete load-bearing piles.
4th International Conference on N.D.T., Grenoble, France, September 1979.

27. DVORAK, A.
Correlation of static and dynamic pile tests.
Proc. Asian Regional Conf. on Soil Mechanics 4, Foundation Engineering 3rd, Haifa, 1967.

28. DVORAK, A.
Dynamic tests of piles and the verification of results by static loading tests.
Acta Technica Scientarium Hungaricae 64, 1969.

29. HIGGS, J.S.
Integrity testing of concrete piles by shock method.
Concrete, October 1979, 31-33.

30. GOBLE, G.G.
Case method of pile capacity determination.
Associated Pile and Fitting Corporation/Case Institute of Technology. Pile-tips, September-October 1975.

31. STEINBACH, J.
Caisson evaluation by the stress wave propagation method.
Illinois Institute of Technology, Ph.D. 1971.

32. STEINBACH, J. and EBEN, V.
Caisson evaluation by the stress wave propagation method.
Journal of Geotechnical Engineering Division ASCE, 101 (No. GT4) April 1975, 361-378.

33. FEGEN, I., FORDE, M.C. and WHITTINGTON, H.W.
Developments in the sonic testing of piles.
Conference on Acoustic Emission.
UKAEA Risley, Warrington, November 1978.

34. T.N.O.
Pile measuring equipment.
Institute T.N.O. for Building Materials and Building Structures.
P.O. Box 49, Delft, Netherlands.

35. WHITTINGTON, H.W., FEGEN, I. and FORDE, M.C.
Signal processing of ultrasonic pulses for non-destructive testing of concrete piles.
Ultrasonics International Conference, Gray, Austria, May 1979.

36. FEGEN, I., FORDE, M.C. and WHITTINGTON, H.W.
The detection of voids in concrete piles using sonic methods.
4th International Conference on N.D.T.
Grenoble, France, September 1979.

37. MENOU, J. and VENEC, Y.
Controle de la continuité des pieux par une méthode d'auscultation dynamique.
Bull. Liaison Labo. et Routiers P.et Ch.No. 44, Mars-Avril 1970, 103-112.

38. ROBERTSON, S.A.
Horizontal pile testing.
Civil Engineering and Public Works Review, January 1979, 17.

39. BLITZ, J.
Fundamentals of ultrasonics.
Butterworths, London, 1967.

40. C.N.S. ELECTRONICS LTD.
24 Holmes Road, London NW5.
1978, Private Communication.

41. GEOPHYSICAL PROSPECTION SERVICES
23 Windsor Court, Clifton, Bristol, BS8 4LJ
1978, Private Communication.

42. POWERS, T.C.
Measuring Young's Modulus of Elasticity by means of sonic vibrations.
Proceedings, ASTM vol. 38, part II, 1938.

43. THOMSON, W.T.
Measuring changes in physical properties of concrete by the dynamic method.
Proceedings, ASTM, vol. 40, 1940, 1113-1129.

44. OBERT, L. and DUVALL, W.
Discussion of dynamic methods of testing concrete with suggestions for standardisation.
Proceedings, ASTMS, vol. 41, 1941, 1053-1071.

45. LONG, B.G., KURTZ, H.J., and SANDENAW, T.A.
An instrument and a technique for field determination of the modulus of elasticity and flexural strength of concrete pavements.
Journal American Concrete Institute, vol. 16, No. 3, January 1945, 217-231.

46. WHITEHURST, E.A.
Dynamic testing of concrete evaluated.
Civil Engineering, December 1957, 57-59.

47. WHITEHURST, E.A.
Evaluation of concrete properties from sonic tests.
American Concrete Institute, 1966, 23-75.

48. PICKETT, G.
Equations for computing elastic constants from flexural and torsional resonant frequencies of vibration of prisms and cylinders.
Proceedings, ASTM, vol. 45, 1945, 846-865.

49. SPINNER, S. and TEFET, W.
A method for determining mechanical resonance frequencies and for calculating elastic moduli from those frequencies.
Proceedings, ASTM, vol. 61, 1961, 1221-1237.

50. LESLIE, J.R. and CHEESMAN, W.J.
An ultrasonic method of studying deterioration and cracking in concrete structures.
Journal American Concrete Institute, Vol. 46, Sept. 1949, 17-36.

51. AKROYD, T.N.W. and JONES, R.
Non-destructive testing of structural concrete by the ultrasonic pulse technique.
Proceedings 4th International Conference on N.D.T., London, 1963, 230-234.

52. ANDERSEN, J. and NERENST, P.
The non-destructive testing of concrete with special reference to the wave velocity method.
Danish National Institute of Building Research, Copenhagen, Report No. 3, 1950, 12-28.

53. ANDERSEN, J. and NERENST, P.
Wave velocity in concrete.
Journal American Concrete Institute, Vol. 48, April 1952, 613-635.

54. RAJAGOPALAN, P.R., PRAKASH, J. and NARASIMHAN, V.
Correlation between ultrasonic pulse velocity and strength of concrete.
Indian Concrete Journal, November 1973, 416-418.

55. GOLIS, M.J.
Pavement thickness measurement using ultrasonic pulses.
47th Annual Meeting of Committee on Mechanical Properties of Concrete, June 1968, 4o-48.

56. MUENOW, R.
A sonic method to determine pavement thickness.
Journal of PCA research and development laboratories September 1963, 8-21.

57. JONES, R.
The non-destructive testing of concrete.
Magazine of Concrete Research, No. 2, June 1949.

58. OGISHI, S. and UCHIDA, T.
A study on the properties of concrete by the ultrasonic method.
4th Japan Congress on Testing Materials - Non-metallic Materials. 104-106.

59. MAYFIELD, B. and BETTISON, M.
Ultrasonic testing of high alumina cement concrete.
Concrete, September 1974, 36-38.

60. LARDINOIS, C.
Quality control of concrete products using the pulse velocity method.
Association Belge pour l'étude de l'emploi des matériaux, no. 399, 1973, 97-103.

61. BUNGEY, J.H.
Ultrasonic pulse testing of H.A.C. on the site.
Concrete, September 1974, 39-41.

62. REYNOLDS, W.N., WILKINSON, S.J. and SPOONER, D.C.
Ultrasonic wave velocities in concrete.
Magazine of Concrete Research, Vol. 30, no. 104.
September 1978, 139-144.

63. GALAN, A.
Estimate of concrete strength by ultrasonic pulse velocity and damping constant.
ACI Journal, October 1967, 678-684.

64. AKASHI, T.
On the measurement of loss of ultrasonic pulse in concrete.
2nd Japan Congress on Testing Materials - Non-Metallic Materials. 165-168.

65. RAYLEIGH, Lord
Theory of sound.
The Macmillan Co., London, 1926 (2nd edition)
vol. 1, 242-305.

66. LOVE, A.E.H.
Mathematical theory of elasticity
Cambridge University Press, 1927 (4th edition), 431.

67. MASON, W.P.
Motion of a bar vibrating in flexure, including the effect of rotatory inertia.
Journal of the Acoustical Society of America
1935, vol. 6, 246.

68. THOMSON, W.T.
The effect of rotatory and lateral inertia on flexural vibrations of prismatic bars.
Journal of the Acoustical Society of America
1939, vol. 11, 198.

69. TIMOSHENKO, S.P.
On the correction for shear of the differential equation for transverse vibration of prismatic bars.
Philosophical Magazine, 1921, vol. 41, 744-746.

70. TIMOSHENKO, S.P.
Vibration of bars of uniform cross-section.
Philosophical Magazine, 1922, vol. 43, 125-131.

71. TIMOSHENKO, S.P.
Vibration problems in engineering.
D. Van Nostrand Co., New York, 1937 (2nd edition)
337-342.

72. GOENS, E.
Über die Bestimmung des Elastizitätsmodulus von Stäben mit Hilfe von Biegungsschwingungen
Annalen der Physik, B. Folge, Band 11, 1931,
649-678.

73. CHREE, C.
On longitudinal vibrations.
Quarterly Mathematics Journal, Vol. 23, 1889, 317-342.

74. LONG, B.G. and KURTZ, H.J.
Effect of curing methods upon the durability of concrete as measured by changes in the dynamic modulus of elasticity.
Proceedings ASTM, vol. 43, 1943.

75. KAPLAN, M.F.
Ultrasonic pulse velocity, dynamic modulus of elasticity, Poisson's ratio and the strength of concrete made with thirteen different coarse aggregates.
Bulletin, Rilem No. 1, March 1959, 58-73.

76. WHITEHURST, E.A.
Effect of variations in mix design or curing conditions on a pulse velocity-strength relationship.
Bull. No. 206, Highway Research Board, Washington,D.C. 1959, 57-63.

77. KAPLAN, M.F.
The effects of age and water/cement ratio upon the relation between ultrasonic pulse velocity and compressive strength of concrete.
Magazine of Concrete Research, Vol. 11, July 1959, 85-92.

78. BRITISH STANDARDS INSTITUTION BS 4408.
Recommendations for non-destructive methods of test for concrete: Measurement of the velocity of ultrasonic pulses in concrete, Part 5, 1974, 20.

79. CHUNG, H.W.
Effects of embedded steel bars upon ultrasonic testing of concrete.
Magazine of Concrete Research, Vol. 30, No. 102, 1978, 19-25.

80. DAVIS, R.E. and TROXELL, G.E.
Modulus of elasticity and Poisson's ratio for concrete and the influence of age and other factors upon these values.
Proceedings, ASTM, vol. 29, 1929, 678-701.

81. THOMAN, W.H. and RAEDER, W.
Ultimate strength and modulus of elasticity of high strength Portland Cement concrete.
Proceedings, ACI, vol. 30, 1934.

82. LARVE, H.A.
Modulus of elasticity of aggregate and its effect on concrete.
Proceedings, ASTM, Vol. 46, 1946, 1298-1310.

83. TROXELL, G.E. and DAVIS, H.E.
Composition and properties of concrete.
McGraw-Hill, 1956.

84. ELVERY, R.H. and IBRAHIM, L.A.M.
Ultrasonic assessment of concrete strength at early stages.
Magazine of Concrete Research, Vol. 28, No. 97, December 1976, 181-190.

85. FACAOARU, I.
Non-destructive testing of concrete in Romania
Institution of Civil Engineers/British National Committee for N.D.T. Symposium on N.D.T. of concrete and timber. June 1969, 39-49.

86. VISVESVARAYA, H.C., RAGHAVENDRA, N. and MAITI, S.C.
Applications of combined methods of N.D.T. for assessment of the quality of construction concrete.
2nd Rilem Symposium on Nondestructive testing of Non-metallic materials, Constanza, Romania, 1974, vol. 3, 141-150.

87. ADIL, N.
The measurement of concrete density by back-scattered gamma radiation.
British Journal of N.D.T., March 1977, 72-77.

88. REYNOLDS, W.N. and WILKINSON, S.J.
The nondestructive physical analysis of concrete.
Materials Physics Division, AERE Harwell,
AERE - R8974, Dec. 1977.

89. HASHIN, Z. and SHTRIKMAN, S.
A variational approach to the theory of the elastic behaviour of multiphase materials.
Journal of Mechanics and Physics of Solids,
Vol. 11, No. 2. March-April 1963, 127-140.

90. WALPOLE, L.J.
On the bounds for the overall elastic modulii of inhomogeneous systems.
Journal of Mechanics and Physics of Solids.
Vol. 14, 1966, 151-169.

91. BOUCHER, S.
Modules effectifs de matériaux composites quasi homogènes et quasi isotropes constitués d'une matrice élastique et d'inclusions élastiques.
Revue Mecanique, Vol. 22, 1976, 1-36.

92. MITCHELL, L.J.
Dynamic testing of materials.
Highway Research Board, V.33, 1954, 242-256.

93. REDWOOD, M.R.
Mechanical wave guides
Pergamon Press, 1960.

94. ABRAMSON, H.N., PLASS, H.J. and RIPPERGER, E.A.
Stress wave propagation in rods and beams.
Advances in applied mechanics, Vol. 5, 1958, 111-194.

95. POCHHAMMER, L.
Uber die Fortpflanzungogeschwindigkeiten kleiner Schwingungen in einem unbegrenzten isotropen Kreiszylinder.
Journal für die reine und angewandte Mathematik 81, 1876, 324-336.

96. CHREE, C.
The equations of an isotropic elastic solid in polar and cylindrical co-ordinates, their solutions and applications.
Trans. Cambridge Phil. Soc. 14, 1889, 250-369.

97. BANCROFT, D.
The velocity of longitudinal waves in cylindrical rods.
Physics Review, 59, 1941, 588-593.

98. FLINN, E.A.
Dispersion curves for longitudinal and flexural waves in solid circular cylinders.
Journal of Applied Physics, 29, 1958, 1261-1262.

99. DAVIES, R.M.
A critical study of the Hopkinson pressure bar.
Phil. Trans. Royal Society, A240, 1948, 375-457.

100. HOLDEN, A.N.
Longitudinal modes of elastic waves in isotropic cylinders and slabs.
Bell Sys. Tech. J. 30, 1951, 956-969.

101. SHEAR, S.K. and FOCKE, A.B.
The dispersion of supersonic waves in cylindrical rods of polycrystalline Ag, Ni and Mg.
Physics Review, 57, 1940, 532-537.

102. TU, L.Y., BRENNAN, J.N. and SAUER, J.A.
Dispersion of ultrasonic pulse velocity in cylindrical rods.
Journal of the Acoustical Society of America, 27, No.3, May 1955, 550-555.

103. OLIVER, J.
Elastic wave dispersion in a cylindrical rod by a wide band short duration pulse technique.
Journal of the Acoustical Society of America, 29, 1957, 189-194.

104. FOLK, R., FOX, G., SHOOK, C.A. and CURTIS, C.W.
Elastic strain produced by sudden application of pressure to one end of a cylindrical bar. Pt. 1,Theory.
Journal of the Acoustical Society of America, 30, 1958, 552-558.

105. McSKIMIN, H.J.
Propagation of longitudinal waves and shear waves in cylindrical rods at high frequencies.
Journal of the Acoustical Society of America, 28, 1956, 484-494.

106. STANFORD, E.G.
A contribution on the velocity of longitudinal elastic vibrations in cylindrical rods.
Nuovo Cimento 7 (suppl. 2), 1951, 332-340.

107. HUDSON, G.E.
Dispersion of elastic waves in solid circular cylinders.
Physical Review 63, 1943, 46-51.

108. VOLTERRA, E.G.
A one-dimensional theory of wave propagation in elastic rods based on the method of internal constraints.
Ingenieur Archiv. 23, 1955, 410-420.

109. VOLTERRA, E.G.
Dispersion of longitudinal waves.
Journal Eng. Division, Proc. ASCE, EM3, July 1957, paper 1322, 1-21.

110. ADEM, J.
On the axially symmetric steady wave propagation in elastic circular rods.
Quarterly Applied Maths, 12, 1954, 261-275.

111. MINDLIN, R.D. and HERRMANN, G.
A one-dimensional theory of compressional waves in an elastic rod.
Proc. 1st U.S. Nat. Cong. Applied Mechanics, Chicago, 1951, 187-191.

112. HERRMANN, G.
Forced motions in elastic rods.
Journal of Applied Mechanics 21, 1954, 221-224.

113. MIKLOWITZ, J.
Travelling compressional waves in an elastic rod according to the more exact one-dimensional theory.
Proc. 2nd U.S. Nat. Cong. Applied Mechanics, June 1954, 179-186.

114. MIKLOWITZ, J.
The propagation of compressional waves in a dispersive rod. Pt. 1, results from the theory.
Journal of Applied Mechanics, 24, 1957,231-239.

115. PLASS, H.J. and STEYER, C.C.
Studies in longitudinal and bending waves in long elastic rods.
University of Texas Defense Research Lab.
Report DRL-376, CM-860, 1956.

116. MALVERN, L.E.
Plastic wave propagation in a bar of material exhibiting a strain rate effect.
Quart. Appl. Maths. 1950, 8, 405.

117. BISHOP, R.E.D.
Longitudinal waves in beams.
Aeronautical Quarterly, Vol. 3, 1952, 280-293.

118. BISHOP, R.E.D.
Longitudinal elastic waves in cylindrical rods.
Nature, 172, 1953, 169.

119. VOLTERRA, E.G.
A one-dimensional theory of wave propagation in elastic rods based on the assumption of constrained elasticity.
Office of Naval Research, Project NOR R (591)05, Rensselaer Poly. Inst. Progress Report 1, 1954.

120. PLASS, H.J.
On longitudinal and transverse waves in elastic rods.
University of Texas, Defense Research Lab.
Report DRL-362, CM-821, 1954.

121. KOLSKY, H.
Stress waves in solids
Oxford Press, 1953.

122. SITTIG, E.
Zur Systematik der Elastischen Eigenschwingungen Isotroper Kreiszylinder.
Acustica 7, 1957, 175-180, 299-305.

123. ABRAMSON, H.N.
Flexural waves in elastic beams of circular cross-section.
Journal Acoustical Society of America, 29, 1957, 42-46.

124. VOLTERRA, E.
A study of the propagation of flexural waves in elastic beams.
Discussion on paper by Ripperger and Abramson.
Journal Applied Mechanics, 25, 1957, 153-155.

125. MINDLIN, R.D.
Influence of rotary inertia and shear on flexural motions of isotropic elastic plates.
Journal Applied Mechanics, 18, 1951, 31-38.

126. MINDLIN, R.D. and DERESIEWICZ, H.
Timoshenko's shear coefficient for flexural vibrations of beams.
Proceedings, 2nd National Congress Applied Mechanics 1955, 175-178.

127. KYNCH, G.J.
The fundamental modes of vibration of uniform beams for medium wavelengths.
British Journal of Applied Physics, 8, 1957, 64-73.

128. OWEN, J.D.
Ph.D. Thesis, University of Wales, 1950.

129. DAVIES, R.M.
Stress waves in solids.
Surveys in mechanics (ed. Batchelor, G.K. and Davies, R.M.), Cambridge University Press, 1956, 64-138.

130. ARENBERG, D.L.
Ultrasonic solid delay lines.
Journal Acoustical Society of America, 20, No. 1, 1948, 1-26.

131. LINDSAY, R.B.
Mechanical Radiation.
McGraw-Hill, 1960, 190-194.

132. STEPHENS, R.W.B. and BATE, A.E.
Wave motion and sound.
Edward Arnold & Co., London, 1950, 113-116.

133. MEYER, E. and NEUMANN, E.G.
Physical and applied acoustics.
Academic Press, London, 1972, 25-26.

134. BREKHOVSKIKH, L.M.
Waves in layered media.
Academic Press, London, 1960, 38-44.

135. MINDLIN, R.D.
Propagation of waves over the surface of a circular cylinder.
Dokl. Akad. Nauk, SSSR, 52, 1946, 107-110.

136. VIKTOROV
Rayleigh type waves on cylindrical surfaces.
Akust. ZH. 4, 1958, 131-136.

137. ELLIOTT, R.S.
Azimuthal surface waves on circular cylinders.
Journal of Applied Physics, 26, 1955, 368-376.

138. MORSE, R.W.
Dispersion of compressional waves in isotropic rods of rectangular cross-section.
Journal of Acoustical Society of America, 20, 1948, 833-838.

139. MORSE, R.W.
The velocity of compressional waves in rods of rectangular cross-section.
Journal of the Acoustical Society of America, 22, 1950, 219-223.

140. KYNCH, G.J. and GREEN, W.A.
Vibration of beams (1) - longitudinal modes.
Quart. Journal Mechanics & Applied Maths. 10, 1957, 63-73.

141. MIRSKY, I. and HERRMANN, G.
Axially symmetric motions of thick cylindrical shells.
Journal of Applied Mechanics, 25, 1958, 97-102.

142. HERRMANN, G. and MIRSKY, I.
Three dimensional and shell theory analysis of axially symmetric motions of cylinders.
Journal of Applied Mechanics, 23, 1956, 563-568.

143. JUNGER, M.C. and ROSATO, F.J.
The propagation of elastic waves in thin walled cylindrical shells.
Journal of the Acoustical Society of America, 26, 1954, 709-713.

144. LIN, T.C. and MORGAN, G.W.
A study of the axisymmetric vibrations of cylindrical shells as affected by rotary inertia and transverse shear.
Journal of Applied Mechanics, 23, 1956, 255-261.

145. NAGHDI, P.M. and COOPER, R.M.
Propagation of elastic waves in cylindrical shells, including the effects of transverse shear and rotary inertia.
Journal of the Acoustical Society of America, 28, 1956, 56-63.

146. SMITH, P.W.
Phase velocities and displacement characteristics of free waves in a thin cylindrical shell.
Journal of the Acoustical Society of America, 27, 1955, 1065-1072.

147. HEIMANN, J.H. and KOLSKY, H.
The propagation of elastic waves in thin cylindrical shells.
Journal of Mechanics and Physics of Solids, 14, 1966, 121-130.

148. PLASS, H.J.
Some solutions of the Timoshenko beam equation for short pulse type loading.
Journal of Applied Mechanics, 25, 1958, 379-385.

149. RIPPERGER, E.A. and ABRAMSON, H.N.
A study of the propagation of flexural waves in elastic beams.
Journal of Applied Mechanics, 24, 1957, 431-434.

150. HUGHES, D.S., PONDROM, W.L. and MIMS, R.L.
Transmission of elastic pulses in metal rods.
Physical Review, 75, 1949, 1552-1556.

151. HUGHES, D.S. and STANBURGH, J.H.
Transmission of elastic pulses in rods.
Texas Journal of Science, 4, 1951, 568-577.

152. RIPPERGER, E.A.
The propagation of pulses in cylindrical bars - an experimental study.
Proceedings 1st Midwestern conference on solid mechanics, Urbana Illinois, 1953, 29-39.

153. MIKLOWITZ, J. and NISEWANGER, C.R.
The propagation of compressional waves in a dispersive elastic rod. Part 2, Experimental results and comparison with theory.
Journal of Applied Mechanics, 24, 1957, 240-244.

154. FOX, G. and CURTIS, C.W.
Elastic strain produced by sudden application of pressure to one end of a cylindrical bar. Part 2, experimental observations.
Journal of the Acoustical Society of America, 30, 1958, 559-563.

155. KOLSKY, H.
The propagation of stress pulses in visco-elastic solids.
Philosophical Magazine, 1, 1956, 693-710.

156. PEKERIS, C.L.
Solution of an integral equation occurring in impulsive wave propagation problems.
Proceedings of the National Academy of Science, 42, 1956, 439-443.

157. REDWOOD, M.
The generation of secondary signals in the propagation of ultrasonic waves in bounded solids.
Proceedings of the Physical Society, 72, 1958, 841-853.

158. REDWOOD, M.
Dispersion effects in ultrasonic waveguides and their importance in the measurement of attenuation.
Proceedings of the Physical Society, B70, 1957, 721-737.

159. SHALEK, R.
Longitudinal impact of a semi-infinite circular elastic bar.
Journal of Applied Mechanics, 24, 1957, 550-555.

160. BULLEN, K.E.
An introduction to theoretical seismology.
Cambridge University Press, 1965.

161. KOLSKY, H.
The propagation of longitudinal elastic waves along cylindrical rods.
Philisophical Magazine, 45, 1954, 712-726.

162. SIMPSON, ROBERT E.
Introducing Electronics for Scientists & Engineers, Allun & Bacon, Boston.

163. MEITZLER, A.H.
Propagation of elastic pulses near the stressed end of a cylindrical bar. Paper presented to the Professional Group on Ultrasonic Engineering, Institute of Radio Engineers, New York, 1956.

164. REDWOOD, M.
The velocity and attenuation of a narrow band, high frequency, compressional pulse in a solid waveguide.
Journal of the Acoustical Society of America, 31, 1959, 442-448.

165. CURTIS, C.W.
Second mode vibrations of the Pochhammer-Chree frequency equations.
Journal of Applied Physics, 25, 1958, 928.

166. HSIEH, D.Y. and KOLSKY, H.
An experimental study of pulse propagation in elastic cylinders.
Proceedings, Physical Society, 71, 1958, 608-612.

167. SUTTON, P.M.
Propagation of sound in plate shaped solid decay lines.
Journal of the Acoustical Society of America, 31, 1959, 34-43.

168. ANDERSON, R.A.
Wave groups in the flexural motion of beams predicted by the Timoshenko theory.
Journal of Applied Mechanics, 21, 1954, 388-394.

169. SHAW, E.A.G.
On the resonant vibrations of thick barium titanate discs.
Journal of the Acoustical Society of America, 28, 1956, 38-50.

170. DAVIES, R.M.
Proceedings 7th International Congress on Applied Mechanics, I, 1948, 404.

171. RIPPERGER, E.A. and ABRAMSON, H.N.
Reflection and transmission of elastic pulses in a bar at a discontinuity in cross-section.
Proceedings 3rd Midwestern conference on solid mechanics, University of Michigan, 1957, 135-145.

172. FISCHER, H.C.
Stress pulse in bar with neck or swell.
Applied Science Review Section A, vol. 4, 1954, 317-328.

173. MUGIONO, H.
Measurement of the reflection of flexural waves at cross-sectional discontinuities in rods.
Acoustica, 5, 1955, 183-186.

174. CHRISTIE, D.G.
Reflection of elastic waves from a free boundary.
Philosophical Magazine, 46, 1955, 527-541.

175. GOODIER, J.N. and BISHOP, R.E.D.
On critical reflection of elastic waves at free surfaces.
Journal of Applied Physics, 23, 1952, 124-126.

176. ROESLER, F.C.
Glancing angle reflection of elastic waves from a free boundary.
Philosophical Magazine, 46, 1955, 517-526.

177. ERGIN, K.
Energy ratio of the seismic waves reflected and refracted at a rock-water boundary.
Bulletin of the Seismological Society of America, 42, 1952, 349-372.

178. EWING, W.M. JARDETSKY, W.S. and PRESS, F.
Elastic waves in 'layered media',
McGraw-Hill, 1957.

179. MUSKAT, M. and MERES, M.W.
Reflection and transmission coefficients for plane waves in elastic media.
Geophysics, Vol. 5, No. 2, April 1940, 115-148.

180. TOLSTOY, I. and USDIN, E.
Dispersive properties of stratified elastic and liquid media: A ray theory.
Geophysics 18, 1953, 844-870.

181. ARONS, A.B. and YENNIE, D.R.
Phase distortion of acoustic pulses reflected obliquely from a medium of higher sound velocity.
Journal of the Acoustical Society of America, 22, 1950, 231-237.

182. CRAGGS, J.W.
The oblique reflection of sound pulses.
Proceedings Royal Society, A237, 1956, 372-382.

183. GUTENBERG, B.
Energy ratio of reflected and refracted seismic waves.
Bulletin Seismological Society of America, 34, 1944, 85-102.

184. NAFE, J.E.
Reflection and transmission coefficients at a solid/solid interface of high velocity contrast.
Bulletin Seismological Society of America, 47, 1957, 205-220.

185. PARKER, J.G.
Reflection of plane sound waves from an irregular surface.
Journal of the Acoustical Society of America, 28, 1956, 672-680.

186. MILES, J.W.
On nonspecular reflection at a rough surface.
Journal of the Acoustical Society of America, 26, 1954, 191-199.

187. NEVILLE, A.M.
Properties of concrete
Pitman, 1973 (2nd edition), 320.

188. GOLDSMITH, W.
Impact - the theory and physical behaviour of collecting bodies.
Arnold, London, 1960, 82-104.

189. HERTZ, H.
Ueber die Beruhrung fester elastischer Korper
Jour. fur die Reine u. Angew, Math. (Crelle's Journal), 92, 1882, 155-171.

190. KORNHAUSER, M.
Structural effects of impact.
Cleaver-Hume Press, London, 1964, 61-65.

191. SEARS, J.E.
On the longitudinal impact of metal rods with rounded ends.
Trans. Camb. Phil. Soc. 21, 1908, 49.

192. HUNTER, S.C.
Energy absorbed by elastic waves during impact.
Journal Mech. Phys. Solids 5, 1957, 162.

193. PROWSE, W.A.
The development of pressure waves during the longitudinal impact of bars.
Phil. Mag. Ser. 7, 22, 1936, 210.

194. ANDREWS, J.P.
Experiments on impact
Proc. Phys. Soc. London, 43, 1931, 8.

195. ANDREWS, J.P.
Theory of collisions of spheres of soft metal.
Phil. Mag. Ser. 7, 9, 1930, 593.

196. VINCENT, J.H.
Experiments on impact.
Proc. Cambridge Phil. Soc. 10, 1900, 332.